Carbon dynamics and greenhouse gas emissions in a tropical dry forest and a pre-alpine Bavarian grassland

by

Sofia Calvo-Rodriguez

A thesis submitted in partial fulfillment of the requirements for the degree of

Doctor of philosophy

Department of Earth and Atmospheric Sciences

University of Alberta

Abstract

The present thesis contains three studies, all of which follow the main trend of quantification and assessment of carbon dynamics and greenhouse gas emissions. The main objectives of the first study **"Dynamics of carbon sequestration in tropical dry forests along two successional gradients under climate change extremes"** were to quantify biomass and carbon accumulation dynamics in two TDF during 12 years along a successional gradient, and assess how climatic events influenced the yearly carbon accumulation. The net primary productivity (NPP) of these TDF varied from 2 Mg C ha^{-1} y^{-1} to 7 Mg C ha^{-1} y^{-1}, depending on the age of the forest stands. Climate variability and drought events like the ENSO of 2015 had a strong influence on carbon dynamics at both sites. The second study "**Seasonality and budgets of soil greenhouse gas emissions from a tropical dry forest successional gradient in Costa Rica"** main objectives were to evaluate seasonal variation and annual budgets of soil greenhouse gas emissions (CO_2, N_2O, and CH_4) in a tropical dry forest successional gradient, and evaluate environmental factors that control temporal dynamics of greenhouse gas emissions. Annual soil emissions of CO_2 were higher for the young forest (8555.7 kg C ha^{-1} y^{-1}) followed by the older forest (7419.6 kg C ha^{-1} y^{-1}) and the pasture (7223.7 kg C ha^{-1} y^{-1}). Annual emissions of N_2O were higher for the forest sites (0.39 and 0.43 kg N ha^{-1} y^{-1}) and lower in the pasture (0.09 kg N ha^{-1} y^{-1}). CH_4 uptake was higher in the older forest (-2.61 kg ha^{-1} y^{-1}) followed by the pasture (-0.69 kg C ha^{-1} y^{-1}) and the young forest (-0.58 kg C ha^{-1} y^{-1}). Fluxes were mainly positively influenced by soil moisture and microbial biomass, and negatively by soil temperature and ammonium concentrations. In the last chapter **"Spatio-temporal variability and uncertainties of greenhouse gas emissions in a pre-alpine Bavarian grassland,"** we compared measured soil gas emissions of CO_2, N_2O, soil temperature and water content against simulated values derived from the biogeochemical model

LandscapeDNDC. For the CO_2 emissions, soil temperature and water content, the model was able to simulate the daily average across different locations. We found a strong correlation between the modeled results and the measured emissions for CO_2 ($r=0.5$, $p<0.01$). For N_2O emissions, we found significant differences between measured emissions and modeled emissions.

Preface

This thesis is an original work by Sofia Calvo-Rodriguez. No part of this thesis has been previously published.

Acknowledgments

I want to express my gratitude to my supervisor Dr. Arturo Sanchez-Azofeifa and co-supervisors Dr. Ralf Kiese and Dr. Ralf Ludwig for welcoming me into their labs and research groups. It has been quite a journey full of professional and personal growth. Thanks for believing in me, and thank you for all the support and guidance.

Many thanks to my family and my husband, for all the love and unconditional support throughout these years. A special thank you to my friends, Dominica Harrison and Sandra Duran, for all the help and support through this process. I also thank Mei Mei Chong, Kati Laakso, Michael Hesketh, Kayla Stan and all my colleagues in the Center for Earth Observation Sciences (CEOS) at the University of Alberta. Without their help, this project would not have been possible. As well, I am grateful to Dr. Benoit Rivard and Dr. Guillermo Hernandez for all their comments and suggestions to improve my research as part of my supervisory committee.

I would also like to thank my colleagues from Costa Rica, Antonio Guzman, Carlos Andres Vargas, Branko Hilje, Maria Montero, and all those who helped me to collect data in the field and gave me support throughout my thesis. Thanks to all the people from Santa Rosa National Park, especially Roger Blanco, Maria Luisa, Maria Marta Chavarria, Lilly, and many others. I also appreciate the IMK-IFU and MICMOR groups for their discussions and suggestions for my research and for making me part of these fantastic research groups. Thanks to collaborators and colleagues from Germany, who include Elija Bleher, Anja Schaefler-Schmid, Alfred Fischer, Anne-Katrin Schwarzer, Ingo Völksch and Benjamin Wolf.

Finally, I would like to acknowledge the University of Alberta, the Inter-American Institute for Global Change Research, the Institute of Meteorology and Climate Research Atmospheric Environmental Research (IMK-IFU), Ludwig Maximilian University of Munich, MICMoR, MITACS, DAAD, and the Rufford Foundation for all the institutional and financial support.

Table of contents

Chapter three – Seasonality and budgets of soil greenhouse gas emissions from a tropical dry forest successional gradient in Costa Rica...39

Chapter four - Spatio-temporal variability and uncertainties of greenhouse gas emissions in a pre-alpine Bavarian grassland..75

List of tables

List of figures

List of abbreviations

TDF	Tropical dry forest
DBH	Diameter at breast height
DOY	Day of the year
NEE	Net Ecosystem Exchange
NPP	Net Primary Productivity
GPP	Gross Primary Productivity
GHG	Greenhouse gases
GWP	Global Warming Potential
SRNP-EMSS	Santa Rosa National Park Environmental Monitoring Super Site
MSSP	Mata Seca State Park
MODIS	Moderate Resolution Imaging Spectroradiometer
NDVI	Normalized Difference Vegetation Index

Chapter one – Introduction

Increases in anthropogenic greenhouse gas (GHG) emissions have been responsible for the rise in global average temperatures since the mid-20th century (IPCC, 2007). Carbon dioxide (CO_2) is the most important anthropogenic GHG (IPCC, 2007). Annual emissions of GHG due to human activity have grown >80% since the 1970s, from 21 to 55 petagrams of CO_{2eq} (carbon dioxide equivalent), which includes emissions from land-use change (Olhoff and Christensen, 2019). On the other hand, the annual amount of GHG absorbed by terrestrial ecosystems (plants and soils) represents ~20% of the anthropogenic GHG emissions or approximately 9.5 petagrams of CO_2-eq annually (Le Quéré, et al. 2015).

About half of the CO_2 assimilated for photosynthesis products are used by plants for the synthesis and maintenance of living cells; the remaining CO_2 is released back into the atmosphere through autotrophic respiration (Amthor and Baldocchi, 2001; Waring and Running, 2010; Mitchard, 2018). The remainder of the photosynthetic products stay in the plant as stored carbon (e.g., foliage, branches, stems, roots, reproductive organs). As plants die or shed leaves and roots, the dead organic matter is used as a substrate by animals and microbes, which release CO_2 back into the atmosphere through heterotrophic respiration (Waring and Running, 2010). Undisturbed forest ecosystems generally have a balance between carbon uptake, storage, and losses, with a small net annual gain, which makes them net carbon sinks overall (Luyssaert et al. 2008). Growing young forests or secondary forests (disturbed forests), on the other hand, can have important annual carbon gains (Pan et al. 2011; Pugh et al. 2019). Because of this, forest growth can delay anthropogenic climate change by slowing the rate of CO_2 that is accumulated in the atmosphere (Pugh et al. 2019). Forests have been assessed globally as representing a sink for 2.4 ± 0.4 petagrams of carbon per year (Pan et al. 2011). However, an ecosystem may lose carbon if photosynthesis is reduced or if there are external perturbations (Houghton, 2013; Brienen et al. 2015).

Climate change could potentially alter the carbon stored in forests and soils, which would lead to a reduction in the strength of the carbon sink (Rowland et al. 2015; Bradford et al. 2016; Mitchard et al. 2018). Changes influence alterations in environmental factors (e.g., increasing temperature, variation in precipitation, droughts) and biological factors (e.g., forest structure and compositional changes, decomposition rates of litter). According to a meta-analysis of 439 studies by Bond-Lamberty and Thomson (2010), climate change will cause a net release of CO_2 from soils because increasing temperatures will trigger microbes to speed up the consumption of plant debris and other organic matter (Bond-Lamberty and Thomson, 2010). Higher temperatures will also increase soil and plant respiration rates (i.e., production of CO_2 when soil organisms respire), which will cause an ecosystem to switch temporarily or permanently from being a sink to a source of carbon (Xu et al. 2004; Castro et al. 2018). Moreover, fires, deforestation, and degradation will continue to reduce forest areas that can act as sinks (Mitchard et al. 2018). Estimates indicate that in a business-as-usual scenario, the world's forests may become a carbon source by 2100 and contribute 6 petagrams of carbon per year to the atmosphere (Bellassen and Luyssaert, 2014).

Predicting the response of stored carbon to changes in global temperature is critical, particularly since the increased release of respired CO_2 to the atmosphere has the potential to exacerbate global warming (Bradford et al. 2016). Globally, soil respiration is estimated to account for 20–38% of the total annual biogenic CO_2 emissions to the atmosphere (Raich and Schlesinger, 1992; Raich and Potter, 1995), which represents the second-largest terrestrial carbon flux (Bond-Lamberty and Thomson, 2010). About 1500 petagrams of total carbon and 136 petagrams of total nitrogen are stored in the top meter of the global soil layer, and this represents the largest terrestrial carbon and nitrogen pools (Schaufler et al. 2010). Climate change can also alter soil emissions of nitrous oxide (N_2O) and methane (CH_4). Although both of these gases occur in lower atmospheric concentrations than CO_2, their global warming potentials per molecule are much higher: 298 times higher for N_2O and 25 times higher for CH_4 (van Groenigen et al. 2011). Agricultural soils are the main source of human-induced N_2O (van Groenigen et al. 2011; Tian et al. 2016). Agriculture is responsible for approximately 50% of the global atmospheric inputs of CH_4 and 75% of the global N_2O emissions (Lassey et al. 2005)

Increases in temperature and atmospheric CO_2 concentrations will generate major changes in ecosystem structure and function, ecological interactions among species, and species' geographic ranges, which will result in predominantly negative consequences for biodiversity and ecosystem goods and services (IPCC 2007). Changes in forest structure and composition can also alter ecosystem carbon and nutrient cycling, thus changing the ecosystem–atmosphere exchange rates of greenhouse gases and affecting climatic drivers on a global scale (Niklaus et al. 2016). Nonetheless, our understanding of how climate changes will affect forest carbon dynamics and greenhouse gas emissions from soils is poor.

This thesis aims to contribute to the quantification and assessment of uncertainties of carbon dynamics and greenhouse gas emissions and to identify and to integrate scientific knowledge for ecosystem characterization. The present thesis compiles four chapters, all of which follow the main trend of quantification and assessment of carbon dynamics and greenhouse gas emissions. This information is much needed to inform and to improve sampling designs for field measurements and the design of biogeochemical models.

The main objectives of Chapter 2 **“Dynamics of carbon sequestration in tropical dry forests along two successional gradients under climate change extremes”** were i) to quantify biomass and carbon accumulation dynamics in two TDF during 12 years along a successional gradient, ii) to assess how precipitation changes and drought (e.g., ENSO) influenced carbon accumulation across forest stands, and iii) to evaluate the influence of forest structure, composition, and soil fertility in the accumulation dynamics of forest carbon. This study was conducted at two TDF, which represent two extremes in the spectrum of TDF along a precipitation gradient. One was a high-rainfall, semi-deciduous TDF (30-75% of deciduous species) with 5 months of dry season located at Santa Rosa National Park, Costa Rica. The other TDF was a low-rainfall, deciduous TDF (90-95% were deciduous species) with a marked dry season (6 months) located at Mata Seca State Park, Brazil.

A total of 28 permanent plots (0.1 ha following Gentry 1988) were established and monitored annually between 2006 and 2018 at Santa Rosa National Park (SRNP-EMSS) in Costa Rica and between 2006 and 2017 at Mata Seca State Park (MSSP) in Brazil. At SRNP-EMSS, 9 permanent plots were established in stands 30 - 90 years old (three plots in the 30-year-old forest, three plots in the 50-year-old forest, and three in the old-growth forest). At MSSP, 18 permanent plots (six plots per forest stand) were established in stands 20 - 70 years old. The young forest stands (age 20) were used for pasture land for 20 years, and cattle were not removed until 2000. At each plot, all tree stems with diameters at breast height (DBH ~1.3 m) $\geq$0.05 m were tagged and measured yearly to record tree mortality, recruitment, and increase in diameter.

Aboveground and belowground biomass was calculated using the annual census of all trees and the allometric equations for tropical tree species from Chave et al. (2014) and the IPCC (2003). We estimated annual losses of aboveground and belowground biomass caused by forest mortality and biomass gain that was caused by recruitment and tree growth. NPP was obtained for both sites from the sum of net changes of aboveground carbon and belowground carbon plus the annual litterfall.

Mortality rates, diameter growth, and recruitment rates were all higher in younger (20-30 year-old) than older (>50 year-old) forest stands. For the site in Brazil, aboveground biomass varied across forest stands from 49.5 to 186.2 Mg ha^{-1} and belowground biomass from 9.0 to 34.0 Mg ha^{-1}. For the site in Costa Rica, aboveground biomass varied across forest stands from 46.5 to 215.3 Mg ha^{-1} and belowground from 13.6 to 38.6 Mg ha^{-1}. The NPP of these TDF varied from 2 Mg C ha^{-1} y^{-1} to 7 Mg C ha^{-1} y^{-1}, depending on the age of the forest stands. At both sites, higher values of NPP were observed in the older forest stands. Climate variability and drought events like the ENSO of 2015 had a strong influence on carbon dynamics by increasing tree mortality rates at both sites.

The main objectives of Chapter 3 "**Seasonality and budgets of soil greenhouse gas emissions from a tropical dry forest successional gradient in Costa Rica**" were (i) to evaluate seasonal variation and annual budgets of soil GHG emissions (CO_2, N_2O, and CH_4) in a TDF successional gradient, (ii) to evaluate environmental factors that control temporal dynamics of GHG exchange, and (iii) to provide total GHG budgets by relating soil GHG emissions to net ecosystem exchange.

This study was conducted in the Santa Rosa National Park (SRNP-EMSS) in Costa Rica at three different land covers (a pasture, an early successional stage forest, and an intermediate successional stage forest). At all three land cover sites, soil CO_2, N_2O, and CH_4 emissions were measured with manual closed static chambers in 2018. The intermediate stage forest site was also equipped with an Eddy Covariance tower and four automated soil flux chambers (8100-104C long term system, LI-COR, Inc., Lincoln, Nebraska, USA) to measure soil CO_2 fluxes. For all three land covers, soil CO_2 fluxes were further measured using a portable, automated, soil flux chamber (8100-103 single survey chamber, LI-COR, Inc., Lincoln, Nebraska, USA). To compare our results with other studies, a literature review of soil GHG fluxes was carried out using online search engines such as Google Scholar, Scopus, and Web of Science.

From the results, after a prolonged drought of 5 months in the year 2018, large emissions pulses of CO_2 and N_2O were observed at all sites following first rain events, caused by the "Birch effect," with a significant effect on the net ecosystem exchange and the annual emissions budget. Annual CO_2 emissions were greatest for the young forest (8555.7 kg C ha^{-1} y^{-1}) followed by the older forest (7419.6 kg C ha^{-1} y^{-1}) and the abandoned pasture (7223.7 kg C ha^{-1} y^{-1}). Annual emissions of N_2O were greatest for the forest sites (0.39 and 0.43 kg N ha^{-1} y^{-1}) and least in the abandoned pasture (0.09 kg N ha^{-1} y^{-1}). CH_4 uptake was greatest in the older forest (-2.61 kg C ha^{-1} y^{-1}) followed by the abandoned pasture (-0.69 kg C ha^{-1} y^{-1}) and the young forest (-0.58 kg C ha^{-1} y^{-1}). Fluxes were mainly influenced by soil moisture, microbial biomass, and soil nitrate and ammonium concentrations. Annual CO_2 and N_2O soil fluxes of tropical dry forests in this study and others from the literature were much lower than the annual fluxes in wetter tropical forests. Conversely, tropical dry forests and abandoned pastures are on average stronger sinks for CH_4 than wetter tropical forests.

The main objectives of Chapter 4, **"Spatio-temporal variability and uncertainties of greenhouse gas emissions in a pre-alpine Bavarian grassland,"** were (i) to compare measured soil gas emissions of CO_2 and N_2O against simulated emissions using the biogeochemical model LandscapeDNDC and (ii) to test the representativeness of the "average" modeling approach by comparing simulated soil emissions with an average site parameterization against the averaged simulation that was derived from multiple spatially explicit simulations.

A combination of manual and automatic soil chambers was used to measure CO_2 and N_2O gas exchanges from the soil at different locations in a Bavarian grassland. Measurements were compared with simulated gas emissions of CO_2 and N_2O using the biogeochemical model LandscapeDNDC. Model applications generally use average site inputs for soil and vegetation initialization with a limited number of samples and do not account for the spatial variability of soil characteristics and environmental conditions (Zacharias et al. 2011).

Measurements from manual and automatic chambers were compared to simulated gas emission of CO_2 and N_2O using the model LandscapeDNDC. The correlation between the modeled results using the specific soil input at each chamber location and the measured emissions at each location was significant but poor for CO_2 ($r=0.2$, $p<0.001$, RMSE=19.97). When we used the modeled results using the averaged parameters from all locations, and the averaged measured emissions from all measured chambers, the relationship for CO_2 improved ($r=0.5$, $p<0.01$, RMSE=12.58). For N_2O, we did not find a significant correlation between modeled and measured fluxes. For the environmental controls we found a good agreement for daily means of soil temperature and moisture at 5 cm depth between modeled and measured values derived from a soil wireless sensor network.

Finally, Chapter 4, **"Conclusions and future work,"** summarizes the major findings from each chapter of the thesis and points out main challenges for future assessment, recommendations, and work necessary for the evaluation of carbon dynamics and greenhouse gases under climate change.

Literature Cited

Amthor, J.S. and Baldocchi, D.D. (2001). Terrestrial Higher Plant Respiration and Net Primary Production. In *Terrestrial Global Productivity*, Academic Press, 33-59

Bellassen, V., & Luyssaert, S. (2014). Carbon sequestration: Managing forests in uncertain times. *Nature*, *506*(7487), 153-155.

Bond-Lamberty, B., Thomson, A. (2010). Temperature-associated increases in the global soil respiration record. *Nature. 464*(7288), 579-582.

Bradford, M. A., Wieder, W. R., Bonan, G. B., Fierer, N., Raymond, P. A., & Crowther, T. W. (2016). Managing uncertainty in soil carbon feedbacks to climate change. *Nature Climate Change*, *6*(8), 751-758.

Brienen RJW, et al. (2015) Long-term decline of the Amazon carbon sink. *Nature,* 519, 344–348.

Castro, S. M., Sanchez-Azofeifa, G. A., & Sato, H. (2018). Effect of drought on productivity in a Costa Rican tropical dry forest. *Environmental Research Letters*, *13*(4), 045001.

Chave, J., Réjou-Méchain, M., Búrquez, A., Chidumayo, E., Colgan, M. S., Delitti, W. B., ... & Henry, M. (2014). Improved allometric models to estimate the aboveground biomass of tropical trees. *Global change biology*, *20*(10), 3177-3190.

Gentry, A. H. (1988). Changes in plant community diversity and floristic composition on environmental and geographical gradients. *Annals of the Missouri botanical garden*, 1-34.

Houghton, R. A. (2013) The emissions of carbon from deforestation and degradation in the tropics: Past trends and future potential. *Carbon Management, 4*:539–546.

IPCC (2007). Intergovernmental Panel on Climate Change Climate Change 2007: Synthesis Report. IPCC Publication, http://www.ipcc.ch/pdf/assessment-report/ar4/syr/ar4_syr.pdf (accessed 10 Dec. 2019).

Lassey, K. R., Scheehle, E. A., & Kruger, D. (2005). Towards reconciling national emission inventories for methane with the global budget. *Environmental Sciences*, *2*(2-3), 193-204.

Le Quéré, C., Moriarty, R., Andrew, R. M., Canadell, J. G., Sitch, S., Korsbakken, J. I., ... & Houghton, R. A. (2015). Global carbon budget 2015. *Earth System Science Data*, *7*(2), 349-396.

Luyssaert S, et al. (2008) Old-growth forests as global carbon sinks. *Nature, 455*, 213–215.

Mitchard, E. T. (2018). The tropical forest carbon cycle and climate change. *Nature*, *559*(7715), 527-534.

Olhoff, A., & Christensen, J. M. (Eds.) (2019). *Lessons from a decade of emissions gap assessments*. United Nations Environment Programme.

Pan, Y., et al. (2011) A large and persistent carbon sink in the world's forests. *Science,* 333, 988–993.

Pugh, T. A., Lindeskog, M., Smith, B., Poulter, B., Arneth, A., Haverd, V., & Calle, L. (2019). Role of forest regrowth in global carbon sink dynamics. *Proceedings of the National Academy of Sciences*, *116*(10), 4382-4387. www.pnas.org/cgi/doi/10.1073/pnas.1810512116

Raich, J.W., Potter, C.S. (1995). Global patterns of carbon dioxide emissions from soils. *Global Biogeochemical Cycles, 9*, 23-36.

Raich, J.W., Schlesinger, W.H. (1992). The global carbon dioxide flux in soil respiration and its relationship to vegetation and climate. Tellus, B44, pp. 81–99

Rowland, L., da Costa, A. C. L., Galbraith, D. R., Oliveira, R. S., Binks, O. J., Oliveira, A. A. R., ... & Ferreira, L. V. (2015). Death from drought in tropical forests is triggered by hydraulics not carbon starvation. *Nature*, *528*(7580), 119-122.

Schaufler, G., Kitzler, B., Schindlbacher, A., Skiba, U., Sutton, M. A., & Zechmeister-Boltenstern, S. (2010). Greenhouse gas emissions from European soils under different land use: effects of soil moisture and temperature. *European Journal of Soil Science*, *61*(5), 683-696.

van Groenigen, K. J., Osenberg, C. W., Hungate, B. A. (2011). Increased soil emissions of potent greenhouse gases under increased atmospheric CO_2. *Nature, 475*(7355), 214-216.

Waring, R. H., Running, S. W. (2010). *Forest ecosystems: analysis at multiple scales*. Elsevier. Pp 59.

Xu, L., Baldocchi, D. D., Tang, J. (2004). How soil moisture, rain pulses, and growth alter the response of ecosystem respiration to temperature. *Global Biogeochemical Cycles, 18*(4).

Chapter two – Dynamics of carbon sequestration in tropical dry forests along two successional gradients under climate change extremes

Abstract

We analyzed forest carbon dynamics and their relationships with climatic conditions across forest stands of different ages in TDF in Brazil and Costa Rica. We determined demographic rates (mortality, recruitment, and diameter growth) by measuring annually all trees >5 cm in diameter at breast height at 27 permanent plots for more than a decade. We also calculated annual aboveground and belowground carbon stocks, losses, and gains. Total net primary productivity (NPP) was obtained for both sites from the sum of net changes of aboveground carbon and belowground carbon plus the annual litterfall. Mortality rates, diameter growth, and recruitment rates were all higher in younger (20-30 year-old) than older (>50 year-old) forest stands. For the site in Brazil, aboveground biomass varied across forest stands from 49.5 to 186.2 Mg ha^{-1} and belowground biomass from 9.0 to 34.0 Mg ha^{-1}. For the site in Costa Rica, aboveground biomass varied across forest stands from 46.5 to 215.3 Mg ha^{-1} and belowground from 13.6 to 38.6 Mg ha^{-1}. The NPP of these TDF varied from 2 Mg C ha^{-1} y^{-1} to 7 Mg C ha^{-1} y^{-1}, depending on the age of the forest stands. At both sites, higher values of total net productivity were observed in the older forest stands. Climate variability and drought events like the ENSO of 2015 had a strong influence on carbon losses at both sites.

Keywords: tree mortality, biomass, carbon sequestration, tropical dry forest, ENSO.

1. Introduction

The current extent of Tropical Dry Forests (TDF) has been reduced globally by 48.5% and 66% in the Neotropics (Portillo-Quintero and Sanchez-Azofeifa 2010). The few remnants of TDF that used to be large continuous tracts of forest cover in lowlands, and submontane areas are now highly fragmented patches under high anthropogenic pressure (Portillo-Quintero and Sanchez-Azofeifa 2010). Secondary TDF are increasingly dominant in tropical regions, and they currently occupy more area than old-growth forests (Gibbs et al. 2010; Poorter et al. 2016); however, it remains unclear how these secondary TDF cope with current and predicted climate change. In the case of TDF, changes in climate, forest structure and diversity loss would add even more stress to these highly fragmented, threatened, disturbed, and understudied ecosystems (Janzen 1988; Portillo-Quintero and Sanchez-Azofeifa 2010; Portillo-Quintero et al. 2014; Calvo-Rodriguez et al. 2017).

From a biological perspective, TDF sustain high biological diversity, which includes a remarkable number of endemic species (Linares-Palomino 2011). In the Americas, endemism levels of TDF in most regions tend to be higher than in adjacent moist forests (Linares-Palomino et al. 2011). Furthermore, TDF have important aboveground and belowground carbon reservoirs. The aboveground live biomass for deciduous TDF in the Americas is estimated to range from 39 to 334 Mg ha^{-1} (Becknell et al. 2012). The belowground biomass ranged from 17 Mg ha^{-1} in Chamela-Cuixmala TDF in Mexico to 66.8 Mg ha^{-1} in Venezuela (Jaramillo et al. 2011).

Moreover, if all world's TDF were restored, this ecosystem could contain 22 Pg of carbon in aboveground biomass, of which 8 Pg of carbon could be from restored TDF in the Americas (Becknell et al. 2012). It is presumed that TDF have the potential to recover its mature-stage biomass more quickly than wet forests (Murphy and Lugo 1986). Secondary TDF regained the aboveground biomass rapidly after disturbance; they can reach maximum potential biomass after approximately 3-5 decades, because of the predominance of sprouting species and wind-dispersed seeds (Becknell et al. 2012).

Even though TDF are ecosystems adapted to dry climatic conditions and seasonal rainfall (Pennington et al. 2004; Pennington et al. 2009; Lasky et al. 2016), carbon dynamics might change under periodic extreme drought events. Increases in temperature and intense droughts can be significant threats to the persistence of TDF (Anderegg et al. 2013; Allen et al. 2015; Catro et al. 2017). The frequency of extreme El Niño Southern Oscillation (ENSO) is predicted to increase (Cai et al. 2014; Steinhoff et al. 2015; Wang et al. 2017), which will bring more extreme droughts to areas where TDF are found. Increases in the frequency and intensity of extreme climatic events will affect plant demography (tree mortality and recruitment) of TDF (Allen et al. 2015; Allen et al. 2017). Persistent changes in the rates of tree mortality can dramatically modify the structure and composition of the forest and compromise forest diversity and productivity and other ecosystem functions and services (van Mantgem et al. 2009). Nonetheless, is still unclear how extreme climate changes (e.g., increase drought and hurricane events) will affect forest carbon dynamics in TDF. Although biomass and carbon accumulation are likely to be affected negatively by increasing droughts, there are fewer data available of long-term studies in TDF that evaluate biomass and carbon accumulation for continuous periods across successional gradients, and there is even less data that evaluate the impact of climate variability on carbon accumulation.

Carbon accumulation is influenced also by time since abandonment or stand age, disturbance history, land-use intensity, and species composition (Brown and Lugo, 1982; Campo and Vázquez-Yanes, 2004). Studies in TDF have found that stand age can be even more influential than rainfall variability for carbon accumulation (Read and Lawrence, 2003), with differences across stands of different ages explained by the changes in species composition during secondary successional changes (Aryal et al. 2015).

To understand and to predict how TDF respond to changes in climate, it is important to assess the synergistic effect of rising temperature and drought on carbon dynamics and how TDF structure and composition mediate forest responses. Here, we quantified biomass and carbon dynamics in two TDF over a 12-year period along a successional gradient to address the following questions: i) How much carbon is being accumulated annually by secondary TDF of different ages? ii) Does structure, composition, and soil fertility influence the dynamics of forest carbon accumulation? iii) How does climate variation (e.g., ENSO) affect growth, mortality, and C fluxes across stand ages? We addressed these questions at two TDF, which represent two extremes in the spectrum of TDF along a precipitation gradient. One was a high-rainfall, semi-deciduous TDF (30-75% of deciduous species), with 5 months of dry season located in Costa Rica. The other TDF was a low-rainfall deciduous TDF (90-95% of deciduous species), with a marked dry season (6 months) located in Brazil.

2. Materials and methods

2.1 Study site

The study was conducted in Santa Rosa National Park Environmental Monitoring Super Site (SRNP-EMSS) in Costa Rica and the Mata Seca State Park (MSSP) in Brazil (Figure 1). The study sites are classified as seasonally TDF (<2000mm annual precipitation), according to the Holdridge life zones (Holdridge 1967). SRNP-EMSS is located in the Guanacaste Conservation Area in northwestern Costa Rica. SRNP-EMSS's mean annual temperature is 27°C, and mean annual precipitation is 1,700 mm. The dry season at SRNP-EMSS extends over five months from December to April (Sanchez-Azofeifa et al. 2013). The MSSP is situated in Minas Gerais in Brazil. Mean annual temperature of the site is 24.4°C, and the mean annual precipitation is 651 mm, which is concentrated during the rainy season (November to April). These two TDF contain a mosaic of different successional stages, defined in Madeira et al. (2009) and Kalacska et al. (2004) as early (~20 in MSSP and ~30 years old in SRNP-EMSS), intermediate (~50 years old), and old growth forest (>100 years) according to the stage of succession based on the years of abandonment since last disturbance and forest composition and structure.

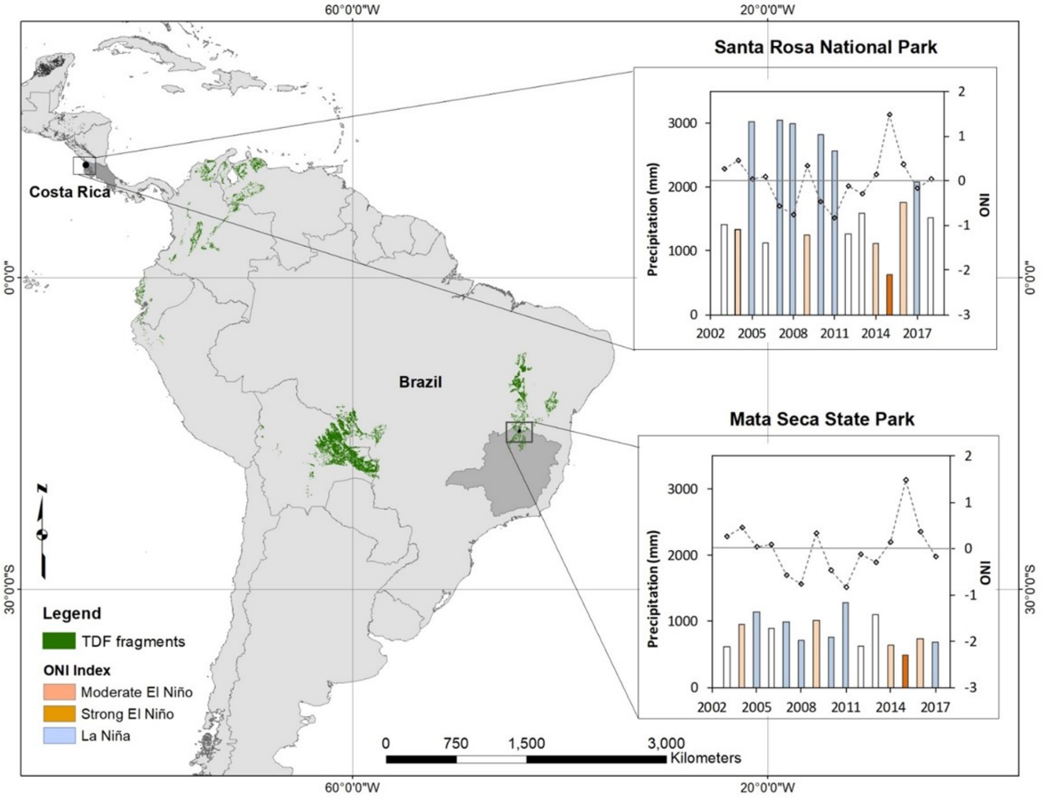

Figure 1. Location of TDF used in this study with insets of temporal variability (2003-2017) of precipitation in bars and the Oceanic Nino Index (ONI). Orange bars represent years for "El Niño" occurrence (less precipitation) and blue bars for "La Niña" occurrence (increase precipitation), according to NOAA (2018).

2.2 Climatic Variables

Climate data for 2006 - 2017 in SRNP-EMSS were obtained from the SRNP-EMSS park administration, where data have been collected and recorded daily for the last 30 y. MSSP monthly climate data for 2006 - 2017 were obtained from a local meteorological station that was managed by the Brazilian National Institute of Meteorology (INMET). Mean annual temperature (MAT), annual precipitation (MAP), days of rain, potential evapotranspiration (PET), and water deficit were calculated for each site using the daily recorded data (Appendix 1). Occurrence and intensity of "El Niño" or "La Niña" events and the Oceanic Nino Index (ONI) at both sites were obtained from NOAA (2018).

2.3 Forest Inventory plots

At the SRNP-EMSS, nine permanent plots were established (three per forest stand). The young forest stands (30-year-old) grew after several pasture fires that occurred in the late 1980s, and the intermediate forest stands (50-year-old forest) regenerated after logging activities and less intense fires in the early 1970s. The old-growth forests (OG) were located in areas where the last reported selected timber harvesting took place >100 years ago (Kalacska et al. 2004). At MSSP, 18 permanent plots were established (six plots per forest stand). The young forest stands (20-year-old) were used for pasture land for 20 years, and cattle were not removed until 2000. The intermediate forest stands (50-year-old forest) were also used for pastureland for an unknown period and were abandoned in the early 1970s. The old-growth (OG) forest have no record of logging over the last 100 years (Madeira et al. 2009; Souza et al. 2019).

At each plot, all tree stems with diameters at breast height (DBH ~1.3 m) $\geq$0.05 m were tagged and measured yearly to record tree mortality, recruitment, and increase in diameter. A total of 1131 individuals were tagged and measured in SRNP-EMSS plots (360 in 30-year-old stands, 330 in 50-year-old stands, 441 in old-growth forests), and 2431 individuals in MSSP plots (845 in 20-year-old stands, 785 in 50-year-old stands, 801 in old-growth forests).

2.4 Forest dynamics and carbon pools

Demographic rates were determined for all individuals (>5cm DBH) for all plots at each site. Tree mortality (m), recruitment (r), and annual growth (g) were calculated using a logarithmic model

(Lieberman and Lieberman 1987; Condit et al. 1999). Tree mortality, recruitment, and growth in each successional stage were calculated using the following formulas:

$$\mathrm{m} = \frac{\ln N_i - \ln N_S}{T} \qquad (1)$$

$$\mathrm{r} = \frac{\ln N_f - \ln N_S}{T} \qquad (2)$$

where N_i is the initial number of individuals, N_S is the number of individuals that survived at time T. For recruitment (r), N_f is the final number of individuals that survived plus the number of individuals recruited during the period T. Individual tree DBH growth rates were calculated using formula 3:

$$\mathrm{DBH_{growth}} = \frac{\mathrm{DBH_f} - \mathrm{DBH_i}}{\mathrm{T}} \qquad (3)$$

where $\mathrm{DBH_i}$ and $\mathrm{DBH_f}$ are the tree diameters at breast height at the initial and final measurements, respectively. For each tree >0.05 m in DBH, we calculated the aboveground biomass at each year of the census using the equation for tropical tree species from Chave et al. (2014):

$$\mathrm{AGB} = 0.0673 \times (\rho \times \mathrm{DBH}^2 \times \mathrm{H})^{0.976} \qquad (4)$$

where AGB is aboveground biomass, ρ is wood density (g cm^{-3}), DBH is the diameter at breast height (cm), and H is tree height (m). For individual trees with multiple stems, we calculated the AGB of each stem and summed them. Total carbon storage per year was converted to Mg C ha^{-1} year^{-1} by using the average wood carbon fraction of 47% (van der Heijden et al. 2015). We then estimated the annual total carbon storage gain ($\mathrm{AGC_{gain}}$) in Mg C ha^{-1} year^{-1} as the gain due to increases in growth plus tree recruitment (new trees entering the census >5cm of DBH each year). The annual total carbon storage loss in Mg C ha^{-1} year^{-1} was estimated as the loss due to tree mortality ($\mathrm{AGC_{loss}}$). Belowground biomass at each year of the census was calculated using the following equation (Penman et al. 2003):

$$\mathrm{BGB} = \exp(-1.0587 + 0.8836 \times \ln \mathrm{AGB}) \qquad (5)$$

where BGB is belowground biomass, and AGB is aboveground biomass. We then estimated the belowground annual gain in total carbon stored in Mg C ha^{-1} year^{-1} ($\mathrm{BGC_{gain}}$) due to tree recruitment and tree growth, and then the annual loss in total carbon stored in Mg C ha^{-1} year^{-1} (BGC_{loss}). The net primary productivity (NPP) in Mg C ha^{-1} year^{-1} was calculated as the aboveground and belowground annual increment obtained from tree growth and recruitment plus the annual litterfall minus the carbon losses due to mortality.

2.5 Litterfall data and fAPAR

Leaf litterfall was collected from May 2007 to March 2010 in SRNP-EMSS and from May 2008 to April 2011 in MSSP. At each plot permanent, eight litter traps were established with an area of 0.5 m^2 following research protocols found in Álvarez et al. (2008) and Souza et al. (2019). Bulk leaf litter (leafs, twigs and reproductive parts) was collected manually from the traps every 4 wk and oven-dried (<70 ° C) to obtain dry matter mass at each collection.

At both sites in Costa Rica and Brazil, wireless sensor networks (WSN) were deployed at one of the plots for each forest stage, under the forest canopy (1.3 m height from forest floor) for permanent fAPAR observations. We used quantum PAR sensors (model SQ-110, Apogee, Logan, UT, USA; field of view 180°) that were connected to self-powered nodes (model ENV-Link-Mini-LXRS, LORD MicroStrain, Cary, NC, USA). Incoming PAR was measured at 30 m high flux towers using two opposite quantum PAR sensors which were synchronized with the WSN observations. The WSN and tower sensors were configured to measure instantaneous PAR every 10 min synchronously. Using the PAR measurements, the fAPAR was calculated using the following equation:

$$fAPAR = \frac{1}{n} \sum_{i}^{n} 1 - \frac{PAR_{tran}}{PAR_{inc}} \tag{6}$$

where i is the sensor location, n is the number of sensors, PAR_{tran} is the PAR transmitted through the canopy measured at 1.3 height and PAR_{inc} is incoming PAR measured from the flux towers above the canopy. For this study, fAPAR data was calculated at the study sites during the respective vegetation periods of the years 2007-2016 for Brazil and years 2013-2019 for Costa Rica. A monthly average fAPAR was calculated for each successional stage.

2.6 Analysis

To evaluate biomass and carbon dynamics over time, we compared all results at each site between years and forest stands using analysis of variance (ANOVA) and subsequent post-hoc Tukey honest significant differences ($p<0.05$ or $p<0.001$). To test how different predictors drive carbon losses and carbon gains, we used linear models in the packages MASS and JTOOLS available in R-software (R Development Core Team 2012). We related biomass dynamics (carbon losses, carbon gain, and carbon growth) to the number of species, the number of stems per plot and the total AGC per plot.

Pearson correlations were used to evaluate inter-specific relationships between carbon loss and the essential climatic variables obtained at each site for all the years of the study. This analysis allowed us to identify statistically significant relationships, and the direction and strength of the relationships between carbon losses and climatic data.

3. Results

3.1 Forest dynamics

At both sites, mortality and recruitment rates varied during the period of measurements. At the MSSP, mortality and recruitment rates tended to be higher compared with the SRNP-EMSS. At both sites, the younger stands had the highest rates of mortality and recruitment compared to older stands (Figure 2). According to the historical climate data obtained for both sites, the annual mean and maximum temperature increased in recent years, but precipitation varied greatly from year to year, depending on the occurrence of ENSO. In 2015 a record low annual precipitation at both sites caused by the ENSO drought was observed (Figure 1). The site in Costa Rica recorded the lowest annual precipitation in 2015 (627 mm) with only 79 d of rain, in contrast to the ~130 d of rain on average for normal years. At MSSP, we also observed low annual precipitation for 2015 (490 mm).

Tree mortality increased, and recruitment rates decreased following the ENSO drought event in 2015 at all successional stages in SRNP-EMSS and MSSP. At MSSP, mortality rates also increased following the “El Niño” event of 2009, although this was a moderate event, and there was not a significant increase at SRNP-EMSS in that year. In addition, in 2016, the first hurricane (Otto) to hit Costa Rica in more than a century passed through SRNP-EMSS, and in the following year (2017), another hurricane (Nate) caused damages and flooding in the area. It is possible that after the ENSO drought of 2015, mortality rates remained high due to these extreme events. After “La Niña” in 2011, there was an increase in mortality at all stages of succession at SRNP-EMSS. This high mortality was explained by strong windstorms that affected the region, which broke several trees.

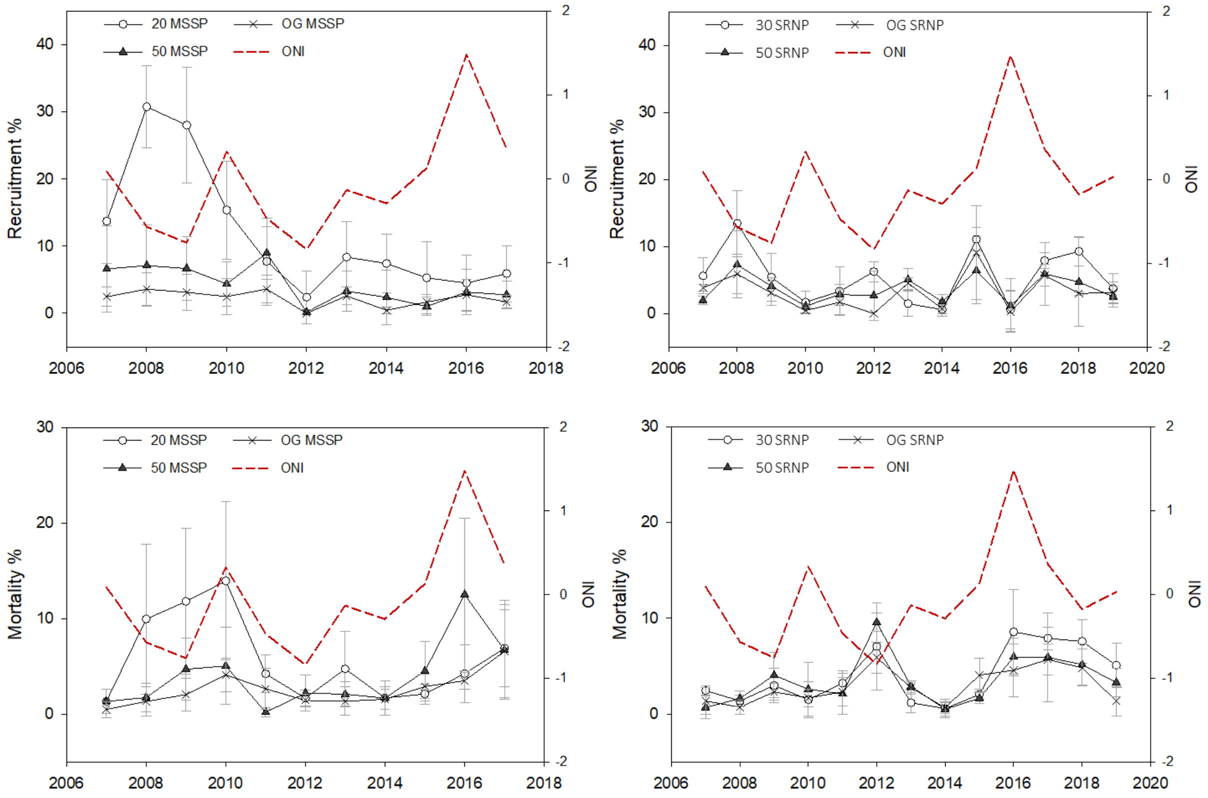

Figure 2. Mortality and recruitment rates per year at the Santa Rosa National Park (SRNP-EMSS) (from 2007 to 2019) and the Mata Seca State Park (MSSP) (from 2007 to 2017). Symbols represent mean values per forest stand, and error bars the standard deviation (20, 30, 50 year-old and old-growth = OG). The red dashed line represents the Oceanic Nino Index (ONI); the more negative the value is, the stronger were the La Nina events, and the more positive the values were, the stronger were the El Nino events.

3.2 Biomass and carbon dynamics

At both sites, aboveground and belowground biomass increased from the first census to the final census (Figure 3), which means that these forests acted as net carbon sinks overall. Values of final AGB for MSSP were initially 12.9, 76.5, and 151.1 Mg ha^{-1} and for the final census, 49.5, 95.0, and 186.2 Mg ha^{-1} for the 20-year old, 50-year old, and old-growth forests stands, respectively. Initial BGB values were 2.7, 17.5, and 31.5 Mg ha$^{-1,}$ and final values were 9.0, 18.0, 34.1 Mg ha^{-1} for the 20-year old, 50-year old, and old-growth forest stands, respectively. At SRNP-EMSS, AGB was initially 40.7, 140.6, and 203.7 Mg ha^{-1} and final values were 46.5, 152.2 and 215.3 Mg ha^{-1} for the 30-year old, 50-year old, and old-growth forest stands, respectively. Initial BGB values were 10.0, 24.8, and 32.3 Mg ha^{-1} and final values were 13.6, 33.4, 38.6 Mg ha^{-1} for the 30-year old, 50-year old, and old-growth forest stands, respectively. The forest stands that grew fastest were the 20-year old forest in Brazil, where AGB increased significantly ($p<0.001$) compared with the initial AGB. Moreover, AGB and BGB in the young forest in Brazil were significantly different ($p<0.001$) from the 50-year old and the old-growth forest. In the TDF of Costa Rica, there was no significant increase in ABG or BGB in any of the forest stands; however, the younger forest was significantly different ($p<0.001$) from the 50-year old and the old-growth forest. We observed significantly higher carbon losses and gains in the 50-year old stands and old forests (Appendix 2).

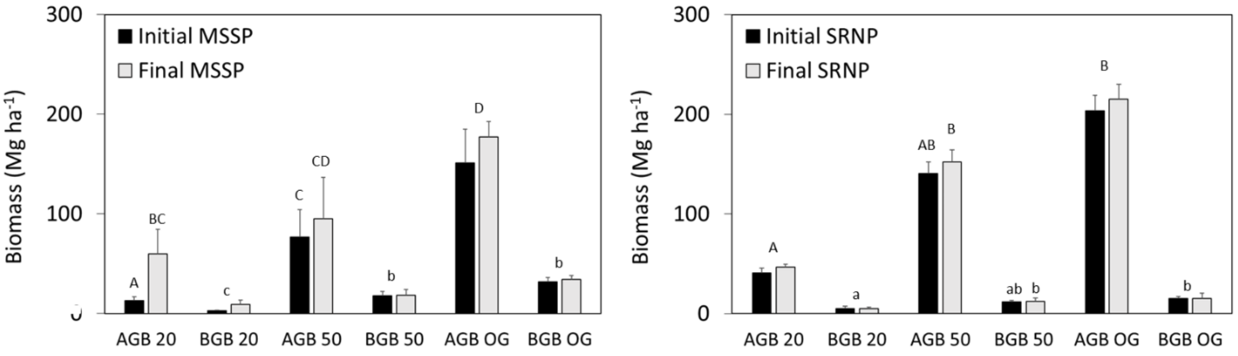

Figure 3. Initial and final aboveground biomass (AGB) and belowground biomass (BGB) at each forest stand (20, 30 and 50 year-old and old-growth = OG) in Mata Seca State Park (MSSP) and Santa Rosa National Park (SRNP-EMSS). Error bars represent the standard deviation. Different capital letters show significant differences of AGB among forest stands ($p<0.001$), and lowercase

letters show significant differences of BGB among forest stands and years ($p<0.001$) according to one-way ANOVA and a Tukey test.

At the Costa Rica site, higher values of NPP were observed in the 50-year old forest stands and the old-growth forest stands (with no significant difference $p>0.001$) and significantly lower NPP was observed at the younger forest stands (Table 1). However, for the Brazilian site, there was no significant difference between the young stands and the older forest stands for NPP.

Table 1. Net changes in aboveground carbon (AGC) and belowground carbon (BGC), litterfall production, and NPP per forest stand (20, 30 and 50 year-old and old-growth = OG) for Mata Seca State Park (MSSP) and Santa Rosa National Park (SRNP-EMSS). Different letters in the same column indicate significant differences between forest stands in a post-hoc Tukey test ($p<0.001$).

Site	**Net AGC change (Mg C ha^{-1} y^{-1})**	**Net BGC change (Mg C ha^{-1} y^{-1})**	**Litterfall (Mg C ha^{-1} y^{-1})**	**NPP (Mg C ha^{-1} y^{-1})**
MSSP				
20	2.3 ± 1.2^{a}	0.4 ± 0.2^{a}	1.9 ± 0.1^{a}	4.6± 1.4^{a}
50	2.8 ± 2.0^{a}	0.7 ± 0.5^{ab}	1.8 ± 0.1^{a}	5.3 ± 2.5^{a}
OG	2.5 ± 1.4^{a}	1.2 ± 0.4^{b}	2.2 ± 0.2^{b}	5.9 ± 1.9^{a}
SRNP-EMSS				
30	1.5 ± 0.4^{a}	0.1 ± 0.1^{a}	0.8 ± 0.6^{a}	2.4 ± 0.9^{a}
50	4.4 ± 2.7^{b}	0.5 ± 0.3^{a}	2.1 ± 0.8^{b}	7.0 ± 4.3^{b}
OG	3.4 ± 3.4^{b}	0.6 ± 0.6^{a}	2.3 ± 0.3^{b}	6.3 ± 1.2^{b}

3.3 Relationship of forest structure and composition on carbon dynamics

At both TDF sites, the number of stems was higher in the older forest stands (1055 stems ha^{-1} in MSSP and 1307 stems ha^{-1} SRNP-EMSS) than in the 50-year old and younger forest stands (295 species ha^{-1} in MSSP and 347 species ha^{-1} SRNP-EMSS). However, the number of species was higher in the 50-year old forest stands (295 species ha^{-1} in MSSP and 347 species ha^{-1} SRNP-EMSS), since we still have the presence of pioneer species and species from more advance stages of succession (Table 2). The number of botanical families' increased with the succession in the

Brazilian site (from 93 to 152 families' ha^{-1}) and for the Costa Rican site, was higher in the 50-year old forest stands (207 families' ha^{-1}).

Table 2. Forest composition (number of stems, species, families) at each forest stands (20, 30, 50 year-old and old-growth = OG) in Santa Rosa National Park (SRNP-EMSS) and Mata Seca State Park (MSSP). Mean and standard deviations were derived from 6 plot replicates per forest age in MSSP and from 3 plot replicates per forest age in SRNP-EMSS.

Site	**Stems (n ha^{-1})**	**Species (n ha^{-1})**	**Families (n ha^{-1})**
MSSP			
20	853 ± 391	168 ± 39	93 ± 19
50	855 ± 181	295 ± 70	137 ± 15
OG	1055 ± 151	265 ± 85	152 ± 15
SRNP-EMSS			
30	967 ± 364	257 ± 35	122 ± 21
50	943 ± 160	347 ± 75	207 ± 6
OG	1307 ± 406	297 ± 50	200 ± 36

The annual time series of fPAR calculated for each site showed that, the fPAR in the rainy season and in the dry season was higher in the older forest and 50-year old stands than in the younger forest stands at both sites (Figure 4). This means that the canopy closure (less lights reaching the understory) increases with the succession since a higher percentage of deciduous trees and trees with smaller specific leaf area are expected at the younger forest stands in TDF.

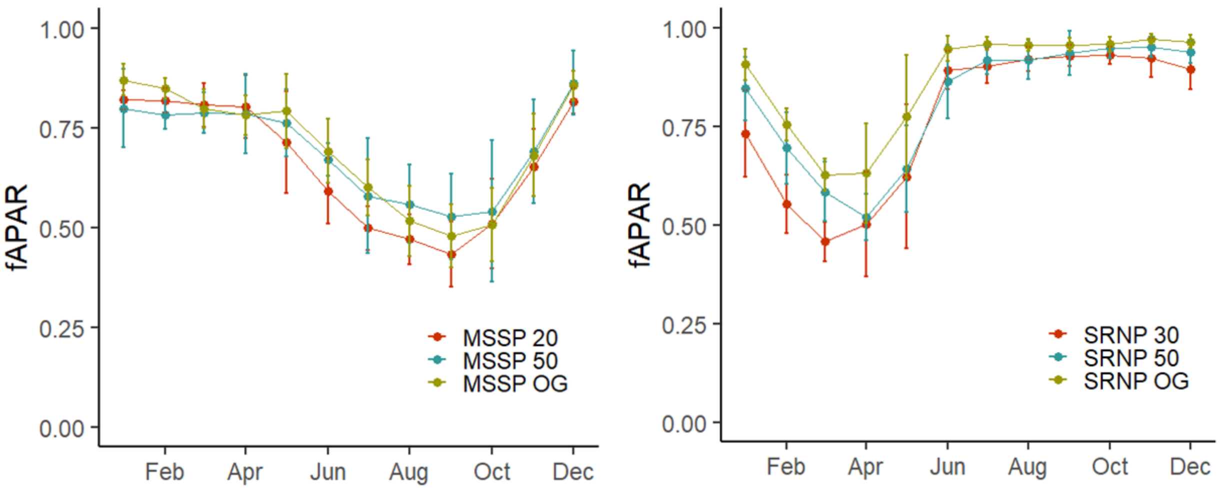

Figure 4. Curve of fPAR at each forest stand (20, 30 and 50 year-old and old-growth = OG) in Mata Seca State Park (MSSP) and Santa Rosa National Park (SRNP-EMSS). Error bars represent the standard deviation.

We also identified the species with highest contribution (more than 5%) to AGB, tree mortality and recruitment at both sites (figure 5). For the Brazilian site *Myracrodruon urundeuva* is the species with highest contribution to AGB in the older forest stand and the younger forest stands. In the 50-year old stand the species with highest contribution is *Terminalia fagifolia*. The species with the highest mortality was *Senna spectabilis* at the younger forest stands and *Combretum duarteanum* at the older growth and 50-year old forests. The species with highest recruitment was *Myracrodruon urundeuva* in the younger forest, *Tabebuia reticulate* at the 50-year old forests and *Combretum duarteanum* at the older growth forests.

For the Costa Rican site *Quercus.oleoides* is the species with highest contribution to AGB in the younger forest stands. In the 50-year old stand the species with highest contribution is *Guettarda macrosperma* and in the old growth forest is *Rehdera trinervis*. The species with the highest mortality was *Cochlospermum vitifolium* at the younger forest stands, *Luehea candida* at the 50-year old forests and *Semialarium mexicanum* at the older growth forests. The species with highest recruitment was *Rehdera trinervis* in the younger forest, *Luehea speciosa* at the 50-year old forests and *Semialarium mexicanum* at the older growth forests.

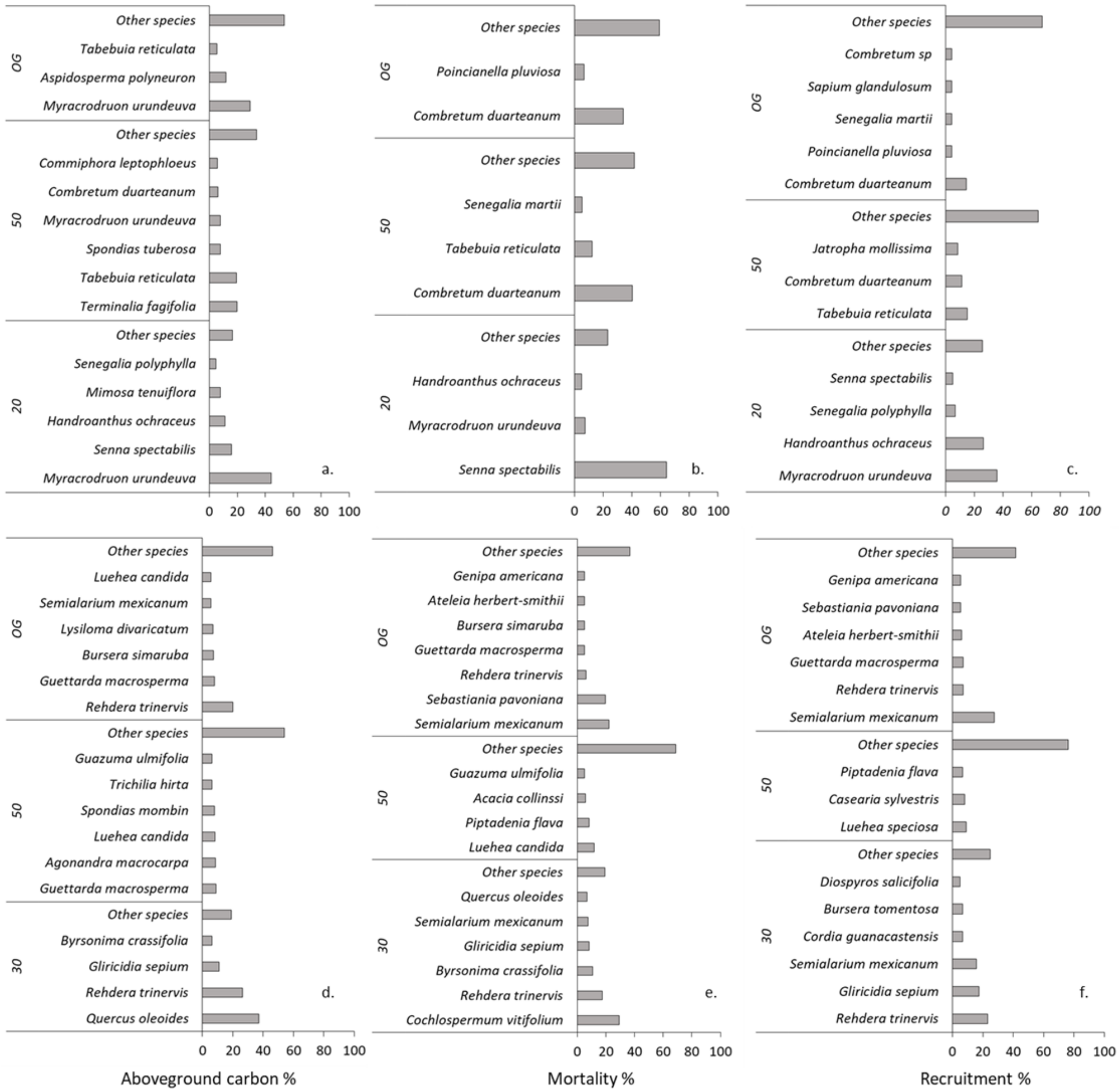

Figure 5. Species with more than 5% contribution in AGB (a. MSSP and d. SRNP-EMSS), tree mortality (b. MSSP and e. SRNP-EMSS) and tree recruitment (c. MSSP and f. SRNP-EMSS) at each forest stand (20, 30 and 50 year-old and old-growth = OG).

Linear models were built to test how carbon storage, carbon gains (recruitment and diameter growth) and carbon losses (mortality) were driven by different predictors, such as time since abandonment (TSA), litterfall, number of species, and stems per plot. From the models built, we found that the time since abandonment had a significant positive effect (Figure 6) on carbon storage ($p<0.05$) and also on carbon loss ($p<0.001$). The number of stems had a significant positive effect on carbon storage ($p<0.05$) and also on carbon gain ($p<0.001$). Litterfall was not a significant predictor ($p>0.05$), although it influenced positively the carbon gains and negatively the carbon losses. The number of species only had a significant positive effect on carbon losses ($p<0.05$) (Appendix 3).

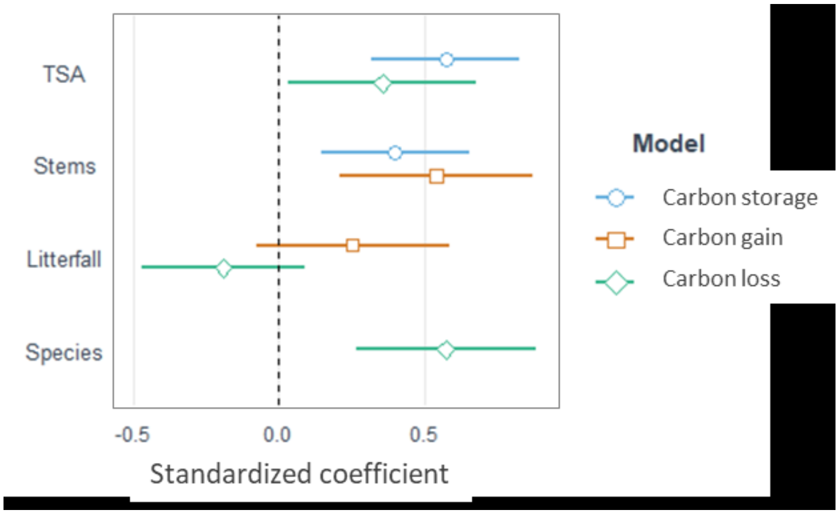

Figure 6. Comparison of the effect of time since abandonment (TSA), averaged annual litterfall per plot, number of species, and stems per plot on carbon storage, carbon gain and carbon loss at both TDF (Mata Seca State Park and Santa Rosa National Park). Standardized regression coefficients can directly be compared among each other; the higher the value, the stronger the relationship observed. If the line crossed the zero, then there was no statistical significance found ($p>0.001$).

3.4 Relationship of climate variability on carbon dynamics

From the correlations between the annual carbon losses caused by mortality at each forest stand and the climatic variables (MAP, MAT, PET, water deficit, and ONI), we found significant correlations only with increasing MAT and PET (Figure 7).

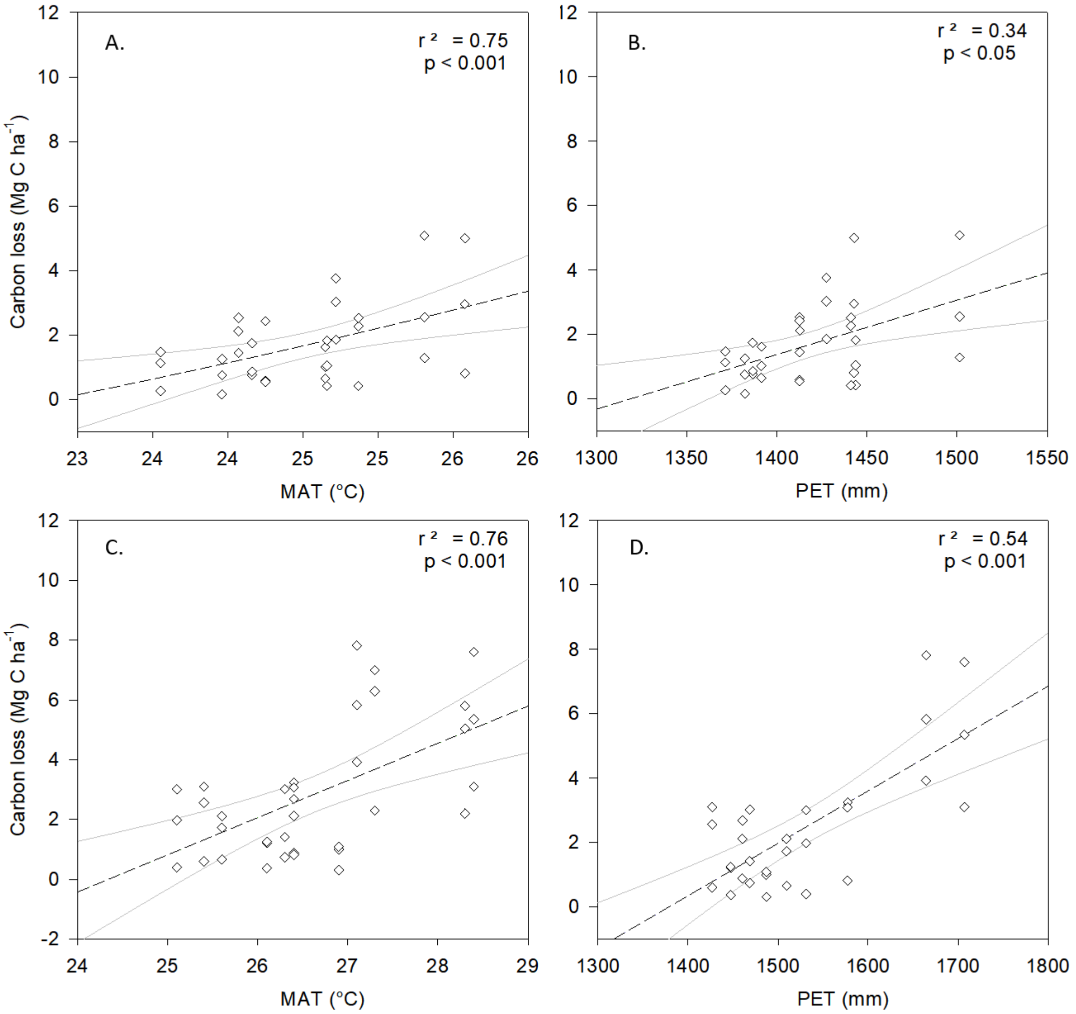

Figure 7 Linear regression between carbon loss and mean annual temperature (A. Mata Seca State Park and C. Santa Rosa National Park) and potential evapotranspiration (B. Mata Seca State Park and D. Santa Rosa National Park).

Furthermore, from the carbon losses and mortality rates calculated highest losses were observed in the years following the ENSO event of 2015 (Figure 8). Only at SRNP-EMSS, the pre-ENSO year was statistically different from the post-ENSO year of 2016 ($p<0.001$), but not from the ENSO year 2015.

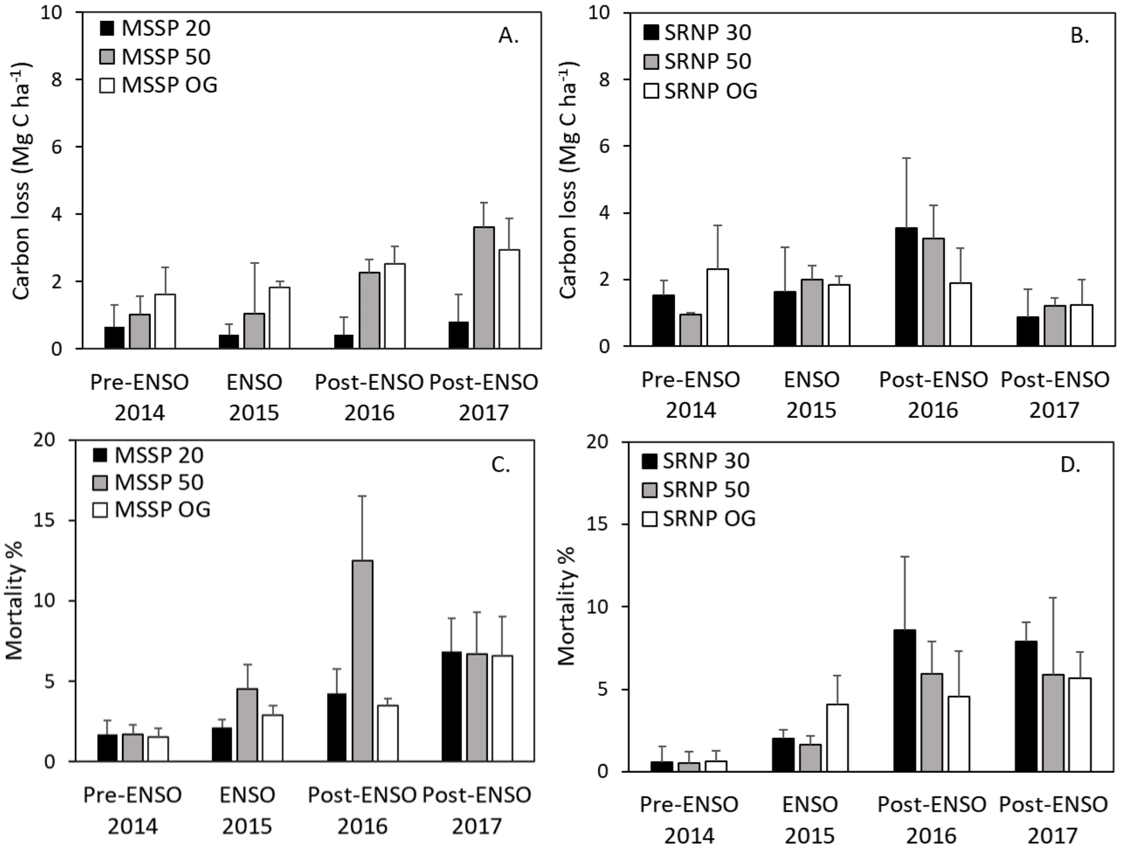

Figure 8 Carbon loss and mortality rates at each forest stands (20, 30 and 50 year-old and old-growth = OG) in Mata Seca State Park (MSSP, A and C) and Santa Rosa National Park (SRNP-EMSS, B and D) calculated for a wet year, a dry year, and the average of all years. Error bars represent the standard deviation.

4. Discussion

4.1 Forests biomass and carbon sequestration dynamics

From our results, the Brazilian TDF had higher rates of recruitment and mortality and more rapid accumulation of biomass in the young forest than the young forest in SRNP-EMSS. Biomass and carbon storage increased in both younger forests and older forests, which may be an indicator of forest recovery of these ecosystems from human disturbances. We obtained values of final AGB of 49.5 to 186.2 Mg ha^{-1} for the site in Brazil, and for the final BGB, we found values between 9.0 and 34.0 Mg ha^{-1}. For the site in Costa Rica, we obtained values of final AGB of 46.5 to 215.3 Mg ha^{-1} and for BGB from 13.6 to 38.6 Mg ha^{-1}. Murphy and Lugo (1986) reported values of total plant biomass (stems, branches, leaves, and roots) for TDF of 78-320 Mg ha^{-1}, which were much lower than the reported values for wet forests (total 269-1186 Mg ha^{-1}). The IPCC (2006) reported values of total AGB for TDF in the Americas of 200-410 Mg ha^{-1} (average of 210 Mg ha^{-1}) and a global average for TDF of 155 Mg ha^{-1}. Also, a meta-analysis with 188 TDF sites across Central and South America reported AGB estimates in mature TDF that ranged from 39 Mg ha^{-1} in Chamela, Mexico to 334 Mg ha^{-1} in Guanacaste, Costa Rica (Becknell et al. 2012). Kalacska et al. (2008) reported AGC for SRNP-EMSS values of 31.8±1.8 Mg C ha^{-1} for 30-year old stands, 60.2±2.5 Mg C ha^{-1} for 50-year old stands, and 88.9±2.0 Mg C ha^{-1} for old-growth forest stands. For the Chamela TDF in Mexico, Kalacska et al. (2008) reported values of 22.4±2.3 Mg C ha^{-1} for the 20 years old forest stands, 29.5±3.0 Mg C ha^{-1} for the undisturbed upper slope forest stands, and 72.6±3.4 Mg C ha^{-1} for the undisturbed riparian forest stands.

The IPCC (2006) reported for the Americas an average annual increment in AGB of 4 Mg ha^{-1} for <20-year-old TDF and tropical moist forests with a long dry season and 1 Mg ha^{-1} for forests >20-year-old. Cifuentes-Jara (2008) measured total AGB in 54 secondary forests that grew along a bioclimatic gradient that encompassed six life zones of Costa Rica from TDF to premontane rain forests. Maximum annual increments in AGB varied from 5.7 Mg ha^{-1} y^{-1} in TDF to 11.4 Mg ha^{-1} y^{-1} in wet forests. Moreover, in <60 y, secondary rain, and wet forests accumulated total biomass between 250 and 300 Mg ha^{-1}, but secondary TDF accumulated only 160 Mg ha^{-1} in 82 years (Cifuentes-Jara, 2008). Another study that compared AGB dynamics of dry and wet tropical forests across the Americas obtained lower annual increments in AGB in TDF, with 2.3 and 1.9 Mg ha^{-1} y^{-1} after 5-15 and 15-25 year after abandonment respectively, than in wet forests (4.7 and 6.1 Mg ha^{-1} y^{-1}) (Rozendaal et al. 2017). Also, these biomass changes were driven mainly by tree growth, which contributed to $\geq$48% of the changes in biomass across forest types and age classes. Mortality also contributed to changes in biomass in the wet forests that were 5-15-year-old, but in TDF, mortality became more important later in succession (Rozendaal et al. 2017).

Regarding the NPP, some components such as root production, are particularly difficult to measure, especially fine root biomass. Few studies that report total ecosystem NPP measured components of belowground production (Eviner 2014). From our estimates, belowground biomass consisted mostly of the standing stock of woody biomass, but it does not capture fine root production, which makes up a great part of the total NPP (Eviner 2014). Woody NPP estimated from the sum of aboveground and belowground components have been estimated to be around 3-14 Mg ha^{-1} $year^{-1}$ in Mexican TDF, of which about 44% on average was allocated belowground (Martínez-Yrízar et al. 1996). Modeled aboveground net primary productivity (ANPP) in SRNP-EMSS using the CASA model (Carnegie-Ames-Stanford Approach, Cao et al. 2016) in the same area as our study showed same successional trends, where NPP for the 30-year old, 50-year old, and old-growth forest were of 3.2 Mg C ha^{-1} yr^{-1}, 8.9 Mg C ha^{-1} yr^{-1}, and 7.6 Mg C ha^{-1} yr^{-1}, respectively (Cao et al. 2016) compared with our respective results of 2.4 Mg C ha^{-1} yr^{-1}, 7.0 Mg C ha^{-1} yr^{-1}, and 6.3 Mg C ha^{-1} yr^{-1}.

4.2 Effects of forest structure and composition on carbon sequestration

Mortality and recruitment rates were higher among younger forest stands. These dynamics likely resulted from the greater competition for space due to the dominance of acquisitive pioneer species with rapid growth and shorter life spans (Chazdon et al. 2007). In contrast, older forest stands had lower rates of mortality and recruitment, because the dominant species specialized in stable low-resource environments and had longer life spans (Condit et al. 1999; Poorter et al. 2008). Tree mortality, recruitment, and growth rates were higher at MSSP than at SRNP-EMSS, because MSSP had younger forest stands and had experienced more recent disturbance (i.e., cattle were taken out of the park in the early 2000s). Greater diameter growth rates and carbon gains in MSSP might also be associated with specific site characteristics, soil depth and texture, water table, and conditions that favored tree growth and minimized the effect of the dry season (Chazdon et al. 2007).

The linear models that were built to test the influence of forest structure and composition on carbon dynamics showed that time since abandonment and number of stems per plot were the best predictors of carbon storage. For carbon gains the number of stems per plot was the best predictor and for carbon losses time since abandonment and number of species per plot were best predictors. Time since abandonment is an important driver of carbon dynamics because the disturbance history, recovery of soil properties, and recovery of forest structure are reflected within it (Brown and Lugo, 1982). Former studies that evaluated biomass across successional gradients in seasonal forests in the Yucatan Peninsula in Mexico and Guanacaste Province in Costa Rica found that stand age explained much of the variation in biomass and basal area (Dupuy et al. 2012; Becknell and Powers 2014).

4.3 Effects of climate variability on carbon sequestration

We found some significant correlations between climatic variables and carbon loss caused by tree mortality at our study sites. Carbon loss did not vary directly with precipitation or water deficit, because mortality increased during both years of droughts and years of high precipitation (years with hurricanes, floods, or wind storms). Martínez-Ramos et al. (2018) also observed an increase in mortality rates during very wet years in the TDF of Chamela-Cuixmala Mexico when the annual precipitation was above normal. They also observed reductions in plant density and species density in very wet years of almost the same magnitude as those produced in very dry years (Martínez-Ramos et al. 2018). Our results confirmed that both dry years and very rainy years can have profound consequences for the demographic rates and carbon dynamics of TDF.

Increases in forest mortality related to the intensification of droughts and temperature in tropical forests have been reported in the literature (e.g., Chazdon et al. 2005; Allen et al. 2010; Maza-Villalobos et al. 2013). At both of our TDF sites, annual mean temperatures have been increasing in recent years (Appendix 1) and precipitation varied greatly; precipitation was lowest during the 2015 drought caused by an ENSO event. In the same year, mortality rates peaked at both TDF sites at all forest stands and remained high in some stands even 3 years after the 2015 event (Figure 2). The increases in mortality rates caused by extreme ENSO events were significantly higher in the younger forest than those in the older stages. Increases in mortality rates were also observed in other years following an ENSO event, which included the “La Niña” event in 2011 at SRNP-EMSS and the “El Niño” event in 2008 at MSSP. These results are similar to the results of others in TDF in Mexico, where prolonged and severe droughts have led to increases in tree mortality rates after ENSO events (Maza-Villalobos et al. 2013; Martínez-Ramos et al. 2018). At a TDF in Chamela-Cuixmala Mexico, Martínez-Ramos et al. (2018) also found that at different stages of forest succession tree mortality and rates of species loss increased as annual rainfall decreased. In particular, mortality and rate of species loss peaked in the ENSO of 2005, and they were still high in the following year. However, they observed recovery from the ENSO effects after subsequent rainy years, where mortality rates returned to normal levels, which led to a net increase in plant density and species density, especially in young forests. Moreover, recruitment rates and species gain increased in extremely dry years (Martínez-Ramos et al. 2018). Long dry seasons triggered flowering and, therefore, seed production, in several woody tropical plant species (Singh and Kushwaha, 2005; Wright and Calderón, 2006).

Under El Niño events, a reduction in photosynthesis rates and increased ecosystem respiration rates have been observed (e.g., De Arruda et al. 2016; Cavaleri et al. 2017), affecting the overall annual carbon sink. Another study in SRNP-EMSS at the 50-year-old forest stands, reported for the net ecosystem exchange an ecosystem uptake between 6.6 and 3.6 t C ha^{-1} for the growing seasons during 2013-2016; the lowest net ecosystem exchange (~40% less than previous year) occurred in 2015 (-3.6 t C ha^{-1}) when a strong El Niño event affected the area (Castro et al. 2018). Verduzco et al. (2015) also found significant interannual and seasonal variations due to seasonal precipitation differences in a TDF in northwest Mexico, where less precipitation switched the annual ecosystem carbon balance to a net source (+1.02 t C ha^{-1} y^{-1}), and higher precipitation led to a net sink (−2.49 t C ha^{-1} y^{-1}). Our main results showed that carbon dynamics in TDF could be greatly influenced by climate variation and global climate change. Depending on their location, some dry forests are more influenced by climate variability than others, and differences between secondary stages are observed, where the youngest forests tend to be more vulnerable.

5. Conclusions

Our results show that mortality and recruitment rates were higher among younger forest stands. Annual NPP was higher in the older forest stages in the Costa Rican site. At the Brazilian site, the annual NPP did not vary significantly between the different forest stages. Our results showed that carbon dynamics in TDF were strongly influenced by time since abandonment and climate variation. The youngest forests tended to be more vulnerable to climatic variations. In the future, we expect to see far greater carbon losses caused by increases in severe droughts and hurricane events (IPCC 2007; Sterl et al. 2008). These events can modify the carbon sequestration capacity of TDF and the recovery rates of secondary TDF in terms of carbon storage, forest structure, and diversity. Under predicted increases in extreme drought events, these changes will jeopardize the ability of secondary TDF to recover faster after human intervention, especially under extreme climatic events such as El Niño. These events will cause significant loss of diversity and biomass that will require time for the ecosystem to recover.

6. Acknowledgments

This work is part of the Research Project TROPI-DRY (Human, Biophysical Dimension on Tropical Dry Forest), which is a collaborative research network funded by the Inter American Institute for Global Change Research (IAI) Collaborative Research Network Program (CRN3-025) and supported by the U.S. National Science Foundation (Grant GEO 0452325) and the Natural Science and Engineering research council of Canada.

7. Literature Cited

Allen, C. D. et al. (2010). A global overview of drought and heat-induced tree mortality reveals emerging climate change risks for forests. *Forest ecology and management*, *259*(4), 660-684.

Allen, C. D., Breshears, D. D., McDowell, N. G. (2015). On underestimation of global vulnerability to tree mortality and forest die-off from hotter drought in the Anthropocene. *Ecosphere*, *6*(8), 1-55.

Allen, K., Dupuy, J. M., Gei, M. G. et al. (2017). Will seasonally dry tropical forests be sensitive or resistant to future changes in rainfall regimes?. *Environmental Research Letters*, *12*(2), 023001.

Álvarez, M. et al. (2008). Ecology procedures. In: Nassar, J. M., Rodríguez, J. P., Sanchez-Azofeifa, G. A., Garvin, T., Quesada, M. eds. Manual of Methods: Human, Ecological and Biophysical Dimensions of Tropical Dry Forests. Caracas: Ediciones IVIC, Instituto Venezolano de Investigaciones Científicas (IVIC). p. 15-46.

Anderegg, W. R., Kane, J. M., Anderegg, L. D. (2013). Consequences of widespread tree mortality triggered by drought and temperature stress. *Nature climate change*, *3*(1), 30.

Aryal, D. R., De Jong, B. H., Ochoa-Gaona, S., Mendoza-Vega, J., & Esparza-Olguin, L. (2015). Successional and seasonal variation in litterfall and associated nutrient transfer in semi-evergreen tropical forests of SE Mexico. *Nutrient cycling in agroecosystems*, *103*(1), 45-60.

Becknell, J. M., & Powers, J. S. (2014). Stand age and soils as drivers of plant functional traits and aboveground biomass in secondary tropical dry forest. *Canadian Journal of Forest Research*, *44*(6), 604-613.

Becknell, J. M., Kucek, L. K., & Powers, J. S. (2012). Aboveground biomass in mature and secondary seasonally dry tropical forests: A literature review and global synthesis. *Forest Ecology and Management*, *276*, 88-95.

Brown, S., & Lugo, A. E. (1982). The storage and production of organic matter in tropical forests and their role in the global carbon cycle. *Biotropica*, 161-187.

Cai, W. et al. (2014). Increasing frequency of extreme El Niño events due to greenhouse warming. *Nature Climate Change*. 4(2): 111-116.

Calvo-Rodriguez, S., Sanchez-Azofeifa, A. G., Duran, S. M., and Espirito-Santo, M. M. (2017). Assessing ecosystem services in Neotropical dry forests: a systematic review. *Environmental Conservation*, *44*(1), 34-43.

Campo, J., & Vázquez-Yanes, C. (2004). Effects of nutrient limitation on aboveground carbon dynamics during tropical dry forest regeneration in Yucatan, Mexico. *Ecosystems*, *7*(3), 311-319.

Cao, S., Sanchez-Azofeifa, G. A., Duran, S. M., & Calvo-Rodriguez, S. (2016). Estimation of aboveground net primary productivity in secondary tropical dry forests using the Carnegie–Ames–Stanford approach (CASA) model. *Environmental Research Letters*, *11*(7), 075004.

Castro, S. M., Sanchez-Azofeifa, G. A., & Sato, H. (2018). Effect of drought on productivity in a Costa Rican tropical dry forest. *Environmental Research Letters*, *13*(4), 045001.

Cavaleri, M. A., Coble, A. P., Ryan, M. G., Bauerle, W. L., Loescher, H. W., & Oberbauer, S. F. (2017). Tropical rainforest carbon sink declines during El Niño as a result of reduced photosynthesis and increased respiration rates. *New Phytologist*, *216*(1), 136-149.

Chave, J., Réjou-Méchain, M., Búrquez, A., Chidumayo, E., Colgan, M. S., Delitti, W. B., ... & Henry, M. (2014). Improved allometric models to estimate the aboveground biomass of tropical trees. *Global change biology*, *20*(10), 3177-3190.

Chazdon, R. L., Letcher, S. G., Van Breugel, M., Martínez-Ramos, M., Bongers, F., & Finegan, B. (2007). Rates of change in tree communities of secondary Neotropical forests following major disturbances. *Philosophical Transactions of the Royal Society B: Biological Sciences*, *362*(1478), 273-289.

Chazdon, R. L., Redondo-Brenes, A., Vilchez-Alvarado, B. (2005). Effects of climate and stand age on annual tree dynamics in tropical second-growth rain forests. *Ecology*, *86*(7), 1808-1815.

Cifuentes Jara, M. (2008). Aboveground biomass and ecosystem carbon pools in tropical secondary forests growing in six life zones of Costa Rica. Oregon State University. https://ir.library.oregonstate.edu/concern/graduate_thesis_or_dissertations/jm214s40j

Clark, D. A. (2004). Sources or sinks? The responses of tropical forests to current and future climate and atmospheric composition. *Philosophical Transactions of the Royal Society of London. Series B: Biological Sciences*, *359*(1443), 477-491.

Condit, R., Ashton, P. S., Manokaran, N., Lafrankie, J. V., Hubbell, S. P., and Foster, R. B. (1999). Dynamics of the forest communities at Pasoh and Barro Colorado: Comparing two 50-ha plots. *Philosophical Transactions of the Royal Society of London. Series B: Biological Sciences*, 354, 1739-1748.

Eviner, V. T. (2014). 10.6 Biogeochemical Interactions Governing Terrestrial Net Primary Production.

De Arruda, P. H. Z., Vourlitis, G. L., Santanna, F. B., Pinto Jr, O. B., Lobo, F. D. A., & Nogueira, J. D. S. (2016). Large net CO_2 loss from a grass-dominated tropical savanna in south-central

Brazil in response to seasonal and interannual drought. *Journal of Geophysical Research: Biogeosciences*, *121*(8), 2110-2124.

Dupuy, J. M., Hernández-Stefanoni, J. L., Hernández-Juárez, R. A., Tetetla-Rangel, E., López-Martínez, J. O., Leyequién-Abarca, E., ... & May-Pat, F. (2012). Patterns and correlates of tropical dry forest structure and composition in a highly replicated chronosequence in Yucatan, Mexico. *Biotropica*, *44*(2), 151-162.

Gibbs, H. K., Ruesch, A. S., Achard, F., Clayton, M. K., Holmgren, P., Ramankutty, N., Foley, J. A. (2010). Tropical forests were the primary sources of new agricultural land in the 1980s and 1990s. *Proceedings of the National Academy of Sciences, 107,* 16732- 16737.

Holdridge, L. R. (1967). *Life zone ecology*. San Jose: Tropical Science Center. 1967.

IPCC (2006). *Guidelines for National Greenhouse Gas Inventories.* Intergovernmental Panel on Climate Change*,* ed. H. Eggleston, L. Buendia, K. Miwa, T. Ngara, & K. Tanabe. Japón: IGES (National Greenhouse Gas Inventories Programme).

IPCC. (2007). Climate change 2007: the physical science basis. In: *Contribution of working group I to the fourth assessment report of the intergovernmental panel on climate change*, ed. S. Solomon, D. Qin, M. Manning, Z. Chen, M. Marquis, K.B. Averyt, M. Tignor and H.L. Miller, pp 996. Cambridge, UK: Cambridge University Press.

Janzen, D. H. (1988). Tropical dry forests. *Biodiversity*, 130-137.

Jaramillo, V. J., Martínez-Yrízar, A., and Sanford, Jr R. L. (2011). Primary productivity and biogeochemistry of seasonally dry tropical forests. In Seasonally dry tropical forests (pp. 109-128). Island Press/Center for Resource Economics.

Kalacska, M., Sanchez-Azofeifa, G. A., Calvo-Alvarado, J. C., Quesada, M., and Janzen, D. (2004). Species composition, similarity and diversity in three successional stages of a seasonally dry tropical forest. *Forest Ecology and Management*, 200, 227-247.

Kalacska, M., Sanchez-Azofeifa, G. A., Rivard, B., Calvo-Alvarado, J. C., & Quesada, M. (2008). Baseline assessment for environmental services payments from satellite imagery: A case study from Costa Rica and Mexico. *Journal of environmental management*, *88*(2), 348-359.

Lasky, J. R., Uriarte, M., and Muscarella, R. (2016). Synchrony, compensatory dynamics, and the functional trait basis of phenological diversity in a tropical dry forest tree community: effects of rainfall seasonality. *Environmental Research Letters*, *11*(11), 115003.

Lieberman, D., and Lieberman. M. (1987). Forest tree growth and dynamics at La Selva, Costa Rica (1969-1982). *Journal of Tropical Ecology*, 3, 347-358.

Linares-Palomino, R., Oliveira-Filho, A. T., & Pennington, R. T. (2011). Neotropical seasonally dry forests: diversity, endemism, and biogeography of woody plants. In *Seasonally dry tropical forests* (pp. 3-21). Island Press, Washington, DC.

Lopez, B. C., Rodriguez, R., Gracia, C. A., & Sabate, S. (2006). Climatic signals in growth and its relation to ENSO events of two Prosopis species following a latitudinal gradient in South America. *Global Change Biology*, *12*(5), 897-906.

Madeira, B., Espírito-Santo, M. M. Do., Sanz D'angelo, V., Nunes, Y. R. F., Sanchez-Azofeifa, G. A., Fernandes, W., and Quesada, M. (2009). Changes in tree and liana communities along a successional gradient in a tropical dry forest in south-eastern Brazil. *Plant Ecology*, 201, 291–304.

Martínez-Ramos, M., Balvanera, P., Arreola Villa, F., Mora, F., Maass, J. M., and Maza-Villalobos Méndez, S. (2018). Effects of long-term inter-annual rainfall variation on the dynamics of regenerative communities during the old-field succession of a neotropical dry forest. *Forest Ecology and Management*, *426*, 91–100. https://doi.org/10.1016/j.foreco.2018.04.048

Martinez-Yrizar, A., Maass, J. M., Pérez-Jiménez, L. A., & Sarukhán, J. (1996). Net primary productivity of a tropical deciduous forest ecosystem in western Mexico. *Journal of Tropical Ecology*, *12*(1), 169-175.

Mattos, P. P., Braz, E. M., Domene, V. D., Sampaio, E. V. D. S. B., Gasson, P., Pareyn, F. G. C., ... & Araújo, E. D. L. (2015). Climate-tree growth relationships of Mimosa tenuiflora in seasonally dry tropical forest, Brazil. *Cerne*, *21*(1), 141-149.

Maza-Villalobos, S., Poorter, L., and Martínez-Ramos, M. (2013). Effects of ENSO and temporal rainfall variation on the dynamics of successional communities in old-field succession of a tropical dry forest. *PloS one*, *8*(12), e82040.

Mendivelso, H. A., Camarero, J. J., Gutiérrez, E., & Castaño-Naranjo, A. (2016). Climatic influences on leaf phenology, xylogenesis and radial stem changes at hourly to monthly scales in two tropical dry forests. *Agricultural and forest meteorology*, *216*, 20-36.

Murphy, P. G., & Lugo, A. E. (1986). Ecology of tropical dry forest. *Annual review of ecology and systematics*, *17*(1), 67-88.

NOAA National Weather Service, National Centers for Environmental Prediction, Climate Prediction Center (2018). Cold and Warm Episodes by Season. Available: https://origin.cpc.ncep.noaa.gov/products/analysis_monitoring/ensostuff/ONI_v5.php

Penman, J., Gytarsky, M., Hiraishi, T., Krug, T., Kruger, D., Pipatti, R., ... & Wagner, F. (2003). Good practice guidance for land use, land-use change and forestry. *Good practice guidance for land use, land-use change and forestry.*

Pennington, R. T., Lavin, M., and Oliveira-Filho, A. (2009). Woody plant diversity, evolution, and ecology in the tropics: perspectives from seasonally dry tropical forests. *Annual Review of Ecology, Evolution, and Systematics*, *40*, 437-457.

Pennington, R. T., Lavin, M., Prado, D. E., Pendry, C. A., Pell, S. K., and Butterworth, C. A. (2004). Historical climate change and speciation: neotropical seasonally dry forest plants show patterns of both Tertiary and Quaternary diversification. *Philosophical Transactions of the Royal Society of London B: Biological Sciences*, *359*(1443), 515-538.

Poorter, L., and Markesteijn, L. (2008) Seedling traits determine drought tolerance of tropical tree species. *Biotropica* 40(3): 321–331.

Poorter, L., Bongers, F., Aide, T. M., Zambrano, A. M. A., Balvanera, P., Becknell, J. M., ... & Craven, D. (2016). Biomass resilience of Neotropical secondary forests. *Nature*, *530*(7589), 211-214.

Portillo-Quintero, C. A., Sanchez-Azofeifa, G. A., Calvo-Alvarado, J. C., Quesada, M., and Espírito-Santo, M. M. Do. (2014). The role of tropical dry forests for biodiversity, carbon and water conservation in the neotropics: lessons learned and opportunities for its sustainable management. *Regional Environmental Change,* 15: 1039-1049.

Portillo-Quintero, C., and Sanchez-Azofeifa, A. (2010). Extent and conservation of tropical dry forests in the Americas. *Biological Conservation*, 143, 144–55.

Powers, J. S., Becknell, J. M., Irving, J., & Perez-Aviles, D. (2009). Diversity and structure of regenerating tropical dry forests in Costa Rica: Geographic patterns and environmental drivers. *Forest Ecology and Management*, *258*(6), 959-970.

Read, L., & Lawrence, D. (2003). Recovery of biomass following shifting cultivation in dry tropical forests of the Yucatan. *Ecological Applications*, *13*(1), 85-97.

Rowland, L., da Costa, A. C. L., Galbraith, D. R., Oliveira, R. S., Binks, O.J. , Oliveira, A. A. R., Pullen, A. M, Doughty, C. E., Metcalfe, D. B., Vasconcelos, S. S., and Ferreira, L. V. (2015). Death from drought in tropical forests is triggered by hydraulics not carbon starvation. *Nature,* 528: 119–121.

Rozendaal, D. M., Chazdon, R. L., Arreola-Villa, F., Balvanera, P., Bentos, T. V., Dupuy, J. M., ... & Martínez-Ramos, M. (2017). Demographic drivers of aboveground biomass dynamics during secondary succession in neotropical dry and wet forests. *Ecosystems*, *20*(2), 340-353.

Sanchez-Azofeifa, G. A., Calvo-Alvarado, J., Espiritu-Santo, M. M., Fernandes, G. W., Powers, J. S., and Quesada, M. (2013). Tropical dry forest in the Americas: the tropi-dry endeavour. *Tropical dry forests in the Americas: Ecology, conservation and management*, 1-16.

Sanchez-Azofeifa, G. A., Quesada, M., Rodríguez, J. P., Nassar, J. M., Stoner, K. E., Castillo, A., ... & Fajardo, L. (2005). Research priorities for Neotropical dry forests 1. *Biotropica: The Journal of Biology and Conservation*, *37*(4), 477-485.

Singh, K. P., & Kushwaha, C. P. (2005). Emerging paradigms of tree phenology in dry tropics. *Current Science*, 964-975.

Souza, S. R., Veloso, M. D., Espírito-Santo, M. M., Silva, J. O., Sanchez-Azofeifa, A., e Brito, B. G. S., & Fernandes, G. W. (2019). Litterfall dynamics along a successional gradient in a Brazilian tropical dry forest. *Forest Ecosystems*, *6*(1), 35.

Steinhoff, D. F., Monaghan, A. J., and Clark, M. P. (2015). Projected impact of twenty-first century ENSO changes on rainfall over Central America and northwest South America from CMIP5 AOGCMs. *Climate Dynamics,* 44(5-6): 1329-1349.

Sterl, A., Severijns, C., Dijkstra, H., et al. (2008). When can we expect extremely high surface temperatures? *Geophysical Research Letters*, *35*(14).

Van Der Heijden, G. M., Powers, J. S., & Schnitzer, S. A. (2015). Lianas reduce carbon accumulation and storage in tropical forests. *Proceedings of the National Academy of Sciences*, *112*(43), 13267-13271.

Van Mantgem, P. J., Stephenson, N. L., and Byrne, J.C. (2009). Widespread increase of tree mortality rates in the western United States. *Science*. 323:521–524.

Verduzco, V. S., Garatuza-Payán, J., Yépez, E. A., Watts, C. J., Rodríguez, J. C., Robles-Morua, A., & Vivoni, E. R. (2015). Variations of net ecosystem production due to seasonal precipitation differences in a tropical dry forest of northwest Mexico. *Journal of Geophysical Research: Biogeosciences*, *120*(10), 2081-2094.

Wang, G., Cai, W., Gan, B., Wu, L., Santoso, A., Lin, X., Chen, Z., and McPhaden, M.J. (2017). Continued increase of extreme El Niño frequency long after 1.5 C warming stabilization. *Nature Climate Change* 7(8): 568-572.

Wright, S. J., & Calderón, O. (2006). Seasonal, El Nino and longer term changes in flower and seed production in a moist tropical forest. *Ecology letters*, *9*(1), 35-44.

Chapter three – Seasonality and budgets of soil greenhouse gas emissions from a tropical dry forest successional gradient in Costa Rica

Abstract

Limited information on greenhouse gas emissions from tropical dry forest soils still hinders the assessment of the sources/sinks from this ecosystem and their contribution at global scales. Particularly, rewetting events after the dry season can have a significant effect on soil biogeochemical processes and associated exchange of greenhouse gases This study evaluated the temporal variation and annual fluxes of CO_2, N_2O, and CH_4 from soils in a tropical dry forest successional gradient. After a prolonged drought of 5 months, large emissions pulses of CO_2 and N_2O were observed at all sites following first rain events, caused by the "Birch effect," with a significant effect on the net ecosystem exchange and the annual emissions budget. Annual CO_2 emissions were greatest for the young forest (8555.7 kg C ha^{-1} y^{-1}) followed by the older forest (7419.6 kg C ha^{-1} y^{-1}) and the abandoned pasture (7223.7 kg C ha^{-1} y^{-1}). Annual emissions of N_2O were greatest for the forest sites (0.39 and 0.43 kg N ha^{-1} y^{-1}) and least in the abandoned pasture (0.09 kg N ha^{-1} y^{-1}). CH_4 uptake was greatest in the older forest (-2.61 kg C ha^{-1} y^{-1}) followed by the abandoned pasture (-0.69 kg C ha^{-1} y^{-1}) and the young forest (-0.58 kg C ha^{-1} y^{-1}). Fluxes were mainly influenced by soil moisture, microbial biomass, and soil nitrate and ammonium concentrations. Annual CO_2 and N_2O soil fluxes of tropical dry forests in this study and others from the literature were much lower than the annual fluxes in wetter tropical forests. Conversely, tropical dry forests and abandoned pastures are on average stronger sinks for CH_4 than wetter tropical forests.

Keywords: soil greenhouse gases, carbon dioxide, nitrous oxide, methane, tropical dry forest, seasonality.

Introduction

Tropical Dry Forests (TDF) are a significant global carbon sink (Jaramillo et al. 2011; Becknell et al. 2012), a hot spot of biodiversity (Linares-Palomino et al. 2011), and are fundamental for the capture, regulation, and supply of regional water resources (Portillo-Quintero et al. 2015). TDF are characterized by the dominance of drought-deciduous trees, with annual average temperatures of $\geq$25°C, annual precipitation of 700-2000 mm per year, and a dry season (precipitation less than 100 mm) that lasts $\geq$3 months (Sanchez-Azofeifa et al. 2005). TDF represent 42% of all tropical forests with 54% of their global coverage (519,597 km^2) located in the Americas, which is equal to 34% of their potential geographic range (Portillo-Quintero and Sanchez-Azofeifa 2010). Due to habitat transformation and land-use changes, TDF are highly fragmented across the continent and continue to be among the most threatened natural ecosystems worldwide (Portillo-Quintero and Sánchez-Azofeifa 2010). The current extent of TDF is represented by a landscape of agricultural fields and patches of secondary forest at different stages of succession (Sanchez-Azofeifa et al. 2005). Secondary TDF are becoming increasingly dominant in tropical regions, and currently occupy more area than old-growth forests (FAO 2010; Gibbs et al. 2010); however, it remains unclear how these secondary TDF cope with current and predicted climate changes.

Climate models predict that under climate change and increased extremes of El Niño and La Niña scenarios, precipitation patterns in Central America will change, with an overall reduction in rainfall and intensification of dry intervals (Cai et al. 2014; Steinhoff et al. 2015; Chadwick et al. 2016; Wang et al. 2017). A reduction in the annual rainfall would lead to greater susceptibility to drought events in the "Dry Corridor" of Central America (Imbach et al. 2012), where 49% of the vegetation is classified as TDF (Lugo et al. 2005). Many ecosystem functions and services of TDF are linked tightly to water availability (Enquist and Leffler 2001; Farrick et al. 2013). Changes in vegetation dynamics and biogeochemical cycling caused by extreme drought events or intensification of dry spells affect forest productivity and ecosystem respiration, which causes an ecosystem to switch temporarily from a carbon sink to a carbon source (Xu et al. 2004; Castro et al. 2018).

The dry season drought and rewetting events have a significant effect on the biogeochemical processes within TDF soils and on carbon and nitrogen dynamics. After rewetting events, large pulses of CO_2 from the soil are released to the atmosphere, a phenomenon known as the "Birch effect" (Birch 1958). These large emission pulses have also been observed for N_2O fluxes in tropical forests at the onset of the wet season (Van Haren et al. 2005; Davidson et al. 1993, 2008; Welch et al. 2019). Overall, the length and intensity of the dry season and weather conditions of the previous wet season have a major influence on the magnitude of these high C and N emission pulses in tropical ecosystems (Butterbach-Bahl et al. 2004; Waring et al. 2016). In abnormally dry and hot years, such as during strong El Niño events, tropical forests can become a major net source of CO_2 (Clark 2004; Castro et al. 2018). Increased N_2O emissions that were associated with rewetting events during El Niño years have also been reported for tropical forests (Butterbach-Bahl et al. 2004; Zhang et al. 2019). Given the high Global Warming Potential (GWP) of N_2O (GWP=265, IPCC, 2014), this will likely further decrease the greenhouse gas sink provided by TDF. These emission pulses often contribute to a substantial portion of the annual soil CO_2 and N_2O flux and highly influence net ecosystem exchange (NEE) in dry ecosystems (Schimel et al. 2007; Castro et al. 2018) and the annual GHG budget.

Furthermore, over many areas of the dry tropics, the quantity and seasonality of precipitation are changing (Feng et al. 2013; Allen et al. 2017), which highlights the importance of studying soil responses to changes in rainfall. Due to the complex interactions among seasonality of precipitation, plant growth, and soil biogeochemical nutrient cycles, terrestrial ecosystem models have difficulty predicting C and N cycle dynamics and associated GHG exchange in TDF, particularly under future climates and extremes such as drought-rewetting events (Waring et al. 2016). This is in large part due to uncertainties in the dynamics of ecosystem C and N turnover to changes in rainfall and soil moisture (Sitch et al. 2008), which can vary widely across space and time (Waring et al. 2016). Even though TDF represent 42% of all tropical forests, and 54% of the total TDF global coverage is located in the Americas (Miles et al. 2006), studies that assess carbon and nitrogen dynamics and associated GHG emissions from TDF soils are still scarce. In particular, studies that evaluate seasonal variations in GHG fluxes from TDF do not include all relevant gases (i.e., CO_2, N_2O, and CH_4). However, these data are crucial to improve annual GHG emissions of TDF and to test and to validate modeling approaches that predict responses of emissions for current and future conditions due to climate change.

The specific objectives of our study, therefore, were (i) to evaluate seasonal variation and annual budgets of soil GHG emissions (CO_2, N_2O, and CH_4) in a TDF successional gradient, (ii) to evaluate environmental factors that control temporal dynamics of GHG exchange, and (iii) to provide total GHG budgets by relating soil GHG emissions to net ecosystem exchange

2. Materials and methods

2.1 Study site

This study was conducted in the Santa Rosa National Park (SRNP-EMSS) in Costa Rica. SRNP-EMSS is located in the Guanacaste Conservation Area (ACG) in northwestern Costa Rica between coordinates 10.866962° and -85.729700° (Figure 9). The study site is classified as seasonally TDF (< 2000 mm annual precipitation), according to the Holdridge life zones (Holdridge 1967). The site's mean annual temperature was 27.0 °C, and the average annual precipitation ranged from 900 to 2600 mm, with a long-term average of 1500 mm. The dry season extended from late December to mid-May (Sanchez-Azofeifa et al. 2014).

2.2 Land cover

The land cover of SRNP-EMSS was a mosaic of secondary forests at different successional stages, which ranged from abandoned pasturelands to a few small patches of old-growth forests. The successional stages at SRNP-EMSS were defined as abandoned pastures, early secondary forest (early stage), intermediate secondary forest (intermediate stage), and old-growth forest (late stage), based on the years of abandonment since last disturbance and forest structure and composition (Kalacska et al. 2004). In this study, we focused on the early and intermediate stages of forest succession and abandoned pastures that were in close vicinity (< 5km).

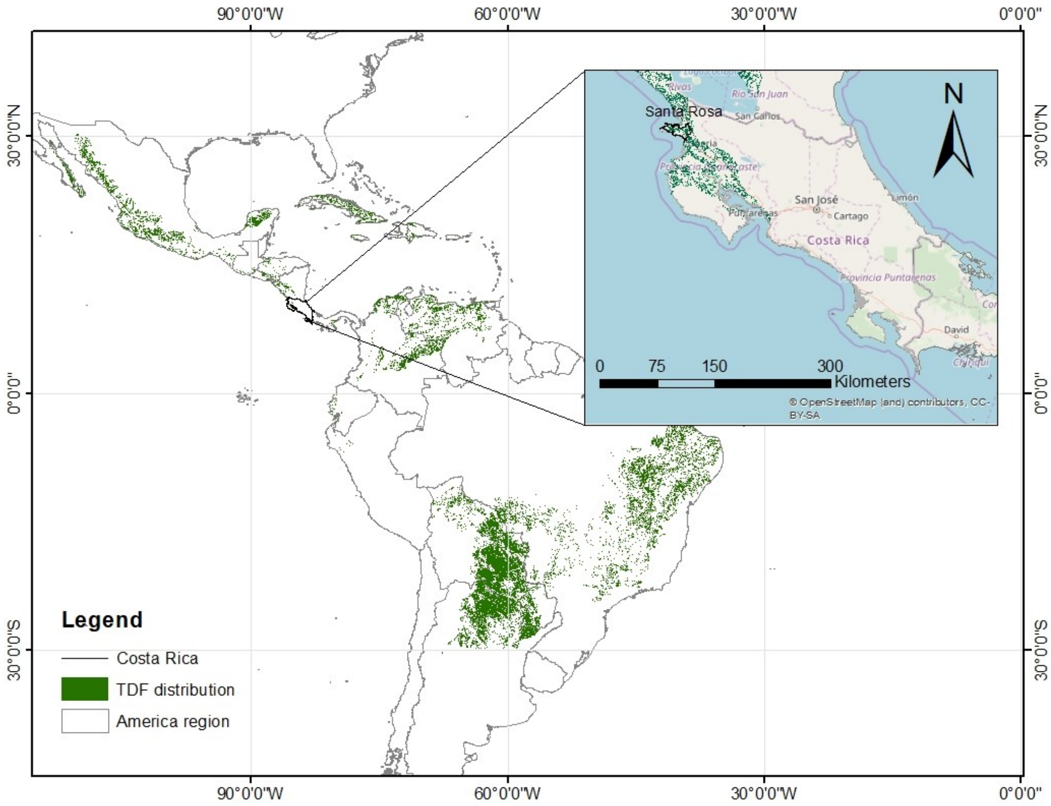

Figure 9. Distribution of Tropical Dry Forest in the Americas and location of the research site in Santa Rosa National Park in Costa Rica.

The abandoned pastures are dominated by the non-native grass *Hyparrhenia rufa* and some shrubs and small trees. The pastures undergo prescribed burns periodically in the dry season and are used as fire-breaks inside the park to protect young forests. After a fire, the pasture grows again and reaches maximum grass heights of up to 2 m in the rainy season. The annual burn of pasturelands is a common practice by the local farmers in the province.

The early stage forest (age~30) grew after several intensive pasture fires that took place late in the 1980s. The superior layer of the canopy is composed of fast-growing deciduous tree species. A second lower stratum is composed of shrubs, small trees, and some grasses (Kalacska et al. 2004). The intermediate stage forest (age~50) regenerated after logging and less intense fires in the early 1970s, and areas where the last reported selected timber harvesting occurred took place >60 years ago (Kalacska et al. 2004). This forest contains a mixture of deciduous and evergreen species, with a dominant canopy layer of 16 m (Table 3).

The soils of SRNP-EMSS have developed on an eroding Ignimbritic plateau made up of volcanic lava flows and ash deposits (Leiva et al. 2009). These soils are dominated by shallow Entisols and Vertisols (Leiva et al. 2009). Table 3 summarizes forest structure, composition, and soil properties of abandoned pasture, early and intermediate stage forest, respectively. Overall, forest sites are characterized by lower bulk density, higher SOC and N contents, and lower C/N ratios than pasture.

Table 3. Forest features and soil properties (0–10 cm depth) of each land cover type in Santa Rosa National Park, Costa Rica. Soil values represent the mean ± standard deviation derived from the six replicated measurements.

Land cover	Abandoned Pasture	Early stage	Intermediate stage
Canopy height	5	12	16
Number of stems per ha	263	1593	1644
Basal area per ha	2.1 ± 0.03	10.9 ± 0.04	21.7 ± 0.04
Tree species number per ha	15	40	66
Bulk density (g cm^{-3})	1.1 ± 0.05	0.8 ± 0.04	0.8 ± 0.01
Texture (%) sand/silt/clay	40/34/26	47/27/26	45/34/21
pH	5.9 ± 0.2	6.0 ± 0.2	6.2 ± 0.1
% Organic Matter	7.3 ± 1.5	8.7 ± 1.5	7.6 ± 0.8
%C	5.1 ± 1.0	6.1 ± 1.0	5.3 ± 0.5
%N	0.3 ± 0.1	0.5 ± 0.1	0.4 ± 0.0
C/N	15.2 ± 0.9	12.4 ± 0.5	12.2 ± 0.3

2.3 Climatic variables, Net Ecosystem Exchange, and NDVI

At the intermediate stage forest site, a climate station (model HOBO U-30-NRC Weather station, Onset Computer Corp., Bourne, MA, USA) included a 35 m × 0.70 m × 2.0 m triangular steel tower that collected eddy covariance (EC) measurements (Baldocchi et al. 1988; Aubinet et al. 1999) of Net Ecosystem Exchange (NEE). For the latter, a closed-path infrared gas analyzer (model EC155, Campbell Scientific Inc., Logan, UT, USA) was used in combination with a three-dimensional sonic anemometer (model CSAT-3A, Campbell Scientific Inc., UK). Further details about the quality check, gap filling, and instrumentation can be found in Castro et al. (2018). The meteorological station provided ancillary climate variables that included air temperature and precipitation (Apogee Instruments Inc., Logan, Utah, USA). Volumetric soil water content sensors at 20 cm soil depth (EC5, Decagon Devices Inc., Pullman, Washington, USA) were installed within the flux footprint and logged continuously at 30-min intervals. Volumetric soil water content data were further transformed into water-filled pore space (WFPS) using the corresponding measured soil porosity and bulk density.

We used the normalized difference vegetation index (NDVI) to relate the influence of the phenology to NEE measured at the intermediate stage forest site. Data for NDVI derived from the MODIS/TERRA and MODIS/AQUA products were obtained for the intermediate plot from ORNL DAAC (2018) using the coordinates of the plot. MODIS provided an 8-d composite at a spatial resolution of 0.25 km x 0.25 km (product MOD13Q1 and MYD13Q1). Data were obtained for 2017 and 2018.

2.4 Measurements of soil CO_2, N_2O, and CH_4 exchange

At the intermediate stage forest, (i.e., the site equipped with the EC tower) soil CO_2 fluxes were measured using four automated soil flux chambers (8100-104C long term system, Clear Chamber automated soil CO_2 flux system, LI-COR, Inc., Lincoln, Nebraska, USA). Soil collars (polypropylene, 20 cm inner diameter) and chambers were installed in June 2016 and logged fluxes continuously at 30-min intervals until December 2018. Flux rates were derived from fitting a linear equation of increase in CO_2 when the chamber was closed using SoilFluxPro software (LI-COR Biosciences Inc., version 4.0n). Quality checks were applied, and flux measurements were discarded if the R^2 of the linear regression was <0.81, which indicated a systematic measuring error (<10% of fluxes).

Soil CO_2 fluxes at all three land covers were further measured using a portable, automated soil flux chamber (8100-103 single survey chamber, automated soil CO_2 flux system, LI-COR, Inc., Lincoln, Nebraska, USA). Soil collars (polypropylene, 20 cm inner diameter) were installed in the field in late April 2018 at each plot (transect with five collars per plot). Measurements using this system took place from 30 April 2018 to 23 February 2019 at the same time as the measurements using the manual chambers (see the section below). All measurements were made during 1-3 d each week in the transition season and 1-3 d per month in the dry and wet season between 9.00 h and 11.00 h when temperatures were nearly at their daily means. Flux calculations and quality checks were the same as for the continuous system.

At all three land cover sites, soil CO_2, N_2O, and CH_4 emissions were measured with manual closed static chambers from 30 April 2018 to 23 February 2019. To do so, at each site, six PVC collars (35 cm by 25 cm) were inserted into the soil approximately one month before the first measurement (end of April), and they remained in place throughout the experimental period. For the measurements, an opaque PVC chamber (12 cm high) that was equipped with a fan, vent, and a sampling port was affixed to the frame by metal clamps with a rubber seal between the frame and chamber to assure gas tightness. For individual chamber measurements, a 60 mL gas sample was taken from the chamber headspace with a gas-tight syringe through a stopcock valve at 10 min intervals (0, 10, 20, 30 min after chamber closure). The 60 mL gas samples were immediately used to flush (40mL via additional flushing needle) and finally over-pressurize (20ml) 10 mL sealed glass vials (SRI, Instruments, Bad Honnef, Germany). The samples were shipped within a maximum of four weeks to KIT, IMK-IFU (Garmisch-Partenkirchen, Germany) for analysis using an autosampler (SRI Instruments, Bad Honnef, Germany, N=200) coupled to a gas chromatograph (8610 C; SRI Instruments, Torrence, USA) that was equipped with an electron capture detector (ECD) and a flame ionization detector/ methanizer (FID) for N_2O and CH_4/CO_2 concentration analysis, respectively. Samples were calibrated continuously with vials (4 out of 16) filled with standard gas (Air Liquide, Düsseldorf, Germany). Linearity of concentration increases were evaluated and single flux rates of CO_2, N_2O, and CH_4 were calculated from changes of gas concentrations in the chamber headspace with time (N_2O/ CH_4: all 4 sampling points; CO_2: 2 or 3 sampling points) and further corrected for temperature and barometric pressure. Quality checks were applied, and single chamber-based CO_2, N_2O, and CH_4 flux measurements were discarded if the R^2 of the linear regression of CO_2 fluxes was <0.81, which indicated a systematic measuring error (<6% of fluxes). Fluxes of CH_4 and N_2O were either set to zero when a $R^2 < 0.6$ or if fluxes were lower than the mean detection limits (<13% for CH_4, <28% for N_2O), which were 4.40 µg CH_4-C and 0.68 µg N_2O-N m^{-2} h^{-1} (Gütlein et al. 2017).

To compare our results with other studies, a literature review of soil GHG fluxes from tropical soils was carried out using online search engines such as Google Scholar, Scopus, and Web of Science. We included in the review only studies from tropical sites in the Americas where soil fluxes have been measured in forests (secondary or primary), savannas, or pastures that have not been managed in recent years (abandoned).

2.5 Physico-chemical soil characterization

For physico-chemical characterization, soil samples from each land cover type were collected shortly before the start of the soil GHG measurements in April 2018. Soil carbon and nitrogen content were determined by an element analyzer (Series II CHNS/O Analyzer 2400, Perkin-Elmer, Norwalk, CT, USA), and pH, bulk density, and soil texture were measured using standard procedures. In 2018, further soil samples (0-5cm depth) were collected at any time that manual chamber measurements were conducted in close vicinity (~0.5m) to the installed collars using a metal cylinder (47 cm diameter and 53 height cm). Soil samples were analyzed for ammonium and nitrate concentrations, and microbial biomass carbon. The methodology used for the determination of microbial biomass was fumigation extraction (Vance et al. 1987). Determination of ammonium and nitrate concentrations was done with Flow Injection Analysis (Hofer, 2003; Knepel, 2012) on 2M KCl soil extracts.

At any time of manual chamber measurements soil temperature and volumetric water content (VWC) were measured for 0–5 cm soil depth with a manual 5TM sensor (DECAGON Devices; WA, USA) after each gas sampling in the center of each chamber collar. Soil water filled pore space (WFPS) was calculated from VWCs according to Werner et al. (2014).

2.6 Statistical analyses

Daily means of N_2O, CH_4 and CO_2 fluxes (+/- SD) were calculated for all land covers from six replicated manual chambers per site, and, for CO_2 fluxes, including measurements from the portable automatic chamber. Seasonal mean gas fluxes were calculated for the dry (30/April – 15/ May), transition (16/May – 19/June), and wet season (20/June – 11/ December) by averaging all available daily measurements during the respective periods. Annual means represent weighted means of seasonal averages (i.e., 131 days of the dry season (1 Jan – 15 May), 35 days of transitioning to the wet season (16 May – 19 June) and 199 days of the wet season (20 June – 31 December). One-way ANOVA (Tukey's HSD) was used to test differences ($\alpha = 0.05$) between land covers and soil properties (microbial biomass, nitrate, ammonium). For all variables analyzed, the Kolmogorov–Smirnov statistic was applied to test for normal distribution. If the data were not distributed normally, we applied a log transformation. When the assumptions for parametric statistical analysis were not fulfilled, even after transformation, the non-parametric Kruskal-Wallis test was used. Soil water filled pore space (WFPS), soil temperature, and greenhouse gas fluxes were analyzed using repeated-measures ANOVA to test the effect of land cover and sampling season.

Pearson correlation analyses were used to identify relationships among all measured variables, which included fluxes and environmental controls. In addition, we used stepwise multiple linear regressions with backward elimination ($\alpha = 0.05$) to test how fluxes varied as a function of soil WFPS and soil nutrient status (microbial biomass, NO_3^-, NH_4^+) both for different land covers and the combined data for all land covers. All statistical analyses and graphs were done using R-software (R Development Core Team 2012).

3. Results

3.1 Seasonal variability of environmental controls

3.1.1 Weather conditions and soil climate

Total annual precipitation during the 2 year of automatic soil respiration measurements was 2079 mm and 1515 mm during 2017, and 2018, respectively (Figure 10). There was an abnormal amount of precipitation (>2000 mm) in 2017, especially in October, when the meteorological station recorded an accumulation of >800 mm of rain, which doubled the monthly historical average. Hurricane Nate caused this unusual precipitation event. Rainfall distribution showed pronounced seasonal differences, with the first four months of the year characterized as the dry season with minimal or no rainfall events. The transition between dry season and wet season started in both years in April or May, and the rainy season ended in December. Mean daily air temperature varied slightly between seasons (Figure 10); maximum daily air temperatures occurred in the dry season (~34 °C) and minimum daily air temperatures occurred in the wet season (~20 °C). The mean annual temperatures in 2017 and 2018 were 25.5 °C and 25.7 °C, respectively.

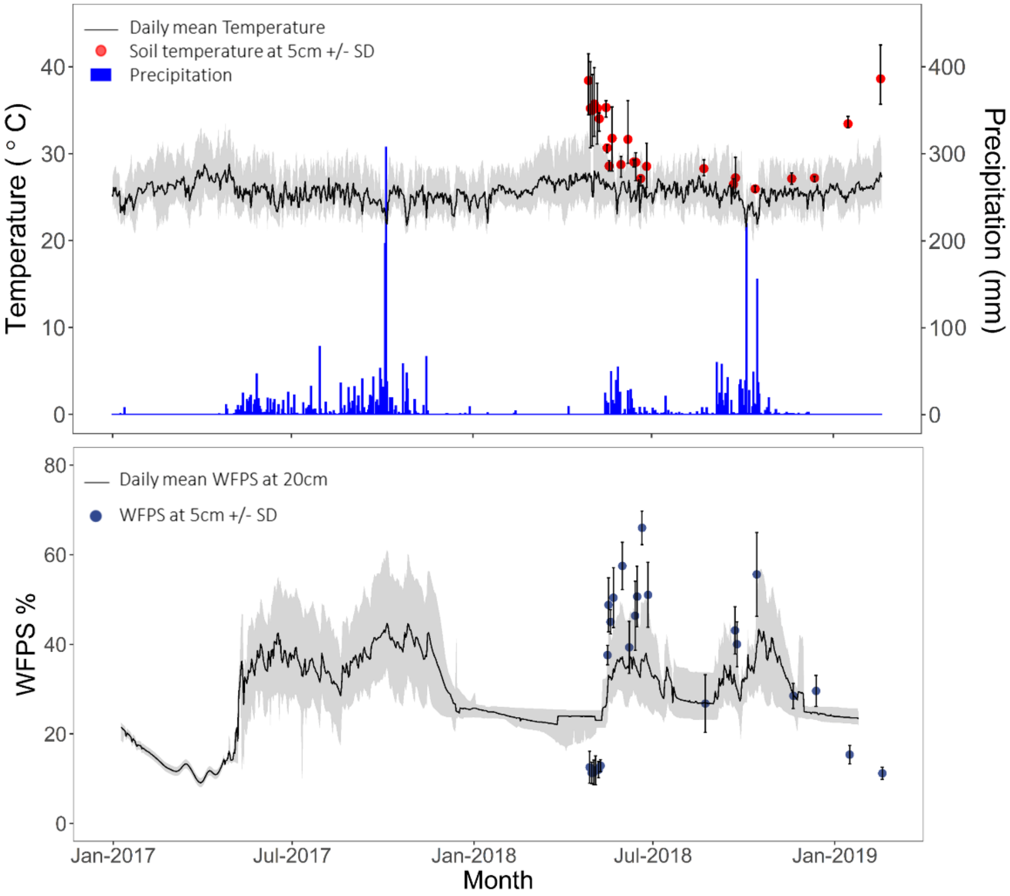

Figure 10. Time series for the intermediate stage forest in Santa Rosa National Park, Costa Rica of daily mean temperature, sum of daily precipitation from the weather station, and soil temperature at chamber sampling days at 5 cm soil depth. Below daily mean soil water content (in water filled pore space: WFPS) at 20 cm, and at chamber sampling days at 5 cm soil depth. The grey area represents maximum and minimum values.

WFPS varied in accordance with the seasonality of precipitation throughout the years. The intermediate stage forest had a maximum WFPS at 5 cm soil depth in the wet season (September-November) when it reached values of >50% WFPS and minimum values (<5% WFPS) at the end of the dry season (March-April) (Figure 10). In addition, in both years we observed a marked reduction in the WFPS in August caused by a short dry season (the *veranillo*, or "little summer"), which is expected and normal for the study region (Janzen and Hallwachs, 2016; Castro et al. 2018). Soil temperature at 5 cm depth followed the seasonal changes in air temperature with maximum temperatures in the dry season (~44 °C) and minimum temperatures during the wet season (~20 °C). Comparison of soil moisture and temperature across the different land-use types revealed significant differences only in the wet season (Table 4), with higher soil moisture and soil temperatures found at the abandoned pasture site.

Table 4. Soil water content (in water filled pore space: WFPS) and temperature at 5 cm soil depth for each land cover type in different seasons in Santa Rosa National Park, Costa Rica. Values represent the mean ± standard deviation derived from the six replicated measurements.

Site	Season	Early	Intermediate	Abandoned Pasture
WFPS	Dry	10.3±3.1^{Aa}	12.3±2.3^{Aa}	11.7±2.7^{Aa}
	Transition	41.9±7.7^{Ab}	46.9±5.4^{Ab}	56.2±6.7^{Ab}
	Wet	36.8±5.2^{Ab}	43.9±6.3^{ABb}	51.9±5.7^{Bc}
Soil temperature (°C)	Dry	36.5±1.3^{Aa}	35.7±2.6^{Aa}	35.4±1.8^{Aa}
	Transition	31.7±1.4^{Ab}	30.6±1.4^{Ab}	33.1±2.2^{Aa}
	Wet	28.5±0.9^{Ab}	26.6±0.8^{Ac}	29.5±1.7^{Ba}

Different capital letters in the superscripts show significant differences among forest stages, and lowercase letters denote significant differences among seasons ($\alpha = 0.05$).

3.1.2 Microbial biomass and soil NH_4^+ and NO_3^- concentration

For the three land covers the measurements of microbial biomass in 2018 were smallest (<100 mg C kg^{-1} SDW) in the dry season (May) and sharply increased during the transition period from dry season to wet season (< 200 mg C kg^{-1} SDW). At all sites, microbial biomass decreased during the wet season (July-December) but values at the end of the wet season were still higher than at the beginning of the dry season (Figure 11a). Overall, no significant differences were found across sites and at any sampling time. In contrast to microbial biomass, soil NH_4^+ and NO_3^- concentrations were highest (30-60 mg N kg^{-1} SDW) in the dry season, sharply decreased during the transition period from dry season to wet season, and remained low (5 - 15 mg N kg^{-1} SDW) during the wet season (July-December). There was little difference between the early and intermediate stage forest sites; both were characterized by nearly equal concentrations of soil NH_4^+ and NO_3^- (Figure 11b,c). By contrast, at the abandoned pasture site, mean soil NH_4^+ concentration (23.6 mg N kg-1 SDW) was ten-fold higher than NO_3^- concentrations (2.2 mg N kg-1 SDW), although the latter showed little variation across different seasons. NO_3^- concentrations were also significantly lower ($p<0.05$) at the abandoned pasture site than at the forest sites.

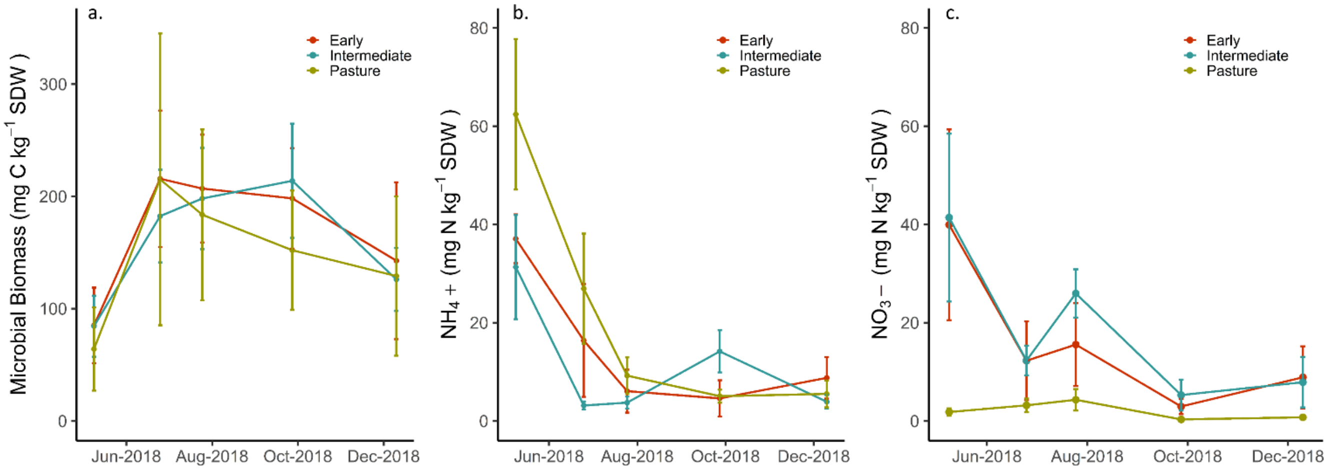

Figure 11. Time series of a) microbial biomass, b) soil ammonium (NH_4^+) concentration, and c) soil nitrate (NO_3^-) concentration measured at the abandoned pasture, early stage forest, and intermediate stage forest in Santa Rosa National Park, Costa Rica in 2018. Values are calculated from n = 6 per site and date; error bars represent SD.

3.2 Seasonal variability of soil CO_2 and N_2O, and fluxes in CH_4

We observed strong seasonality at all sites for the soil CO_2 and N_2O fluxes measured by manual chambers in 2018 (Figure 12). Large emission pulses were observed for CO_2 and N_2O at the transition period from dry season to wet season, which ranged annually from 0.1 to 525.1 mg C $m^{-2} h^{-1}$ and -4.1 to 184.7 µg N $m^{-2} h^{-1}$, respectively. For all sites, the largest CO_2 and N_2O emissions were observed in the transition season ($p<0.05$). These high pulses lasted longer for CO_2 (more than one month) than for N_2O, which returned to background levels in a few days'. For all sites, mean CO_2 and N_2O fluxes were higher during the wet season than the dry season. There were no significant ($p<0.05$) differences in CO_2 and N_2O emissions between land covers during the dry season or the wet season. However, in the transition from dry season to wet season, the two forest sites were characterized by higher CO_2 and N_2O emissions than the abandoned pasture.

At all sites, seasonal variation of soil CH_4 exchange was less pronounced than for CO_2 and N_2O emissions. Overall, CH_4 fluxes ranged from -66.4 to 215.7 µg C m^{-2} h^{-1}. Although we observed occasional emissions of CH_4 associated with heavy precipitation events mainly at the early stage forest and abandoned pasture, all sites were net sinks for atmospheric CH_4 on an annual basis. Significantly higher CH_4 uptake rates over all seasons ($p<0.05$) were found for the intermediate stage forest (annual average of -30.91 µg C m^{-2} h^{-1}). Uptake rates at the abandoned pasture and early stage forest were lower and not significantly different from each other (Figure 12).

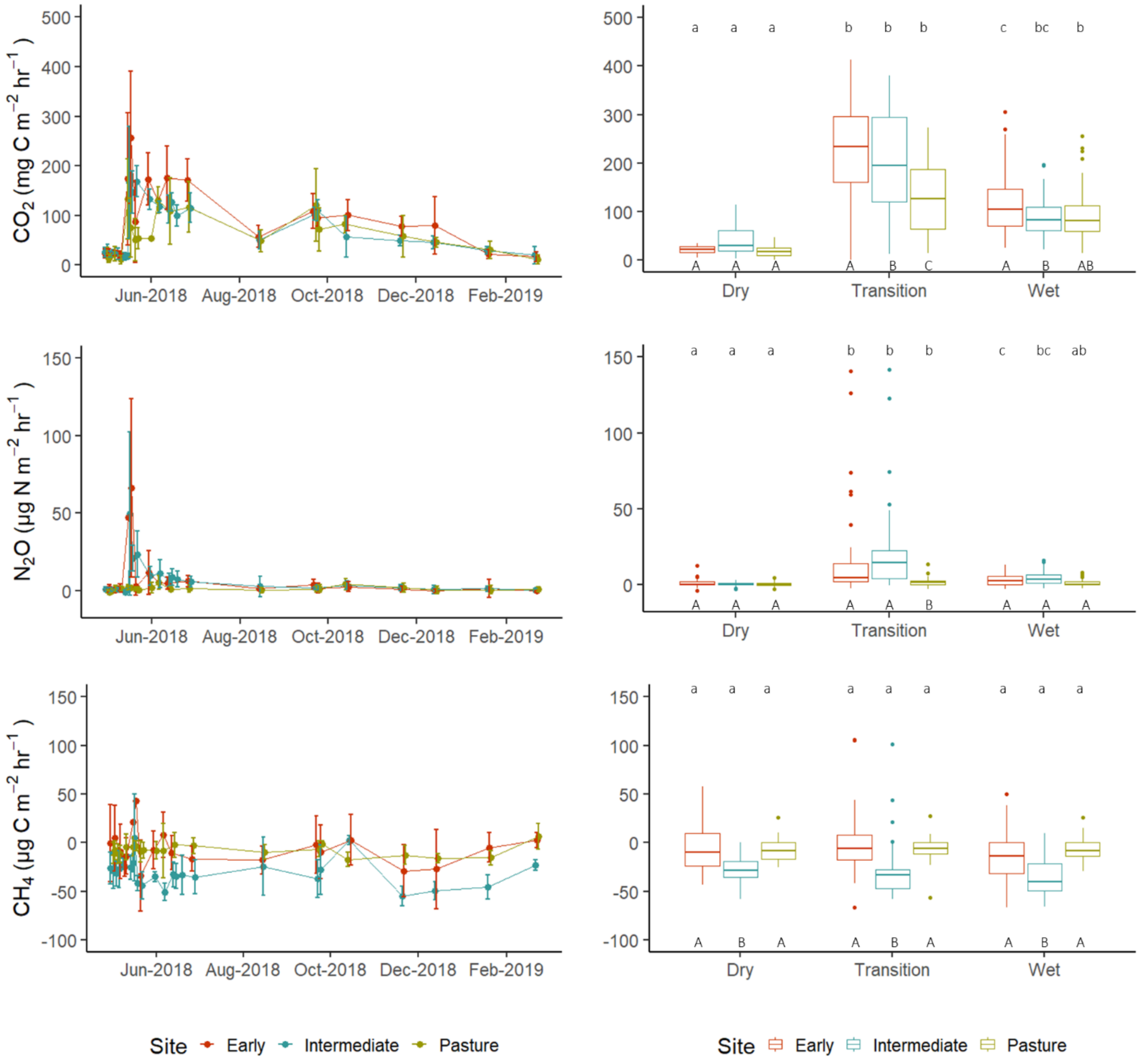

Figure 12. Left panel: Time series of daily CO_2, N_2O, and CH_4 fluxes measured at the different land covers in Santa Rosa National Park, Costa Rica in 2018. Right panel: Seasonal means of CO_2, N_2O, and CH_4 fluxes at the different land covers. Different capital letters in the right panel show significant differences among forest stages, and lowercase letters denote significant differences among seasons ($p<0.05$).

Annual soil CO_2 emissions were significantly higher ($p<0.05$) for the early forest stage (8555.74 kg C ha^{-1} y^{-1}) followed by the intermediate forest stage (7419.65 kg C ha^{-1} y^{-1}) and the abandoned pasture (7223.76 kg C ha^{-1} y^{-1}). Annual emissions of N_2O were significantly higher ($p<0.05$) for the early and intermediate forest sites (0.39 kg N ha^{-1} y^{-1} and 0.43 kg N ha^{-1} y^{-1}) and lower in the abandoned pasture (0.09 kg N ha^{-1} y^{-1}). Annual CH_4 uptake was significantly higher ($p<0.05$) in the intermediate forest stage (-2.61 kg C ha^{-1} y^{-1}) followed by the abandoned pasture (-0.69 kg C ha^{-1} y^{-1}) and the early forest stage (-0.58 kg C ha^{-1} y^{-1}), although there was no significant difference between the latter two sites (Table 5).

Table 5. Seasonal, annual emissions of N_2O, CO_2, and CH_4 fluxes (±SD) for each land cover in Santa Rosa National Park, Costa Rica. Annual means (2018) represent weighted means of seasonal averages (i.e., 131 days of dry season, 35 days of transition to wet season, and 199 days of wet season).

Plot	**Season**	**N_2O flux (μg N m^{-2} h^{-1})**	**N_2O (kg N ha^{-1})**	**CO_2 flux (mg C m^{-2} h^{-1})**	**CO_2 (kg C ha^{-1})**	**CH_4 flux (μg C m^{-2} h^{-1})**	**CH_4 (kg C ha^{-1})**
Early	dry	0.88±2.73	0.03±0.09^{Aa}	24.64±9.71	774.75±305.13^{Aa}	-4.46±50.41	0.13±1.54^{Aa}
	transition	25.88±48.09	0.22±0.40^{Ab}	233.16±96.19	1958.57±807.97^{Ab}	-7.88±22.81	-0.06±0.19^{Aa}
	wet	3.05±3.70	0.15±0.18^{Aa}	121.91±62.64	5822.42±2991.77^{Ac}	-13.83±24.03	-0.65±1.14^{Aa}
	annual	**9.28**±28.48	**0.39**±0.67^{A}	**175.34**±110.75	**8555.74**±1368.29^{A}	**-6.78**±34.15	**-0.58**±2.87^{A}
Intermediate	dry	0.39±1.46	0.01±0.05^{Aa}	42.89±26.99	1308.90±866.69^{Aa}	-23.41±27.60	-0.74±0.87^{Ba}
	transition	24.24±31.94	0.20±0.27^{Bb}	222.14±87.20	1866.00±732.45^{Cb}	-35.85±15.52	-0.30±0.13^{Ba}
	wet	4.39±4.52	0.21±0.22^{Aab}	88.88±42.82	4244.75±2045.29^{ABb}	-33.00±20.98	-1.58±1.00^{Ba}
	annual	**7.86**±18.10	**0.43**±0.53^{A}	**123.43**±91.34	**7419.65**±1214.81^{B}	**-30.91**±22.44	**-2.61**±2.00^{B}
Abandoned Pasture	dry	0.31±1.80	0.01±0.06^{Aa}	25.61±29.05	805.05±913.43^{Aa}	-7.98±11.51	-0.25±0.36^{Aa}
	transition	1.69±2.57	0.01±0.02^{Bb}	141.23±76.73	1186.34±644.49^{Cb}	-5.54±13.22	-0.05±0.11^{Aa}
	wet	1.33±2.52	0.06±0.12^{Bab}	109.56±56.50	5232.37±2698.45^{ABb}	-8.32±9.20	-0.40±0.44^{Aa}
	annual	**1.21**±2.43	**0.09**±0.20^{B}	**102.72**±72.29	**7223.76**±1418.79^{B}	**-7.22**±11.36	**-0.69**±0.91^{A}

Different capital letters show significant differences among forest stages, and lowercase letters denote significant differences among seasons ($p<0.05$).

3.3 Environmental controls of CO_2, CH_4, and N_2O exchange

Using Pearson correlation coefficients (Figure 13), a significant correlation between CO_2 and WFPS was found for the abandoned pasture (R=0.63), the early stage forest (R=0.87), and intermediate stage forest (R=0.78). The magnitude of soil CO_2 emissions was correlated with N_2O emissions in the early stage forest (R=0.65) and intermediate stage forest (R=0.64), but not in the abandoned pasture. Considering data from all sites, soil CO_2 emissions were better correlated with WFPS than N_2O and microbial biomass (R=0.69, 0.49, 0.36) and with soil ammonium concentration (R=-0.42) and soil temperature (R=-0.51); however, the latter two were correlated negatively with WFPS (Figure 13).

Soil N_2O emissions were correlated positively with WFPS (R=0.46) in the early stage forest and intermediate stage forest (R=0.52) and negatively with nitrate in the intermediate stage forest (R=-0.53). Using all data from all sites, N_2O was correlated positively with WFPS (R=0.29) and negatively with CH_4 fluxes (R=-0.31). CH_4 fluxes were correlated with environmental controls only in the intermediate stage forest (i.e., negatively with WFPS (R=0.45) and positively to soil temperature (R=0.51)), but there were no significant correlations between CH_4 fluxes and potential environmental controls at the early stage forest and abandoned pasture. Considering data from all sites, CH_4 fluxes were correlated with soil temperature (Figure 13), however, note that soil temperature was correlated negatively with WFPS.

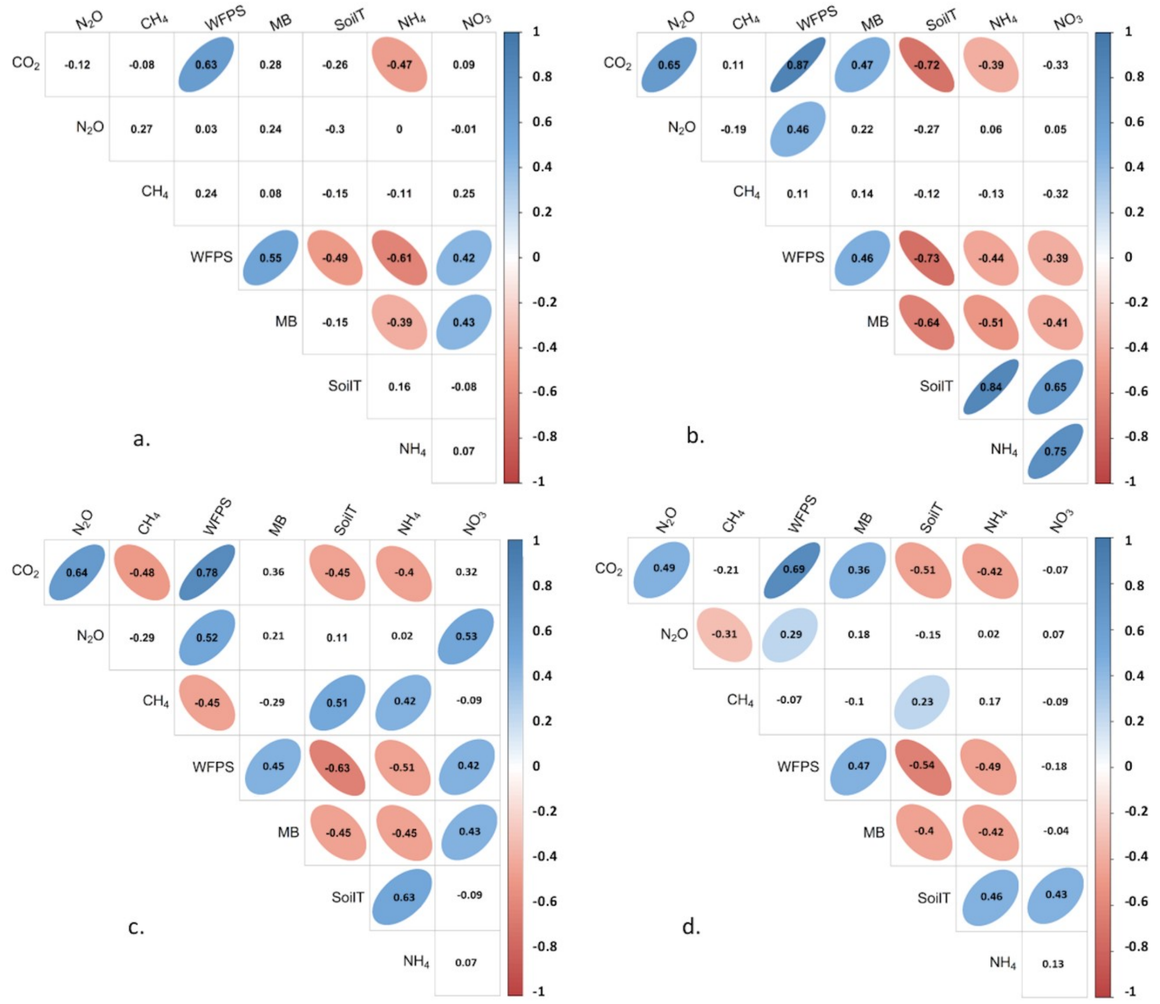

Figure 13. Pearson correlation coefficients for greenhouse gas fluxes and soil environmental conditions (a=abandoned pasture, b=early stage forest, c=intermediate stage forest, and d=all sites combined). Variable abbreviations are as follows: WFPS = water-filled pore space, Soil T = soil temperature, MB = microbial biomass, and NH_4 = soil ammonium concentration, and NO_3 = soil nitrate concentration. All variables were recorded and collected at 5 cm of soil depth. Only significant correlations ($p<0.05$) are shown in red or blue circles in the graph.

From the stepwise multiple regression to identify the best combinations of environmental factors that controlled soil GHG exchange, we found that for CO_2 fluxes, WFPS was the only predictor for single sites and for all data. N_2O fluxes were best explained by a combination of WFPS either with soil NH_4 concentration or with microbial biomass (Appendix 4). However, the regression was only significant at the forest sites or using the combined data for all sites. CH_4 fluxes were controlled mainly by WFPS and soil nitrate concentration; however, the regression was only significant at the intermediate stage forest and abandoned pasture site.

3.4 Seasonal variability of NDVI, NEE, and soil CO_2 emissions from automatic chamber measurements

Similar to the manual chamber measurements, CO_2 fluxes from the automated chambers in the intermediate stage forest also showed a strong "Birch Effect" after the first precipitation events in both 2017 and 2018. The large pulses of soil CO_2 emissions caused the NEE to become positive (i.e., turning the intermediate stage forest into a carbon source), which lasted 41 d in 2017 and 35 d in 2018 (Figure 14, 15). During this short period, soil CO_2 emissions measured with the automatic chambers in the footprint of the EC tower summed to 1427.9 kg C ha^{-1} and 1896.5 kg C ha^{-1} in 2017 and 2018, respectively. These numbers represented 21% and 22% of the annual soil CO_2 emissions, which were 6778.6 ± 797.8 kg C ha^{-1} y^{-1} and 8638.4 ± 1006.2 kg C ha^{-1} y^{-1} in 2017 and 2018, respectively. Overall, the magnitude of daily and annual CO_2 emissions of automatic and manual chambers (7419.65 ± 1214.8 kg C ha^{-1} y^{-1}) at the intermediate stage forest in 2018 compared well and were not statistically different, due to high spatial variability of fluxes (Figure 14, Table 5). During the transition period, leaves began to grow again, and as the NDVI became higher, NEE returned to negative values, switching the forest to a carbon sink (Figure 14). The soil CO_2 pulse emissions during the transition period offset 45% of annual NEE in 2017 (-2796.5 kg C ha^{-1} y^{-1}), but only 13% in 2018 as the NEE in 2018 was a stronger carbon sink (-3934.9 kg C ha^{-1} y^{-1}) (Figure 15).

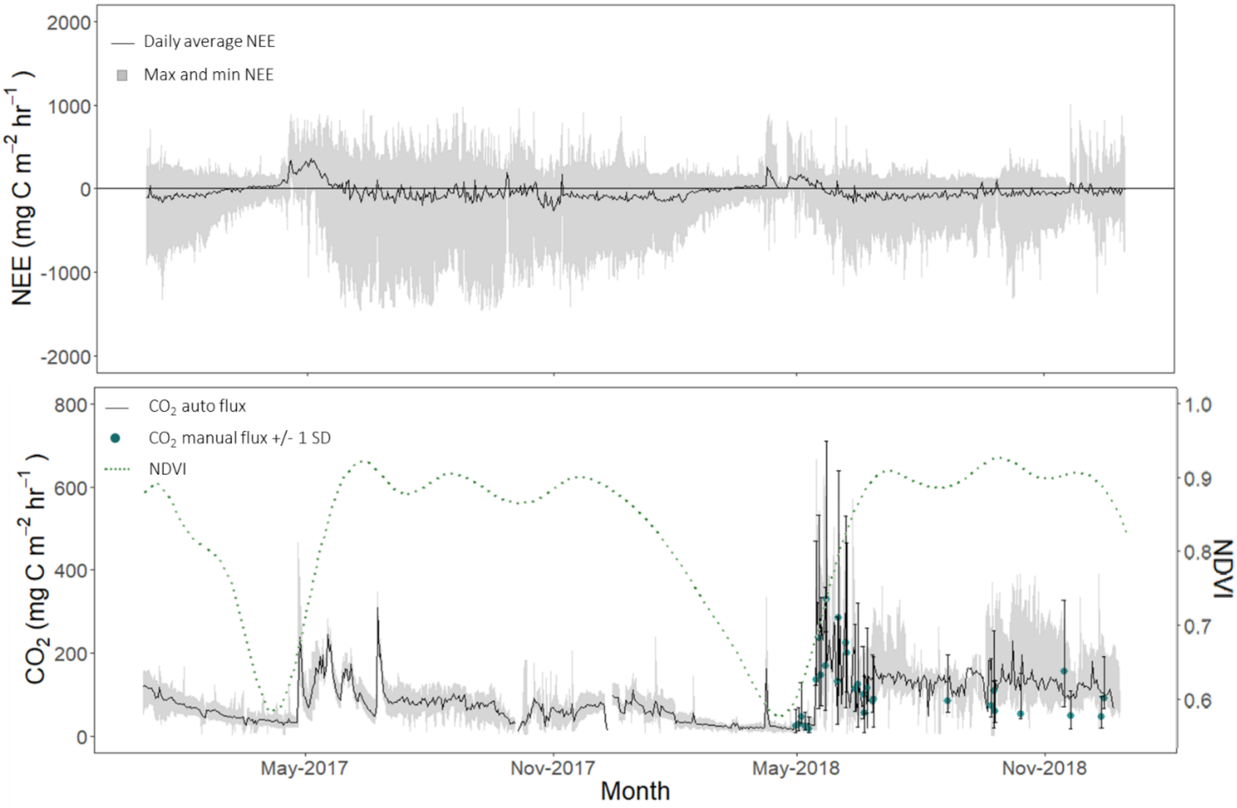

Figure 14. Time series of net ecosystem CO_2 exchange (NEE mg C $m^{-2}h^{-1}$) and MODIS NDVI and soil CO_2 fluxes (panel below) measured with automatic and manual chambers at the intermediate stage forest (CO_2 mg C m^{-2} h^{-1}) in 2017 and 2018 (grey area represents max and min values).

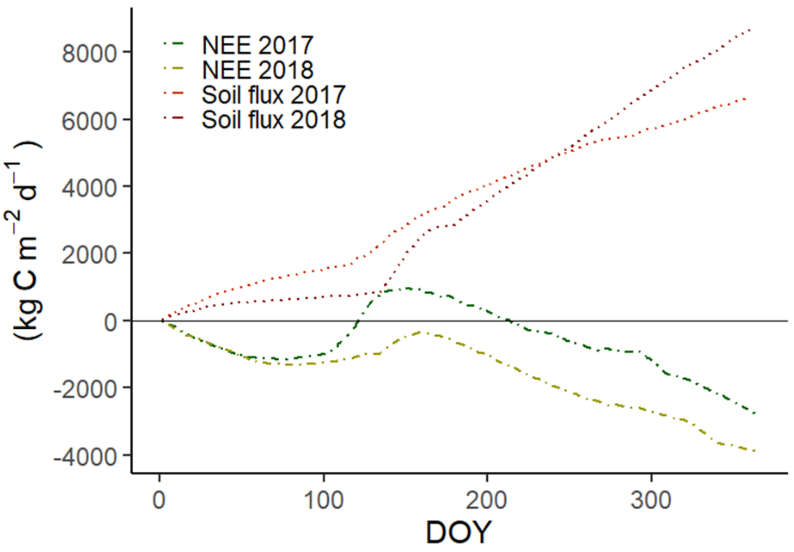

Figure 15. Time series with day of the year (DOY) and cumulative net ecosystem CO_2 exchange (NEE kg C m^{-2} d^{-1}), and cumulative soil CO_2 fluxes (CO_2 kg C m^{-2} d^{-1}) measured with automatic chambers at the intermediate stage forest in Santa Rosa National Park Costa Rica.

4. Discussion

4.1. GHG exchange of tropical dry forests and abandoned pastures

GHG exchange of TDF ecosystems depend on various factors, such as soil temperature, soil moisture, chemo-physical soil properties, and vegetation interactions, all of which control substrate availability (Raich and Schlesinger 1992; Schlesinger and Andrews 2000; Lebrija-Trejos et al. 2011) for ecosystem C and N turnover. According to our results, dynamics of soil GHG fluxes were linked strongly to soil water dynamics induced by the seasonality of precipitation and, thus, soil moisture that varied between <10% (dry season) to >60% WFPS in the peak of the wet season. Soil moisture affects microbial activity and decomposition processes in soils (Curiel Yuste et al. 2007), and it also determines the soil diffusivity and, therefore, the gas exchange with the atmosphere (Moldrup et al. 2003). At our sites, soil CO_2 and N_2O emissions, and CH_4 uptake markedly differed between seasons with overall lowest fluxes observed in the dry season induced by dry soil conditions that slowed microbial activity and, thus, slowed C and N turnover (Muhr et al. 2008). Soil temperature was not an important predictor for soil fluxes in TDF, which was related to the low seasonal variation in air temperature (Figure 10). Regarding different land-use types, soil GHG fluxes were higher in forest sites than in the abandoned pasture site, which can be explained by the difference in soil microclimatic conditions and substrate availability that was controlled by different soil and vegetation characteristics.

4.1.1 CO_2 fluxes

In our study, soils of the different land covers sampled were strong atmospheric sources of CO_2, in the transition from dry season to wet season after soil rewetting. Annual soil emissions of CO_2 in 2018 were higher for the early stage forest (8.6 t C ha^{-1} y^{-1}) followed by the intermediate stage forest (7.4 t C ha^{-1} y^{-1}) and the abandoned pasture (7.2 t C ha^{-1} y^{-1}). The lower CO_2 fluxes at the abandoned pasture site were related to differences in soil and vegetation characteristics as indicated by lower soil C and N concentrations and by lower leaf litter production compared with the forest sites as indicated by much lower stem number and basal area (Table 3). Aryal et al. (2017) also related higher soil respiration rates in Mexican mature forests and secondary forests (>35 y) compared with younger secondary forests (<20 y) to differences in substrate availability and microclimate conditions created by the vegetation. Root density at each site can also contribute to differences in soil respiration rates (Vargas et al. 2007).

According to our results, eddy covariance measurements at the intermediate stage showed that the net uptake of CO_2 is put on hold during the transition from dry season to rainy season, where large CO_2 emission pulses from the soil caused the forest to become a carbon source (Figure 14). This is related to the "Birch Effect" when there is limited decomposition during the dry season, but large quantities of accumulated soil organic matter are mobilized during rewetting events at the onset of the wet season (Campo and Vazquez-Yanes, 2004). This is consistent with Castro et al. (2018) and other studies from TDF (Perez-Ruiz et al. 2010; Waring et al. 2016) and forests in seasonally dry regions (Myklebust et al. 2008; Yepez et al. 2007; O'Connell et al. 2018). These studies report that at the onset of the wet season, NEE was characterized by a net CO_2 efflux from the ecosystem to the atmosphere that was induced by elevated soil respiration rates that lasted for several days before the ecosystem returning to a carbon sink caused by decreasing soil respiration; this process simultaneously increased gross primary productivity (Figure 14; Perez-Ruiz et al. 2010; Waring et al. 2016; Castro et al. 2018; O'Connell et al. 2018). Verduzco et al. (2015) also found significant temporal variations in NEE in a TDF in northwest Mexico, where the ecosystem was a net carbon source in years with low annual precipitation ($+1.02$ t C ha^{-1} y^{-1}), and a net carbon sink (-2.49 t C ha^{-1} y^{-1}) during years with higher annual precipitation.

Model simulations have shown that large changes in the soil water potential can lead to larger CO_2 pulse emissions and greater total losses of CO_2 in TDF. In their study, Waring et al. (2016) suggested that more severe droughts that resulted in very dry soils led to increasing ecosystem C losses through intensification of the "Birch effect" during rewetting events. Their simulations were based on a model that assumed first-order decay rates of soil organic matter and an enzyme-catalyzed soil C mineralization introduced by Allison et al. (2010), also showed that CO_2 losses were greater under larger but more sporadic precipitation events compared with smaller but more frequent ones. As predicted as a consequence of climate change, changes in rainfall patterns and intensification of droughts (Cai et al. 2014; Steinhoff et al. 2015; Wang et al. 2017) will likely reduce the C sink strength of TDF in the future.

4.1.2 N_2O fluxes

Our study reports slightly lower N_2O emissions for TDF (0.5 kg N ha^{-1} y^{-1}) and abandoned pastures (0.3 kg N ha^{-1} y^{-1}), as previously reported by studies in similar ecosystems (Appendix 5). Across our study sites, N_2O emissions from the forest (0.39-0.43 kg N ha^{-1} y^{-1}) were significantly higher than in the abandoned pasture (0.09 kg N ha^{-1} y^{-1}), which can be first explained by higher nitrogen availability maintained by much higher rates of litter production as indicated by much higher stem numbers and basal area in the forest stands (Table 3). Based on estimates for leaf N concentration as reported by Powers and Tiffin (2010) for TDF in Costa Rica, annual nitrogen input from litterfall in forest ecosystems can be up to 80 kg N ha^{-1} y^{-1}, which is much higher than at the burned pasture site. Furthermore, significantly lower soil nitrate concentration and lower soil nitrate to ammonium ratios at the abandoned pasture site (Figure 11) demonstrated lower N turnover by nitrification, which would result in much lower N_2O emissions from the abandoned pasture site (Neill et al. 1997).

The mechanisms for N_2O emissions are a tight linkage between nitrification and denitrification processes, which mainly depend on abundance of soil water. Thus, in our seasonally dry ecosystems, the highest N_2O emissions were observed at the transition from dry season to wet season (Figure 12). In a TDF in Mexico, Garcia-Mendez et al. (1991) also found a large but short-lived pulse of N_2O fluxes after a major rewetting event, which attained a maximum value of 120 $\mu g\ m^{-2}\ h^{-1}$: this value is in the same range as we observed at our study sites (Figure 12). Although N_2O fluxes in tropical forest soils are mostly driven by denitrification in the wet season (e.g., Breuer et al. 2000; Garcia-Montiel et al. 2001; Kiese et al. 2008b), the N_2O emission pulses after rewetting of dry soil are caused mainly by nitrification (Davidson et al. 1993). In the dry season, low water content limits the activity of soil microorganisms, which reduced the amount of N transformation in the ecosystem (Castaldi and Aragosa 2002). The primary controlling factor for nitrogen transformation and associated N_2O emissions were increasing pool sizes of organic and inorganic nitrogen during dry soil conditions, which are processed rapidly by soil microbes during rewetting events (Garcia-Mendez et al. 1991; Davidson 1993; Borken and Matzner 2009). Possible mechanisms mentioned in the literature include disruption of soil aggregates, which cause a release of new N and C substrates (Navarro-García et al. 2012) and the release of nitrogen-enriched microbial osmolytes (Wood et al. 2012). Conversely, after vegetation starts growing, as indicated by a sharp increase of NDVI (Figure 14), soil NH_4 and NO_3 concentration decrease (Figure 11), which might cause lower N_2O production and emissions during the wet season as also reported by Castaldi et al. (2006) for other tropical dry ecosystems.

Overall, a greater degree of soil drying before rewetting is associated with higher concentrations of microbial, soluble, and respiratory pools of C and accumulation of soil inorganic N (Williams and Xia 2009). Thus, as observed for CO_2 pulse emissions, Guo et al. (2014) found that drier soils triggered higher N_2O emissions at rewetting events. However, comparing importance of CO_2 and N_2O emissions during rewetting events and also for calculating annual budgets by use of global warming potentials reveal that the contribution of N_2O emissions to total GHG emissions to be of minor importance (<5%).

4.1.3 Soil CH_4 exchange

In our study, we found greatest uptake rates (-2.6 kg C $ha^{-1}y^{-1}$) in the intermediate stage forest and lower uptake rates in the early stage secondary forest (-0.58 kg C $ha^{-1}y^{-1}$) and abandoned pasture (-0.69 kg C ha^{-1} y^{-1}). Overall, these numbers were comparable with earlier studies conducted in tropical dry ecosystems as compiled in our literature review (Appendix 5). Lower uptake rates in the abandoned pasture can be explained by higher bulk density (Tab. 1) and higher water content (Tab. 2) that limited diffusion of atmospheric CH_4 into the soil (Kiese et al. 2008a). Differences in uptake rates between the two forest types remained unclear because physical and chemical soil properties, and soil temperature and moisture, were similar between the two forest types (Table 4, 5). As for N_2O and CO_2, seasonality of CH_4 uptake was driven by temporal dynamics of soil moisture, particularly in the intermediate stage forest (Figure 12). As observed in other studies (Fest et al. 2017; O'Connell et al. 2018), we also found sporadic CH_4 emissions after high rainfall events at the transition from dry season to wet season but only in the early stage forest and the abandoned pasture site. Due to the lowest Global Warming Potential of methane (GWP=25), CH_4 fluxes were of lowest (<1%) importance for the total GHG balance at both forest and abandoned pasture sites.

4.2 Soil GHG exchange of tropical ecosystems and global upscaling

There are few studies that report on simultaneous measurements of soil emissions of CO_2, N_2O, and CH_4 from TDF, although it represents 42% of all tropical forests (Miles et al. 2006). From the literature review, we found a total of 19 studies where one or more soil GHG fluxes were measured at tropical forest sites across the Americas (Figure 16). Seven studies were from TDF sites; however, none of the studies analyzed CO_2, N_2O, and CH_4 simultaneously, and most of them had limited datasets mainly due to very small number of campaigns across the year. Six studies of TDF measured N_2O, four measured CH_4, and only one measured soil CO_2 emissions.

Overall, our study and the literature review revealed that soil CO_2 and N_2O emissions, and CH_4 uptake rates, were lower in pastures compared with forests, but differences were more pronounced in wet tropical compared to dry tropical ecosystems (Figure 16, Appendix 5). TDF tend to be a stronger sink for atmospheric CH_4 than wetter tropical forests. Nonetheless, this trend was not statistically different (Appendix 5). On the other hand, annual N_2O and CO_2 emissions were higher in wet tropical forests. We found a significant positive correlation ($p<0.001$) between the annual fluxes of N_2O and mean annual precipitation for tropical sites (Figure 13). The correlation was stronger if only forest sites were included in the analysis. For methane and CO_2 fluxes, this relationship was not as clear. For CO_2 emissions, we found a better correlation with mean annual temperature by using only the forest sites (Figure 16). Mean annual temperature has been found in previous studies to be highly correlated with annual rates of soil respiration at global scales (Raich and Schlesinger 1992; Raich et al. 2002; Chen et al. 2014; Hursh et al. 2017). Although at local scales, such as our TDF study site, with little seasonality in temperature, temporal variability in soil respiration rates was controlled mainly by the seasonality of rainfall and soil moisture.

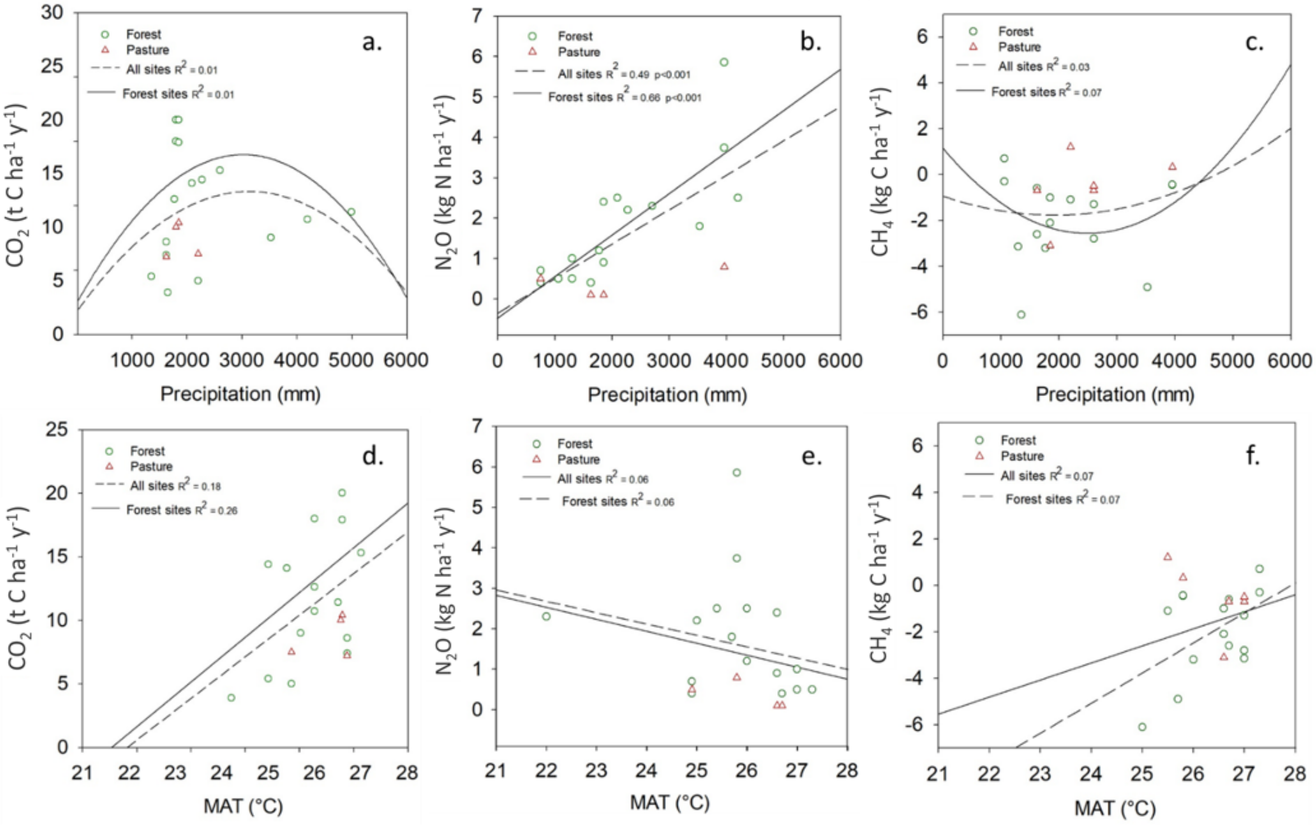

Figure 16. Relationships between annual precipitation and CO_2, N_2O, and CH_4 fluxes (a,b,c) and Mean Annual Temperature (MAT) and CO_2, N_2O, and CH_4 fluxes (d,e,f) derived from the literature review of studies measuring greenhouse gases in the American tropics at pastures or forest sites.

Castaldi et al. (2006) calculated for seasonally dry tropical forests an average annual emission rate of 1.53 kg N_2O-N ha^{-1} and a mean annual uptake rate of methane of -1.31 kg CH_4-C ha^{-1} y^{-1}. This resulted in a total annual global flux of 2.3 Tg N_2O-N per year and a total global methane sink of -1.96 Tg CH_4-C per year by using an area of 15.0 x 10^6 km^2 for tropical seasonally-dry ecosystems. Using the same area and mean values for TDF as reported in Appendix 5, our estimates of 0.75 Tg N_2O-N and -3.00 Tg CH_4-C resulted in a much lower global N_2O source strength but a larger soil CH_4 sink for TDF. Dalal and Allen (2008) estimated a global mean flux from tropical forests, which included seasonally dry and wet tropical forests for CH_4 of -2.9 kg C ha^{-1} y^{-1} and N_2O emissions of 3.03 kg N ha^{-1} y^{-1}. For tropical dry savannas, they determined a global average CH_4

uptake rate of -0.60 kg C ha^{-1} y^{-1} and N_2O emissions of 0.60 kg N ha^{-1} y^{-1}. The estimates for tropical dry savannas were more comparable with numbers of N_2O and CH_4 fluxes of our study (Table 5) and values for TDF that resulted from our literature review (Appendix 5). This indicated that TDF in the case of Dalal and Allen (2008) would be better represented by dry savannas than integrated into a general tropical forest class. Overall, the still low number of measurements and the different quality and classification criteria applied in upscaling procedures demonstrate the need for harmonization of data and criteria used to differentiate GHG source and sink strength of tropical wet forests, dry forests, and savanna ecosystems.

5. Conclusions

Overall, our observations suggested that TDF soils were important sources (CO_2, N_2O) and sinks (CH_4) of GHGs, but emissions were significantly lower and more seasonal than in tropical wet forest ecosystems. We found a strong control due to precipitation events and, thus, soil water content control of soil GHG fluxes. Other soil environmental variables were less important, such as temperature, microbial biomass, and inorganic N concentration. Particularly, pulse emissions of CO_2 and N_2O at the transition from dry season to wet season significantly influenced the respective annual emission budget, particularly in the forest sites. However, contributions to total ecosystem GHG budgets were dominated mainly by soil CO_2 emissions (>95%). For the intermediate stage forest, elevated CO_2 emissions during the transition from dry season to wet season significantly offset annual net ecosystem exchange, and a predicted increase in the frequency and duration of drought events could potentially reduce the ecosystem carbon sink strength of tropical dry forests and pastures with ongoing climate change.

6. Acknowledgments

This work was supported by The Rufford Foundation, The Helmholtz Research School MICMoR (*Mechanisms and Interactions of Climate Change in Mountain Regions*), The U.S. National Science Foundation (Grant GEO 0452325), The Natural Science and Engineering Research Council of Canada, and the TROPI-DRY project (Human, Biophysical Dimension on Tropical Dry Forest), which is a collaborative research network funded by the Inter American Institute for Global Change Research (IAI) Collaborative Research Network Program (CRN3-025).

7. Literature Cited

Allen, K., Dupuy, J. M., Gei, M. G., Hulshof, C., Medvigy, D., Pizano, C., et al. (2017). Will seasonally dry tropical forests be sensitive or resistant to future changes in rainfall regimes?. *Environmental Research Letters*, *12*(2), 023001.

Allison, S., Wallenstein, M., and Bradford, M. (2010). Soil-carbon response to warming dependent on microbial physiology. *Nature Geosciences. 3,* 336-40.

Aryal, D. R., Hendricus, B., Jong, J. De, Mendoza-Vega, J., Ochoa-Gaona, S., & Esparza-Olguín, L. (2017). Soil Organic Carbon Stocks and Soil Respiration in Tropical Secondary Forests in Southern Mexico. Global Soil Security, 153–165. https://doi.org/10.1007/978-3-319-43394-3.

Aubinet, M., Grelle, A., Ibrom, A., Rannik, Ü., Moncrieff, J., Foken, T., Kowalski, A.S., Martin, P.H., Berbigier, P., Bernhofer, C. et al. (1999). Estimates of the annual net carbon and water exchange of forests: The EUROFLUX methodology. In *Advances in Ecological Research*; Academic Press: Cambridge, MA, USA, Volume 30, pp. 113–175.

Baldocchi, D.D., Hincks, B.B., Meyers, T.P. (1988). Measuring biosphere-atmosphere exchanges of biologically related gases with micrometeorological methods. *Ecology*, *69*, 1331–1340.

Becknell, J. M., Kucek, L. K., & Powers, J. S. (2012). Aboveground biomass in mature and secondary seasonally dry tropical forests: A literature review and global synthesis. *Forest Ecology and Management*, *276*, 88-95.

Borken, W., & Matzner, E. (2009). Reappraisal of drying and wetting effects on C and N mineralization and fluxes in soils. *Global Change Biology*, *15*(4), 808-824.

Breuer, L., Papen, H., & Butterbach-Bahl, K. (2000). N_2O emission from tropical forest soils of Australia. *Journal of Geophysical Research Atmospheres*, *105*(D21), 26353–26367. https://doi.org/10.1029/2000JD900424

Butterbach-Bahl, K., Kock, M., Willibald, G., Hewett, B., Buhagiar, S., Papen, H., Kiese, R. (2004). Temporal variations of fluxes of NO, NO_2, N_2O, CO_2, and CH_4 in a tropical rain forest ecosystem. *Global Biogeochemical Cycles*, 18, doi:10.1029/2004GB002243

Cai, W., Borlace, S., Lengaigne, M., Van Rensch, P., Collins, M., Vecchi, G., et al. (2014). Increasing frequency of extreme El Niño events due to greenhouse warming. *Nature Climate Change. 4*(2): 111-116.

Campo, J., & Vázquez-Yanes, C. (2004). Effects of nutrient limitation on aboveground carbon dynamics during tropical dry forest regeneration in Yucatán, Mexico. *Ecosystems*, *7*(3), 311-319.

Castaldi, S., & Aragosa, D. (2002). Factors influencing nitrification and denitrification variability in a natural and fire-disturbed Mediterranean shrubland. *Biology and Fertility of Soils*, *36*(6), 418–425. https://doi.org/10.1007/s00374-002-0549-2

Castaldi, S., Ermice, A., & Strumia, S. (2006). Fluxes of N_2O and CH_4 from soils of savannas and seasonally dry ecosystems. *Journal of Biogeography*, *33*(3), 401–415. https://doi.org/10.1111/j.1365-2699.2005.01447.x

Castro, S. M., Sanchez-Azofeifa, G. A., & Sato, H. (2018). Effect of drought on productivity in a Costa Rican tropical dry forest. *Environ. Res. Lett*, *13*. Retrieved from https://doi.org/10.1088/1748-9326/aaacbc

Chadwick, R., Good, P., Martin, G., & Rowell, D. P. (2016). Large rainfall changes consistently projected over substantial areas of tropical land. *Nature Climate Change*, *6*(2), 177.

Chen, S., Zou, J., Hu, Z., Chen, H., & Lu, Y. (2014). Global annual soil respiration in relation to climate, soil properties and vegetation characteristics: Summary of available data. *Agricultural and Forest Meteorology*, *198*, 335-346.

Clark, D. A. (2004). Sources or sinks? The responses of tropical forests to current and future climate and atmospheric composition. *Philosophical Transactions of the Royal Society B: Biological Sciences*, *359*(1443), 477–491. https://doi.org/10.1098/rstb.2003.1426

Curiel Yuste, J., Baldocchi, D. D., Gershenson, A., Goldstein, A., Misson, L., & Wong, S. (2007). Microbial soil respiration and its dependency on carbon inputs, soil temperature and moisture. *Global Change Biology*, *13*(9), 2018–2035. https://doi.org/10.1111/j.1365-2486.2007.01415.x

Dalal, R. C., & Allen, D. E. (2008). Greenhouse gas fluxes from natural ecosystems. *Australian Journal of Botany*, *56*(5), 369. https://doi.org/10.1071/bt07128

Davidson, E. A., Matson, P. A., Vitousek, P. M, et al. (1993). Processes regulating soil emissions of NO and N_2O in a seasonally dry tropical forest. *Ecology*, 74(1): 130–139.

Davidson, E. A., Nepstad, D. C., Ishida, F. Y., & Brando, P. M. (2008). Effects of an experimental drought and recovery on soil emissions of carbon dioxide, methane, nitrous oxide, and nitric oxide in a moist tropical forest. *Global Change Biology*, *14*(11), 2582-2590.

Didan, K. (2015). MOD13Q1 MODIS/Terra, MYD13Q1 MODIS/Aqua Vegetation Indices 16-Day L3 Global 250m SIN Grid V006. NASA EOSDIS Land Processes DAAC. https://doi.org/10.5067/MODIS/MYD13Q1.006

Enquist, B. J., & Leffler, A. J. (2001). Long-term tree ring chronologies from sympatric tropical dry-forest trees: individualistic responses to climatic variation. *Journal of Tropical Ecology*, *17*(1), 41-60.

Farrick, K. K., & Branfireun, B. A. (2013). Left high and dry: a call to action for increased hydrological research in tropical dry forests. *Hydrological Processes*, *27*(22), 3254-3262.

Fest, B. J., Hinko-Najera, N., Wardlaw, T., Griffith, D. W., Livesley, S. J., & Arndt, S. K. (2017). Soil methane oxidation in both dry and wet temperate eucalypt forests shows a near-identical relationship with soil air-filled porosity. *Biogeosciences,* 14, 467-479. https://doi:10.5194/bg-14-467-2017

Garcia-Montiel, D. C., Steudler, P. A., Piccolo, M. C., Melillo, J. M., Neill, C., & Cerri, C. C. (2001). Controls on soil nitrogen oxygen emissions from forest and pastures in the Brazilian Amazon. *Global Biogeochemical Cycles*, *15*(4), 1021–1030. https://doi.org/10.1029/2000GB001349

Guo, X., Drury, C. F., Yang, X., Daniel Reynolds, W., & Fan, R. (2014). The Extent of Soil Drying and Rewetting Affects Nitrous Oxide Emissions, Denitrification, and Nitrogen Mineralization. *Soil Science Society of America Journal*, *78*(1), 194. https://doi.org/10.2136/sssaj2013.06.0219

Gütlein, A., Gerschlauer, F., Kikoti, I., & Kiese, R. (2018). Impacts of climate and land use on N_2O and CH_4 fluxes from tropical ecosystems in the Mt. Kilimanjaro region, Tanzania. *Global Change Biology*, *24*(3), 1239–1255. https://doi.org/10.1111/gcb.13944

Hofer, S. (2003). QuikChem Method 12-107-06-2-A. Determination of ammonia (Salicylate) in 2M KCl soil extracts by Flow Injection Analysis. Lachat Instruments. Colorado, USA. 10p.

Holdridge, L. R., & Tosi, J. A. (1967). *Life zone ecology*. San José, CR: Centro Científico Tropical.

Hursh, A., Ballantyne, A., Cooper, L., Maneta, M., Kimball, J., & Watts, J. (2017). The sensitivity of soil respiration to soil temperature, moisture, and carbon supply at the global scale. *Global change biology*, *23*(5), 2090-2103.

Imbach, P., Molina, L., Locatelli, B., Roupsard, O., Mahé, G., Neilson, R., et al. (2012). Modeling potential equilibrium states of vegetation and terrestrial water cycle of Mesoamerica under climate change scenarios. *Journal of Hydrometeorology*, *13*(2), 665-680.

IPCC (2014). Climate Change 2014: Synthesis Report. Contribution of Working Groups I, II and III to the Fifth Assessment Report of the Intergovernmental Panel on Climate Change, 2–26. Cambridge University Press, Cambridge, United Kingdom and New York, NY, USA. https://doi.org/10.1017/CBO9781107415324.

Janzen, D. H., Hallwachs, W., & Kappelle, M. (2016). Biodiversity conservation history and future in Costa Rica: The case of Área de Conservación Guanacaste (ACG). *Costa Rican Ecosystems. The University of Chicago Press, Chicago and London*, 290-341.

Jaramillo, V. J., Martinez-Yrizar, A., & Sanford, R. L. (2011). Primary productivity and biogeochemistry of seasonally dry tropical forests. In *Seasonally dry tropical forests* (pp. 109-128). Island Press, Washington, DC.

Kalacska, M., Sanchez-Azofeifa, G. A., Calvo-Alvarado, J. C., Quesada, M., Rivard, B., & Janzen, D. H. (2004). Species composition, similarity and diversity in three successional stages of a seasonally dry tropical forest. *Forest ecology and management*, *200*(1-3), 227-247.

Kiese, R., Hewett, B., Butterbach-Bahl, K. (2008b). Seasonal dynamic of gross nitrification and N_2O emission at two tropical rainforest sites in Queensland, Australia. *Plant and Soil*, 309, 211-226.

Kiese, R., Wochele, S., Butterbach-Bahl, K. (2008a). Site specific and regional estimates of methane uptake by tropical rainforest soils of north-eastern Australia. *Plant and Soil*, 309, 105-117.

Knepel, K. (2012). QuikChem Method 12-107-04-1-B. Determination of nitrate in 2M KCl soil extracts by Flow Injection Analysis. Lachat Instruments. Loveland, USA. 11p.

Lebrija-Trejos, E., Pérez-García, E. A., Meave, J. A., Poorter, L., & Bongers, F. (2011). Environmental changes during secondary succession in a tropical dry forest in Mexico. *Journal of Tropical Ecology*, *27*(5), 477–489. https://doi.org/10.1017/s0266467411000253

Leiva, J. A., Rocha, O. J., Mata, R., & Gutiérrez-Soto, M. V. (2009). Cronología de la regeneración del bosque tropical seco en Santa Rosa, Guanacaste, Costa Rica: II. La vegetación en relación con el suelo. *Revista de Biología Tropical*, *57*(3), 817-836.

Linares-Palomino, R., Oliveira-Filho, A. T., & Pennington, R. T. (2011). Neotropical seasonally dry forests: diversity, endemism, and biogeography of woody plants. In *Seasonally dry tropical forests* (pp. 3-21). Island Press, Washington, DC.

Lugo, P. M. A., Medina, E., Money, H. A., Murphy, P. G., & Bullock, S. H. (2005). Dry forests of Central America and the Caribbean. *Seasonally dry tropical forests*, 9-34.

Miles, L., Newton, A., DeFries, R., Ravilious, C., May, I., Blyth, S., Kapos, V., Gordon J. (2006). A global overview of the conservation status of Tropical Dry Forests. *Journal of Biogeography*. 33, 491-505.

Moldrup, P., Olesen, T., Komatsu, T., Yoshikawa, S., Schjønning, P., & Rolston, D. E. (2003). Modeling diffusion and reaction in soils: X. A unifying model for solute and gas diffusivity in unsaturated soil. *Soil Science*, *168*(5), 321–337. https://doi.org/10.1097/00010694-200305000-00002

Muhr, J., Goldberg, S. D., Borken, W., & Gebauer, G. (2008). Repeated drying-rewetting cycles and their effects on the emission of CO_2, N_2O, NO, and CH_4 in a forest soil. *Journal of Plant Nutrition and Soil Science*, *171*(5), 719–728. https://doi.org/10.1002/jpln.200700302

Myklebust, M. C., Hipps, L. E., & Ryel, R. J. (2008). Comparison of eddy covariance, chamber, and gradient methods of measuring soil CO2 efflux in an annual semi-arid grass, Bromus tectorum. *Agricultural and forest meteorology*, *148*(11), 1894-1907.

Navarro-García, F., Casermeiro, M. Á., & Schimel, J. P. (2012). When structure means conservation: Effect of aggregate structure in controlling microbial responses to rewetting events. *Soil Biology and Biochemistry*, *44*(1), 1–8. https://doi.org/10.1016/j.soilbio.2011.09.019

Neill, C., Piccolo, M.C., Cerri, C.C., Steudler, P.A., Melillo, J.M., Brito, M. (1997). Net nitrogen mineralization and net nitrification rates in soils following deforestation for pasture across the southwestern Brazilian Amazon Basin landscape. *Oecologia*, 110, 243 - 252

O'Connell, C. S., Ruan, L., & Silver, W. L. (2018). Drought drives rapid shifts in tropical rainforest soil biogeochemistry and greenhouse gas emissions. *Nature Communications*, *9*(1). https://doi.org/10.1038/s41467-018-03352-3

ORNL DAAC. (2018). MODIS and VIIRS Land Products Global Subsetting and Visualization Tool. ORNL DAAC, Oak Ridge, Tennessee, USA. Accessed October 24, 2019. Subset obtained for MOD13Q1/MYD13Q1 product at 10.8427N,85.6165W, time period: 2016-10-23 to 2019-09-22, and subset size: 0.25 x 0.25 km. https://doi.org/10.3334/ORNLDAAC/1379

Perez-Ruiz, E. R., Garatuza-Payan, J., Watts, C. J., Rodriguez, J. C., Yepez, E. A., & Scott, R. L. (2010). Carbon dioxide and water vapour exchange in a tropical dry forest as influenced by the North American Monsoon System (NAMS). *Journal of Arid Environments*, *74*(5), 556–563. https://doi.org/10.1016/j.jaridenv.2009.09.029

Portillo-Quintero, C. A., & Sanchez-Azofeifa, G. A. (2010). Extent and conservation of tropical dry forests in the Americas. *Biological conservation*, *143*(1), 144-155.

Portillo-Quintero, C., Sanchez-Azofeifa, A., Calvo-Alvarado, J., Quesada, M., & do Espirito Santo, M. M. (2015). The role of tropical dry forests for biodiversity, carbon and water conservation in the neotropics: lessons learned and opportunities for its sustainable management. *Regional Environmental Change*, *15*(6), 1039-1049.

Powers, J.S., Tiffin, P. (2010). Plant functional type classifications in tropical dry forests in Costa Rica: leaf habit versus taxonomic approaches. *Functional Ecology*, 24, 927–936.

Raich, J. W., Potter, C. S., & Bhagawati, D. (2002). Interannual variability in global soil respiration, 1980–94. *Global Change Biology*, *8*(8), 800-812.

Raich, J. W., Schlesinger, W. H. (1992). The global carbon dioxide flux in soil respiration and its relationship to vegetation and climate. Tellus B. 44(2), 81-99.

Sanchez-Azofeifa, G.A., Calvo-Alvarado, J.C., Espírito-Santo, M.M.Do., Fernandes, G.W., Powers, J., Quesada, M. (2014). Tropical Dry Forests in the Americas: The Tropi-Dry Endeavor. In: Tropical Dry Forests in the Americas: Ecology, Conservation, and Management. CRC Press, Boca Raton. pp 1-16

Sanchez-Azofeifa, G.A., Castro, K. L., Rivard, B., Kalacska, M. R. (2005). Research priorities for neotropical dry forests. *Biotropica*. 37, 477-485.

Schimel, J., Balser, T. C., & Wallenstein, M. (2007). Microbial stress-response physiology and its implications for ecosystem function. *Ecology*, *88*(6), 1386-1394.

Singh, J. S., Singh, S., Raghubanshi, A. S., Singh, S., Kashyap, A. K., & Reddy, V. S. (1997). Effect of soil nitrogen, carbon and moisture on methane uptake by dry tropical forest soils. *Plant and Soil*, *196*(1), 115–121. https://doi.org/10.1023/A:1004233208325

Sitch, S., Huntingford, C., Gedney, N., Levy, P. E., Lomas, M., Piao, S. L., et al. (2008). Evaluation of the terrestrial carbon cycle, future plant geography and climate-carbon cycle feedbacks using five Dynamic Global Vegetation Models (DGVMs). *Global Change Biology*, *14*(9), 2015-2039.

Steinhoff, D. F., Monaghan, A. J., and Clark, M. P. (2015). Projected impact of twenty-first century ENSO changes on rainfall over Central America and northwest South America from CMIP5 AOGCMs. *Climate Dynamics* 44(5-6): 1329-1349.

van Haren, J. L. M., Handley, L. L., Biel, K. Y., Kudeyarov, V. N., McLain, J. E. T., Martens, D. A., & Colodner, D. C. (2005). Drought-induced nitrous oxide flux dynamics in an enclosed tropical forest. *Global Change Biology*, *11*(8), 1247–1257. https://doi.org/10.1111/j.1365-2486.2005.00987.x

Vance, E. D., Brookes, P. C., & Jenkinson, D. S. (1987). An extraction method for measuring soil microbial biomass C. *Soil biology and Biochemistry*, 19 (6), 703-707.

Veldkamp, E., Keller, M. & Nunez, M. (1998) Effects of pasture management on N2O and NO emissions from soils in the humid tropics of Costa Rica. *Global Biogeochemical Cycles*, 12, 71–79.

Verduzco, V. S., Garatuza-Payán, J., Yépez, E. A., Watts, C. J., Rodríguez, J. C., Robles-Morua, A., & Vivoni, E. R. (2015). Variations of net ecosystem production due to seasonal precipitation differences in a tropical dry forest of northwest Mexico. *Journal of Geophysical Research: Biogeosciences*, *120*(10), 2081–2094. https://doi.org/10.1002/2015JG003119

Wang, G., Cai, W., Gan, B., Wu, L., Santoso, A., Lin, X., Chen, Z., and McPhaden, M. J. (2017). Continued increase of extreme El Niño frequency long after 1.5 C warming stabilization. *Nature Climate Change* 7(8): 568-572.

Waring, B. G., & Powers, J. S. (2016). Unraveling the mechanisms underlying pulse dynamics of soil respiration in tropical dry forests. *Environmental Research Letters*, *11*(10). https://doi.org/10.1088/1748-9326/11/10/105005

Welch, B., Gauci, V., & Sayer, E. J. (2019). Tree stem bases are sources of CH_4 and N_2O in a tropical forest on upland soil during the dry to wet season transition. *Global Change Biology*, *25*(1), 361–372. https://doi.org/10.1111/gcb.14498

Williams, M. A., & Xia, K. (2009). Characterization of the water soluble soil organic pool following the rewetting of dry soil in a drought-prone tallgrass prairie. *Soil Biology and Biochemistry*, *41*(1), 21–28. https://doi.org/10.1016/j.soilbio.2008.08.013

Vargas, R., & Allen, M. F. (2008). Environmental controls and the influence of vegetation type, fine roots and rhizomorphs on diel and seasonal variation in soil respiration. *New Phytologist*, *179*(2), 460-471.

Wood, T. E., & Silver, W. L. (2012). Strong spatial variability in trace gas dynamics following experimental drought in a humid tropical forest. *Global Biogeochemical Cycles*, *26*(3), 1–12. https://doi.org/10.1029/2010GB004014

Xu, L., Baldocchi, D. D., Tang, J. (2004). How soil moisture, rain pulses, and growth alter the response of ecosystem respiration to temperature. *Global Biogeochemical Cycles, 18*(4), 1-10.

Yepez, E. A., Scott, R. L., Cable, W. L., & Williams, D. G. (2007). Intraseasonal variation in water and carbon dioxide flux components in a semiarid riparian woodland. *Ecosystems*, *10*(7), 1100–1115. https://doi.org/10.1007/s10021-007-9079-y

Zhang, K., Zhu, Q., Liu, J., Wang, M., Zhou, X., Li, M., et al. (2019). Spatial and temporal variations of N_2O emissions from global forest and grassland ecosystems. *Agricultural and Forest Meteorology*, *266*, 129-139.

Chapter four - Spatio-temporal variability and uncertainties of greenhouse gas emissions in a pre-alpine Bavarian grassland

Abstract

Model applications generally use average site inputs for soil and vegetation, most often originating from a limited number of samples, thus limiting the representation of the spatial variability of soil characteristics and environmental conditions. We used a combination of manual and automatic soil chambers to measure the CO_2 and N_2O gas exchanges from soils at different locations in a Bavarian grassland. Measurements were compared to simulated gas emission of CO_2 and N_2O using the biogeochemical model LandscapeDNDC. The correlation between the modeled results using the specific soil input at each chamber location and the measured emissions at each location was significant but poor for CO_2 ($r=0.2$, $p<0.001$, $RMSE=19.97$). When we used the modeled results using the averaged parameters from all locations, and the averaged measured emissions from all measured chambers, the relationship for CO_2 improved ($r=0.5$, $p<0.01$, $RMSE=12.58$). For N_2O, we did not find a significant correlation between modeled and measured fluxes. For the environmental controls we found a good agreement for daily means of soil temperature and moisture at 5 cm depth between modeled and measured values derived from a soil wireless sensor network.

Keywords: soil greenhouse gases, carbon dioxide, nitrous oxide, LandscapeDNDC.

1. Introduction

Predicting the response of soil carbon and emissions of greenhouse gases (GHG) to changes in global temperature is critical, particularly since the increased release of soil carbon dioxide (CO_2) and nitrous oxide (N_2O) to the atmosphere can exacerbate global warming (IPCC, 2007). Agricultural croplands are a significant source of anthropogenic GHG emissions (Schulze et al. 2009). However, uncertainties in estimates of annual GHG from farmlands are still high (Schulze et al. 2009). Thus, there is still a high need to monitor and evaluate the scale and spatial uncertainties of emissions of GHG from farmlands and incorporate these results in the development of management practices that can help minimize these emissions.

Emission factors generated from chamber-based measurements of GHG fluxes from land-use categories are typically based on relatively few measurements in time and space, propagating errors and uncertainty into the total national accounts (He et al. 2016). Some practical constraints for the chamber-based measurements are the limited number of chambers (or collars) that can be deployed on the study area, the limited number of gas samples that can be collected and analyzed or the limited number of chambers that can be multiplexed together in automatic systems (He et al. 2016). Furthermore, the IPCC (2006) "Guidelines for National Greenhouse Gas Inventories" advise consideration of the impact of specific conditions (e.g., management practice and crop type) when estimating direct emissions from croplands. A sufficient spatial and temporal resolution is also essential since some GHG emissions are characterized by short emission pulses with a high spatial variation. This creates a need for data from long-time monitoring studies (Zacharias et al. 2011). The up-scaling of short-term measurements or measurements with an insufficient frequency can lead to a severe over or underestimation of annual emissions (Flessa et al. 2002; Wolf et al. 2010; Barton et al. 2015). Chamber-based measurements from soils at local scales (less than 1 km^2) are compulsory in the Kyoto accord reporting, especially in agriculture (IPCC, 2006).

Soil GHG emissions can also be estimated using numerical biogeochemical models such as the DNDC (de-nitrification de-composition model, Li et al. 1992a; Li et al. 1992b), LandscapeDNDC (Haas et al. 2013; Butterbach-Bahl et al. 2019), DayCent (Parton et al. 1998) and APSIM (Agricultural Production Systems Simulator, Keating et al. 2003). These models are developed by fitting equations to multiple field and laboratory data and require input parameters to represent soil and vegetation characteristics, agricultural management, and meteorological conditions to drive the model as predictive variables. However, biogeochemical models cannot alone substitute for monitoring biophysical conditions and soil GHG exchange of agricultural systems since their applicability is still governed by the availability of measurements for calibration and validation. Comparisons between simulation results and observations are necessary to evaluate the model capacity to represent and predict biogeochemical processes under various conditions (Haas et al. 2013).

Model applications generally use for simulations average site conditions of soil and vegetation, with a limited number of samples and do hardly account for the spatial variability of soil characteristics and environmental changes (Zacharias et al. 2011). For these reasons, modeling must be coupled with biophysical properties and GHG data collection. According to Oertel et al. (2016) review on GHG from soils, more experimental and monitoring data are needed with an area-representative distribution, for a better validation of numerical models. Understanding the uncertainty at spatial scales in the predictive outputs of the model is also critical to develop strategies to minimize the emissions of biogenic GHG. Mitigation of GHG emissions can be done on field-scale by adapting agricultural management practices (e.g., timing of fertilization; Adegbeye et al. 2019). More importantly, there needs to be an understanding of the spatial variability of soil properties regulating nutrient and water supply for crop growth. This information can be used by farmers (e.g., by precision farming) to adapt fertilization rates on smaller scales and increase nutrient use efficiency (Adegbeye et al. 2019).

As such the main objectives of this study were (i) comparing measured soil gas emission of CO_2 and N_2O in a high spatial resolution against simulated emissions and assessing the capability of LandscapeDNDC to resolve spatial patterns of soil GHG emissions and (ii) testing the representativeness of the “average” modeling approach by comparing simulated soil emissions with an average site parameterization against the averaged simulation derived from multiple spatially explicit simulations. This approach will help in the quantification of the model uncertainties in order to extrapolate from fine to coarse scales and quantify the errors that accompany extrapolations across scales.

2. Materials and methods

2.1 Study site

The study was conducted at the grassland site Fendt located in the TERENO (Terrestrial Environmental Observatories; Zacharias et al. 2011; Bogena et al. 2015) Pre-Alpine Observatory in S-Germany (Kiese et al. 2018). The grassland is located at the head of a small tributary stream to the Rott River at an elevation of 595 m.a.s.l (47° 49' N, 11° 03' E). The site’s mean annual temperature is 8.6 °C, and the mean annual precipitation is 959 mm, as measured from an on-site weather station since 2011. The soil type, according to the US Soil Taxonomy, is Cambic Stagnosol (Kiese et al. 2018).

The land use of the area is dominated by grassland, with some small patches of cropland. The grasslands are mainly used for forage production for dairy cattle (mean harvest is about 11 tons DM ha^{-1} y^{-1}) and are managed intensively with up to 6 cuts and 5 manure applications per year (Kiese et al. 2018). The most abundant and dominant species of grasses and herbs are *Arrhenatherum elatius*, *Festuca rubra*, *Lolium perenne, Plantago lanceolate, Prunella vulgaris, Ranunculus repens, Taraxacum officinalis* and the clover *Trifolium repens* (Fu et al. 2019).

2.2 Measuring design

For the data sampling of environmental parameters, we used the deployed wireless sensor network equipped with soil moisture and temperature sensors throughout the grassland in order to assess moisture and temperature dynamics. The sensors were placed at three different depths in the soil (5, 20, and 50 cm) in each node. The network has 20 nodes spaced in a 70- by 70-m regular grid (figure 17). Measurements were performed in a temporal resolution of 15 min using two electromagnetic soil water content sensors (SMT100, Truebner GmbH) that were installed horizontally into the soil (~5–10 cm from each other). Both sensors also record soil temperature (Kiese et al. 2018).

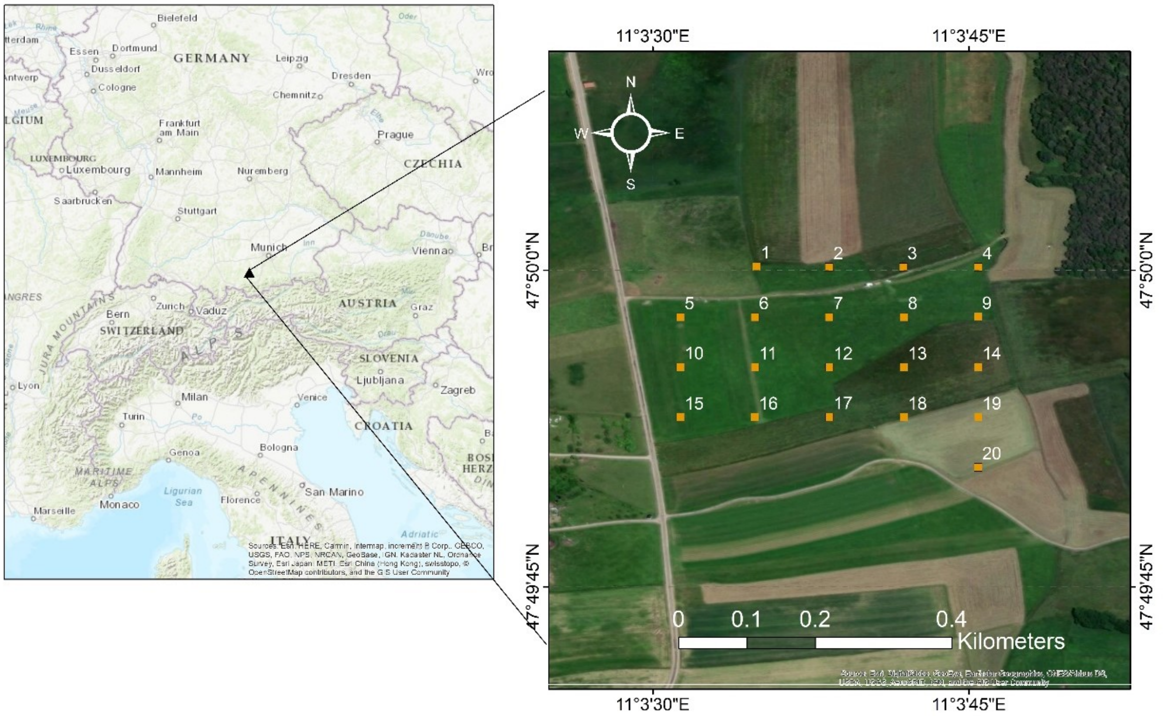

Figure 17. On the left, location of the grassland site Fendt in the TERENO Pre-Alpine Observatory, S-Germany. On the right, mapped points represent the positions of nodes in the soil wireless sensor network.

For physico-chemical characterization, soil samples were collected at the depths of each of the soil sensors (Figure 17) at installation in 2015. From these samples, bulk density, pH, soil texture, and total carbon and nitrogen content (Table 6, Appendix 6) were measured.

Table 6. Physico-chemical properties found at 5, 20, and 50 cm of depth. Values are means ± SD of replicated measurements (n=20).

Depth	Bulk density	Clay	Silt	Sand	Organic C	Total N	pH
cm	g cm^{-3}	----------------------------------	----------------------------------	%	----------------------------------	----------------------------------	
5	1.1±0.2	51.3±12.3	41.7±5.0	7.0±8.7	7.4±1.9	0.8±0.2	5.9±1.0
20	1.3±0.3	56.7±15.3	37.7±7.1	5.6±9.4	2.7±1.3	0.3±0.1	5.6±0.6

50	1.0±0.6	51.0±19.5	40.1±10.8	8.9±14.7	6.1±7.6	0.4±0.4	5.3±0.4

2.4 Measurements of soil CO_2 and N_2O exchange

Manual chambers (n=16) consisting of dark PVC were used to measure the CO_2 and N_2O gas exchanges in the regular grid of the wireless sensor network (figure 17). PVC frames 35 by 25 cm (collars) were inserted into the soil (10cm depth) approximately one month before the first measurement and remained in place throughout the experimental period. For the measurements, 12cm high PVC chambers, equipped with fans, vents, and sampling ports, were affixed to the frame by metal clamps, and a rubber seal between the frame and chamber assures an air-tight seal. For individual chamber measurements, a 60 ml gas sample was taken from the chamber headspace with a gas-tight syringe through a stopcock valve at 10 min intervals (0, 10, 20, 30, and 40 min after chamber closure). The 60 ml gas samples were immediately used to flash (40 ml) 10 ml sealed glass vials, which were over pressurized (10ml) by the remaining sample volume (20ml). The samples were transported the same day to KIT, IMK-IFU (Garmisch-Partenkirchen, Germany) for analysis using an autosampler (SRI Instruments, Bad Honnef, Germany, N=200) coupled to a gas chromatograph (8610 C; SRI Instruments, Torrence, USA) equipped with an electron capture detector (ECD) and a flame ionization detector/ methanizer (FID) for direct N_2O and indirect CO_2 concentration analysis, respectively. Samples were continuously calibrated with vials (4 out of 16) filled with standard gas (Air Liquide, Düsseldorf, Germany). Flux rates of CO_2 and N_2O were calculated from the linear change in gas concentrations in the chamber headspace with time. Single flux rates were corrected for chamber headspace temperature and barometric pressure. Quality checks were applied, and single chamber-based CO_2 flux measurements were discarded if the R^2 of the linear regression of CO_2 fluxes was <0.88, indicating a systematic measuring error (<10% of fluxes). Fluxes of N_2O were either set to zero with respective $R^2 < 0.6$ or if fluxes were lower than the mean detection limits (<18% for N_2O), which were 0.68 µg N_2O-N m^{-2} hr^{-1} (Gütlein et al. 2017).

The experiment was conducted from 1st of June to 30 of July in 2016 and repeated using the same approach from the 1st of June to 30 of July in 2017. Measurements were taken between 8 am and 10 am to represent the best daily average conditions of temperature. Because of the large number of chambers, sample collection was divided into two cycles, taking about two hours to collect gas samples for all chambers. Measurements on the site from 5 automatic chambers complement the manual chamber dataset for 2016. The automatic chambers have a base area of 40 cm x 40 cm and are fitted with a top that can be automatically opened and closed using pneumatic actuators. Chambers were adapted using aluminum foil to be dark chambers and placed on the field on metal bases inserted into the ground. Chambers were installed in the field from June to July of 2016. Gas samples were taken at a rate of 200 ml min^{-1}. Air samples were analyzed in the field using a gas chromatograph equipped with an electron capture detector for the detection of N_2O and flame ionization detector for CO_2. This automated measuring system has been previously described in detail (e.g., Papen and Butterbach-Bahl 1999; Rosenkranz et al. 2006; Remy et al. 2017).

2.5 LandscapeLDNDC

LandscapeDNDC combines the soil biogeochemical processes of the agricultural DNDC (Li et al. 1992) and the Forest-DNDC (Li et al. 2000; Stange et al. 2000; Kesik et al. 2005) into a general soil biogeochemistry module. LandscapeDNDC simulates ecosystem C and N turnover, changes in soil C and N stocks, and associated losses for various land use types and periods of land-use change (Haas et al. 2013; Butterbach-Bahl et al. 2019). The model combines plant growth, micrometeorology, water cycling, microbial C, and N cycling and exchange processes with the atmosphere and hydrosphere of terrestrial ecosystems (Molina et al. 2016). The main feature of LandscapeDNDC is its capability to concurrently and synchronously simulate multiple grid cells (multiple sites) in a regional simulation (Butterbach-Bahl et al. 2019).

Soil data collected from the site were used to initialize the model. These data included soil properties, such as soil texture, bulk density, porosity, pH, field capacity, saturated hydraulic conductivity, and soil carbon and nitrogen content (Appendix 6). Soil data were collected at three depths at the Fendt site thus, the model was initialized down to 100 cm. Daily weather data required by the model, including minimum and maximum temperature, precipitation, wind speed, solar radiation, and relative humidity, were available from the on-site weather station. Management data, including tillage and fertilizer scheduling and application rates, were obtained from direct cooperation with the local farmer. Data required for the LDNDC model of maximum and minimum water content in the soil at each location was derived from the soil wireless sensor network. To stabilize the carbon and nitrogen dynamics, the model was initialized by simulating for five years using the soil, crop and management data available for the site.

2.6 Statistical analyses

Daily mean N_2O and CO_2 fluxes were calculated from sub-daily measurements of five replicated automatic chambers and compared to the N_2O and CO_2 flux measurements from the manual chambers conducted once per day. To test how daily fluxes compared between automatic chambers and manual chambers, we used Pearson correlation analyses.

The effect of uncertainty on the model inputs on predicted CO_2 and N_2O emissions was quantified in this study first by running the model using the average of each parameter at all locations and then running the model for each of the 20 locations individually, i.e., single and specific initializations of soil characteristics for each of the 20 sampling locations using the corresponding measured soil parameters. We then compared results of modeled emissions of CO_2 and N_2O and modeled soil temperature and soil moisture against measured variables at each location using Pearson correlation and Root Mean Square Error (RMSE), which is the standard deviation of the residuals or prediction errors (if the correlation coefficient approx. 1 then the RMSE should approx. 0 and therefore there are no errors). All analyses and graphs were carried using the R-software (R Development Core Team 2012).

3. Results

3.1 Soil CO_2 and N_2O fluxes

Mean hourly N_2O and CO_2 fluxes measured in 2016 (June-July) from five automatic chambers at the grassland site Fendt showed variations across the day. While CO_2 emissions varied across the day with a peak of maximum emissions close to noon (10-3 pm) and minimum emissions over the night time, N_2O emissions showed no diurnal patterns (Figure 18).

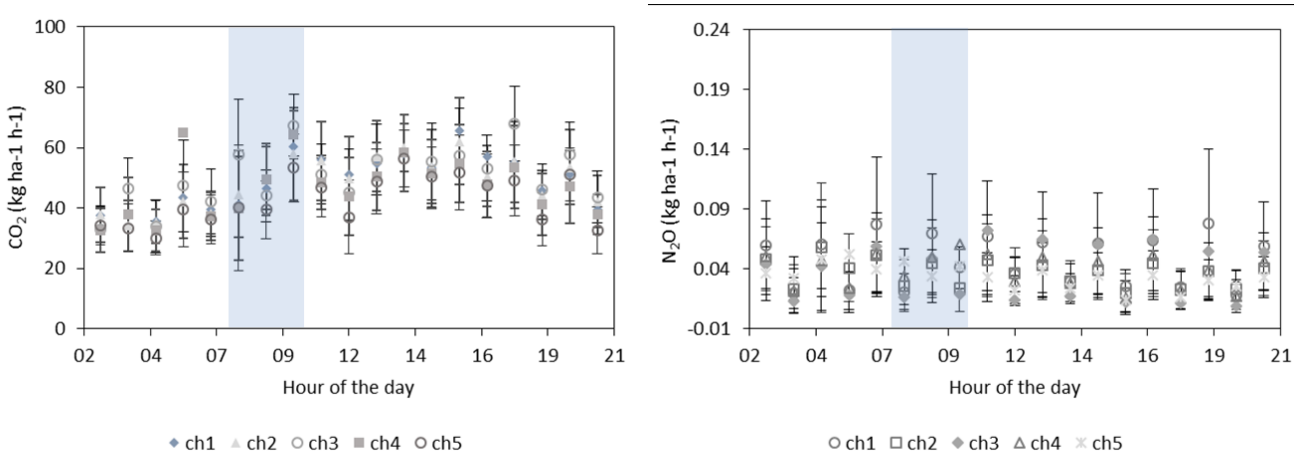

Figure 18. Mean hourly CO_2 and N_2O fluxes measured at the grassland site Fendt in 2016 (June-July) using automatic chambers (5 replicates: ch1, ch2, ch3, ch4, ch5). The blue area represents the time when data was collected with the manual chambers.

In order to test how daily fluxes calculated from sub-daily measurements of automatic chambers compared to fluxes from single measurements of manual chambers, we analyzed the correlation between datasets (Figure 19). For CO_2 measurements, we found a significant correlation (R = 0.87, p<0.001); however, for the N_2O fluxes, we did not found a significant correlation.

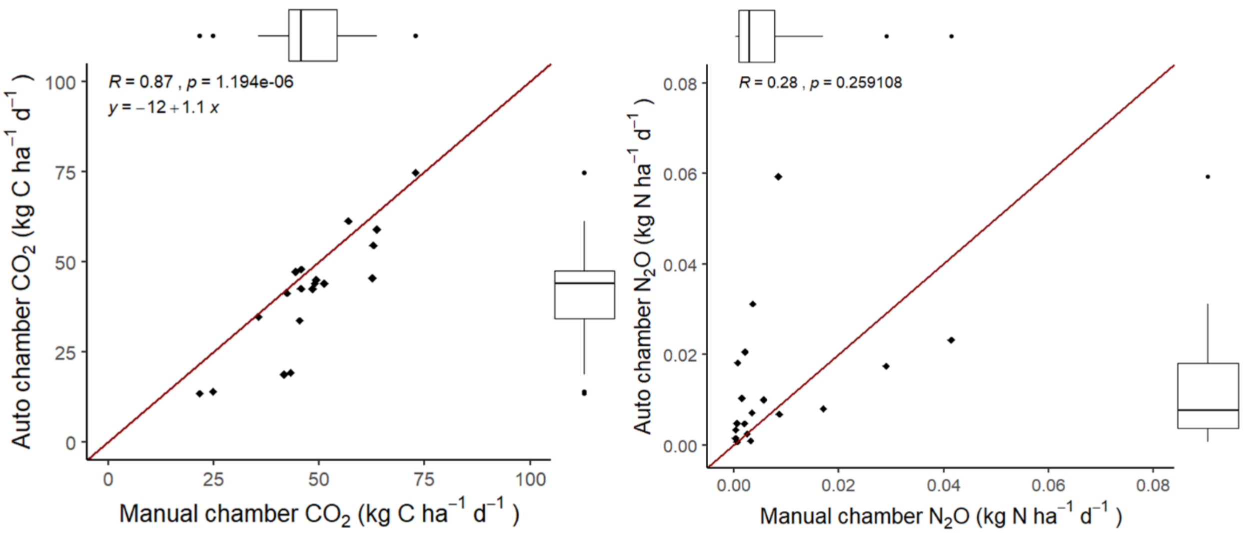

Figure 19. Pearson correlation and marginal boxplots between measured CO_2 and N_2O fluxes using manual chambers (n=16) and automatic chambers (n=5) at the grassland site Fendt in 2016 (June-July).

3.2 LandscapeDNDC simulations of CO_2 and N_2O fluxes

CO_2 fluxes in the year 2016 and 2017 measured using both manual chambers and automatic chambers, and modeled with LandscapeDNDC all showed a strong seasonality and similar patterns at all measured locations (Figure 20). High emissions for CO_2 were observed in the summer when measurements with automatic and manual chambers were carried on the site. However, measurements of N_2O fluxes using manual chambers, automatic chambers and modeled results showed some agreements (Figure 20). Higher values in the model were observed in the spring and winter and mainly induced by fertilization events and freezing and thawing cycles.

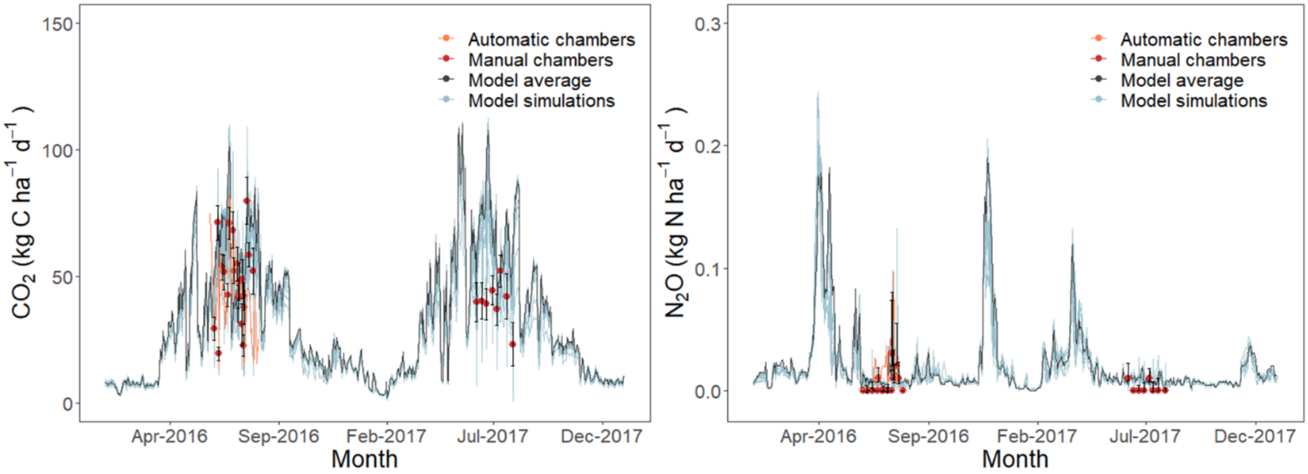

Figure 20. Time series of the daily average of CO_2 and N_2O fluxes measured using the automatic chambers (n=5), manual chambers (n=16) and modeled emissions at the grassland site Fendt in 2016 and 2017.

We compared the LandscapeDNDC model results using site against field measurements of CO_2 and N_2O fluxes collected across the grassland (Figure 21). Only a significant correlation was obtained between the LandscapeDNDC from the average of all site simulations for CO_2 fluxes and the average of the CO_2 measured fluxes ($R = 0.66$, $p<0.05$). No significant correlation was found for N_2O fluxes.

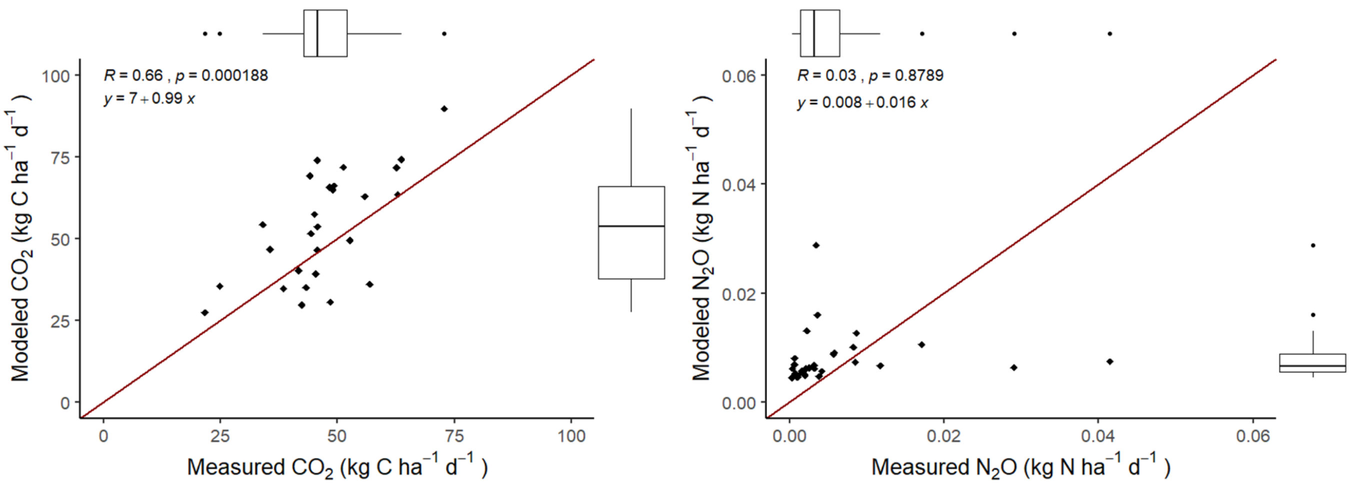

Figure 21. Pearson correlation between average measured CO_2 and N_2O fluxes using manual chambers (n=16) and modeled fluxes (n=16) at the grassland site Fendt in 2016 (June-July).

Moreover, for CO_2, the correlation between the LandscapeDNDC results using the specific soil input at each chamber location and the measured emissions at each location was significant for CO_2 (Table 7; R = 0.2, $p<0.05$). When we used the LandscapeDNDC results using the averaged parameters from all locations, and the averaged measured emissions from all measured chambers, the relationship improves for CO_2 (R = 0.42, $p<0.05$).

Table 7. Performance Statistics of correlations using daily CO_2 fluxes from manual chambers (n=16) and simulations from LandscapeDNDC (n=16) at the grassland site Fendt in 2016 (June-July).

Performance Statistics	**p-value**	**R**	**RMSE**
Measured CO_2 vrs modeled CO_2	<0.05	0.2	18.97
Measured average CO_2 vrs average modeled CO_2	<0.05	0.66	8.28
Measured average CO_2 vrs simulation with averaged parameters	<0.05	0.42	9.97

3.3 LandscapeLDNDC simulations of environmental controls of CO_2 and N_2O exchange

We found generally strong agreement for daily means of the soil temperature at 5 cm depth between modeled and measured datasets (Figure 22). The model accurately captured the seasonal patterns of soil temperature except in the winter season, where the modeled temperatures decreased below zero, but the data derived from the soil network does not. For soil moisture, the results showed some discrepancies between the simulated and measured results (Figure 22). The model failed to simulate some of the drying and rewetting events that we observed from the data derived from the wireless sensor network.

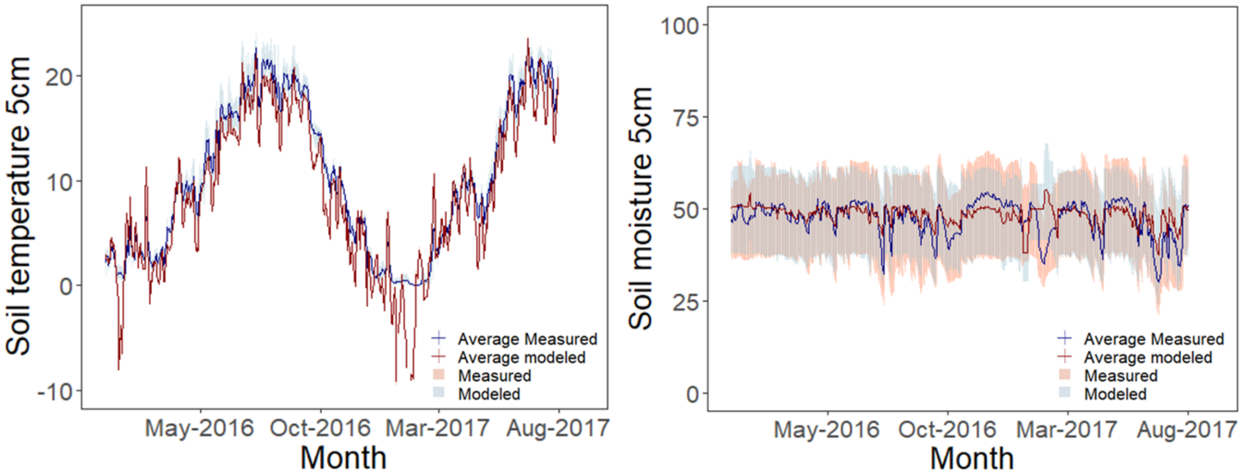

Figure 22. Time series of the daily average of soil temperature and moisture measured at 5cm depth at 20 positions and modeled for the same positions in the grassland site Fendt in 2016 and 2017. Colored areas in the graph represent max and min values for each variable.

For soil temperature, a significant correlation ($p < 0.001$) was obtained between daily modeled and measured values (RMSE = 2.07 and R = 0.97; Figure 23). A significant correlation ($p < 0.001$) was also obtained between daily modeled and measured soil moisture (RMSE = 5.10 and R = 0.81; Figure 23). Density plots of daily values of soil moisture and soil temperature showed a good agreement between modeled and on site measurements (Figure 23).

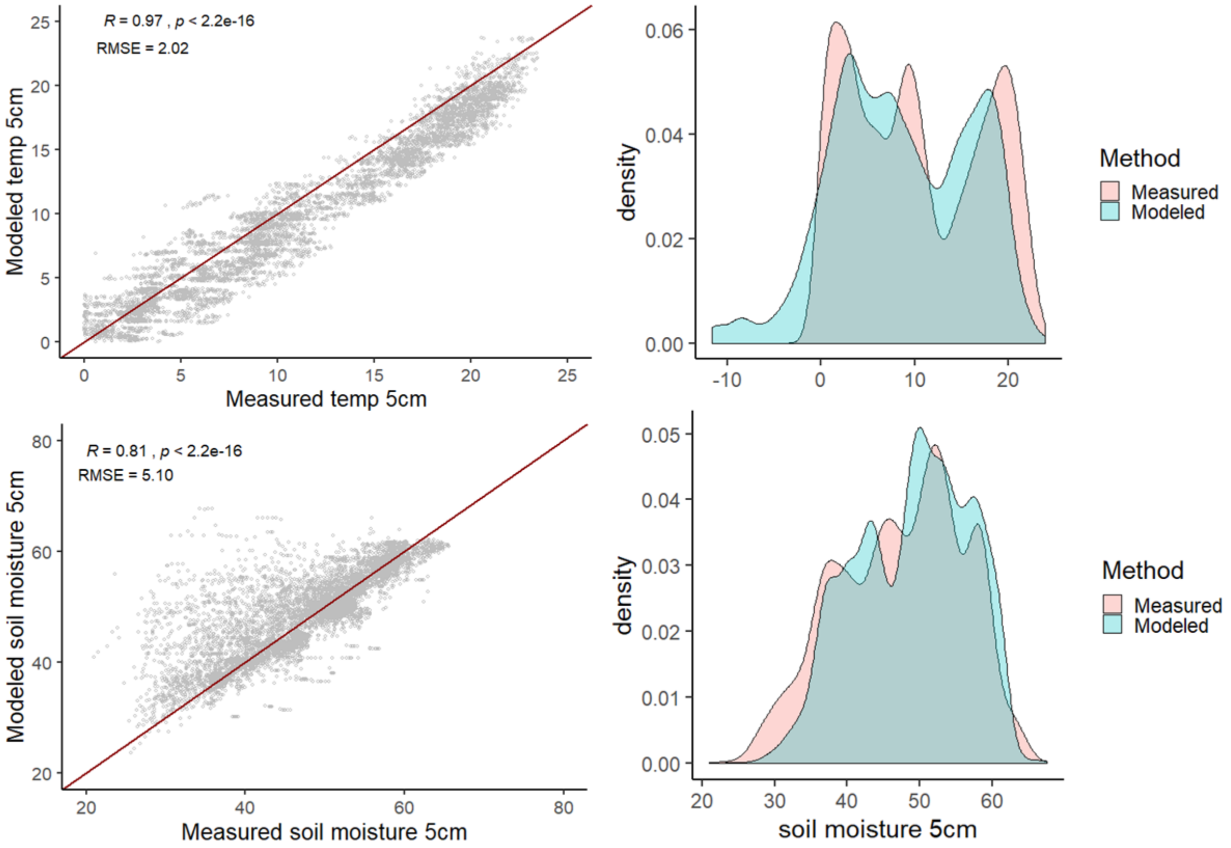

Figure 23. Pearson correlation and density plots between measured soil temperature and moisture (n=20) and modeled soil temperature and moisture (n=20) at 5cm depth in the grassland site Fendt in 2016 (June-July).

4. Discussion

For the CO_2 emissions, the LandscapeDNDC model was able to simulate the daily average across locations of CO_2 fluxes. The resulting simulations were comparable to fluxes derived from manual chamber measurements. However, at refined spatial scales, the model had more difficulties simulating the observed emissions for each individual soil profile. At local scales, the results from the model improve when we used the average of all the simulations for the site than by using the resulting simulation from averaged parameters to initialize the model. This could be explained by the field heterogeneity of the soil parameters used, which increases the variance of model results (Appendix 6). Discrepancies between modeled and measured results could also arise from inconsistencies or systematic errors in the input data of the model or biological processes that the model fails to fully characterize at refined scales (Leip et al. 2011).

For N_2O emissions, we found significant differences between measured emissions using automatic and manual chambers in the field, and also between measured and modeled fluxes. Simulating and predicting N_2O fluxes is challenging, given a large number of factors involved. N_2O emissions from soils are mainly produced through microbial-mediated nitrification and denitrification processes and are controlled by numerous environmental factors, such as concentrations of mineral N, availability of dissolvable organic carbon, redox potential, and temperature (e.g., Robertson and Groffman, 2007; Butterbach-Bahl et al. 2013). The temporal and spatial variability of these controlling factors results in enormous heterogeneity in N_2O fluxes (e.g., Bouwman et al. 2002; Groffman et al. 2009), making it more difficult to model and predict N_2O emissions at local scales.

For the environmental controls of CO_2 and N_2O, such as soil moisture and temperature, the model was able to simulate the seasonal patterns. Soil moisture and temperature are important environmental controls regulating the microbial production, consumption, and emissions of N_2O (Ruser et al. 2006). The discrepancies between measured N_2O using manual chambers and modeled emissions could also be linked to some disagreements in the rewetting events of the soil moisture in the model simulations if compared to the measured values of soil moisture derived from the wireless sensor network at the grassland. Another study that compared the DNDC, LandscapeDNDC and IAP-N-GAS biogeochemical models found that simulations of N_2O emissions by the three models agreed well with annual observations, but not with daily observations because all three models underestimated the daily average of soil moisture (Zhang et al. 2015). Inaccurate soil moisture simulations can result in the under-prediction of large N_2O peaks (Zhang et al. 2015).

Moreover, N_2O emissions are strongly affected by field management practices (fertilization, yield) influencing N_2O production and consumption. Since agricultural practices may change from farm to farm and may vary at different years, the LandscapeDNDC model setup is based on statistics at the district level (Haas et al. 2013). The disagreement observed between modeled and measured fluxes in our study could also be influenced by a discrepancy between the timing of the actual management activities in the grassland (e.g., fertilization events) and the management activities established in the model set up.

5. Conclusions

Testing and validating models under diverse conditions is required in order to ensure the uncertainty of a model for making large-scale estimates. In this study, the LandscapeDNDC model was tested for estimating CO_2 and N_2O emissions from a grassland. The model was able to simulate the seasonal and daily trends of the measured CO_2 fluxes. For N_2O emissions, we found significant differences between measured emissions and modeled emissions. For the environmental controls of CO_2 and N_2O, soil moisture and temperature, the model was able to simulate the seasonal patterns. Discrepancies between modeled and measured fluxes could arise from inconsistencies or systematic errors in the input data of the model or biological processes that the model fails to characterize at local scales. Although process-based models have been used for extensive scale simulations, more improvement is still required to enhance their performance, especially to assess the spatial variability of greenhouse gas emissions at local scales and the validity of upscaling model estimates to larger regions.

6. Acknowledgments

This work was supported by The Helmholtz Research School MICMoR (*Mechanisms and Interactions of Climate Change in Mountain Regions*).

7. Literature Cited

Adegbeye, M. J., Reddy, P. R. K., Obaisi, A. I., Elghandour, M. M. M. Y., Oyebamiji, K. J., Salem, A. Z. M., ... & Camacho-Díaz, L. M. (2019). Sustainable agriculture options for production, nutritional mitigation of greenhouse gasses and pollution, and nutrient recycling in emerging and transitional nations- An overview. *Journal of Cleaner Production*, 118319.

Barton L., Wolf B., Rowlings D., Scheer C., Kiese R., Grace P., Stefanova K., Butterbach-Bahl K. (2015). Sampling frequency affects estimates of annual nitrous oxide fluxes. Scientific Reports 5, DOI: 10.1038/srep15912.

Bogena, H. R., Bol, R., Borchard, N., Brüggemann, N., Diekkrüger, B., Drüe, C., ... & Missong, A. (2015). A terrestrial observatory approach to the integrated investigation of the effects of deforestation on water, energy, and matter fluxes. *Science China Earth Sciences*, *58*(1), 61-75.

Bouwman, A. F., Boumans, L. J. M., & Batjes, N. H. (2002). Modeling global annual N2O and NO emissions from fertilized fields. *Global Biogeochemical Cycles*, *16*(4), 28-1.

Butterbach-Bahl, K., Baggs, E. M., Dannenmann, M., Kiese, R., & Zechmeister-Boltenstern, S. (2013). Nitrous oxide emissions from soils: how well do we understand the processes and their controls?. *Philosophical Transactions of the Royal Society B: Biological Sciences*, *368*(1621), 20130122.

Butterbach-Bahl, K., Denk, T., Grote, R., Haas, E., Havermann, F., Petersen, C. W., Kiese, R., Klatt, S., Kraus, D., Molina Herrera, S., Petersen, K., Werner, C., & Wolf, B. (2019). LandscapeDNDC v1. 30.0. https://ldndc.imk-ifu.kit.edu/products/ldndc-usersguide.pdf

Flessa, H., Ruser, R., Schilling, R., Loftfield, N., Munch, J.C., Kaiser, E.A., Beese, F. (2002). N_2O and CH4 fluxes in potato fields: Automated measurement, management effects and temporal variation. *Geoderma*, 105, 307-325.

Fu, J., Gasche, R., Wang, N., Lu, H., Butterbach-Bahl, K., & Kiese, R. (2019). Dissolved organic carbon leaching from montane grasslands under contrasting climate, soil and management conditions. *Biogeochemistry*, *145*(1-2), 47-61.

Groffman, P. M., Butterbach-Bahl, K., Fulweiler, R. W., Gold, A. J., Morse, J. L., Stander, E. K., ... & Vidon, P. (2009). Challenges to incorporating spatially and temporally explicit phenomena (hotspots and hot moments) in denitrification models. *Biogeochemistry*, *93*(1-2), 49-77.

Gütlein, A., Gerschlauer, F., Kikoti, I., & Kiese, R. (2018). Impacts of climate and land use on N_2O and CH_4 fluxes from tropical ecosystems in the Mt. Kilimanjaro region, Tanzania. *Global Change Biology*, *24*(3), 1239–1255. https://doi.org/10.1111/gcb.13944

Haas, E., Klatt, S., Fröhlich, A., Kraft, P., Werner, C., Kiese, R., et al. (2013). LandscapeDNDC: a process model for simulation of biosphere–atmosphere–hydrosphere exchange processes at site and regional scale. *Landscape ecology*, 28(4), 615-636.

He, Y., Gibbons, J., & Rayment, M. (2016). A two-stage sampling strategy improves chamber-based estimates of greenhouse gas fluxes. *Agricultural and Forest Meteorology*, 228, 52-59.

IPCC (2006). Intergovernmental Panel on Climate Change 2007: guidelines for national greenhouse gas inventories. Vol. 4. Agriculture, forestry and other land use. Institute for Global Environmental Strategies, Hayama, Japan.

IPCC (2007). Intergovernmental Panel on Climate Change 2007: Synthesis Report. IPCC Publication, http://www.ipcc.ch/pdf/assessment-report/ar4/syr/ar4_syr.pdf (accessed 10 Dec. 2019).

Keating, B. A., Carberry, P. S., Hammer, G. L., Probert, M. E., Robertson, M. J., Holzworth, D., ... & McLean, G. (2003). An overview of APSIM, a model designed for farming systems simulation. *European journal of agronomy*, *18*(3-4), 267-288.

Kesik, M., Ambus, P., Baritz, R., Bruggemann, NB., Butterbach- Bahl, K., Damm, M., Duyzer, J., Horvath, L., Kiese, R., Kitzler, B., Leip, A., Li, C., Pihlatie, M., Pilegaard, K., Seufert, G., Simpson, D., Skiba, U., Smiatek, G., Vesala, T., Zechmeister- Boltenstern, S. (2005). Inventories of N_2O and NO emissions from European forest soils. *Biogeosciences*, 2, 353-375.

Kiese, R., Fersch B., Baessler C., Brosy C., Butterbach-Bahl K., Chwala C., Dannenmann M., Fu J., Gasche R., Grote R., Jahn C., Klatt J., Kunstmann H., Mauder M., Rödiger T., Smiatek G., Soltani M., Steinbrecher R., Völksch I., Werhahn J., Wolf B., Zeeman M., Schmid H.P. (2018). The TERENO-preAlpine Observatory: integrating meteorological, hydrological and biogeochemical measurements and modelling. *Vadose Zone Journal*. 10.2136/vzj2018.03.0060.

Leip, A., Busto, M., Corazza, M., Bergamaschi, P., Koeble, R., Dechow, R., ... & De Vries, W. (2011). Estimation of N2O fluxes at the regional scale: data, models, challenges. *Current Opinion in Environmental Sustainability*, *3*(5), 328-338.

Li, C. (2000). Modeling trace gas emissions from agricultural ecosystems. *Nutrient Cycling Agro ecosystems*, 58, 259-276.

Li, C., Frolking, S., & Frolking, T. A. (1992a). A model of nitrous oxide evolution from soil driven by rainfall events: 1. Model structure and sensitivity. *Journal of Geophysical Research: Atmospheres*, *97*(D9), 9759-9776.

Li, C., Frolking, S., & Frolking, T. A. (1992b). A model of nitrous oxide evolution from soil driven by rainfall events: 2. Model applications. *Journal of Geophysical Research: Atmospheres*, *97*(D9), 9777-9783.

Molina-Herrera, S., Haas, E., Klatt, S., Kraus, D., Augustin, J., Magliulo, V., ... & Skiba, U. (2016). A modeling study on mitigation of N2O emissions and NO3 leaching at different agricultural sites across Europe using LandscapeDNDC. *Science of the Total Environment*, *553*, 128-140.

Oertel, C., Matschullat, J., Zurba, K., Zimmermann, F., Erasmi, S. (2016). Greenhouse gas emissions from soils - A review. *Chemie der Erde*. 76, 327–352.

Papen, H., & Butterbach-Bahl, K. (1999). A 3-year continuous record of nitrogen trace gas fluxes from untreated and limed soil of a N-saturated spruce and beech forest ecosystem in Germany: 1. N_2O emissions. *Journal of Geophysical Research: Atmospheres*, *104*(D15), 18487-18503.

Parton, W. J., Hartman, M., Ojima, D., & Schimel, D. (1998). DAYCENT and its land surface submodel: description and testing. *Global and planetary Change*, *19*(1-4), 35-48.

Remy, E., Gasche, R., Kiese, R., Wuyts, K., Verheyen, K., & Boeckx, P. (2017). Edge effects on N2O, NO and CH4 fluxes in two temperate forests. *Science of the Total Environment*, *575*, 1150-1155.

Robertson, G. P., & Groffman, P. M. (2007). Nitrogen transformations. In *Soil microbiology, ecology and biochemistry* (pp. 341-364). Academic Press.

Rosenkranz, P., Brüggemann, N., Papen, H., Xu, Z., Seufert, G., & Butterbach-Bahl, K. (2006). N 2 O, NO and CH 4 exchange, and microbial N turnover over a Mediterranean pine forest soil.

Ruser, R., Flessa, H., Russow, R., Schmidt, G., Buegger, F., & Munch, J. C. (2006). Emission of N2O, N2 and CO2 from soil fertilized with nitrate: effect of compaction, soil moisture and rewetting. *Soil Biology and Biochemistry*, *38*(2), 263-274.

Schulze, E.D., Luyssaert, S., Ciais, P., Freibauer, A., Janssens, I.A., Soussana, J.F., et al. (2009). Importance of methane and nitrous oxide for Europe's terrestrial greenhouse-gas balance. *Nature Geoscience*, 2, 842-850.

Stange, F., Butterbach-Bahl, K., Papen, H., Zechmeister-Boltenstern, S., Li, C., Aber, J. (2000). A process-oriented model of N2O and NO emissions from forest soils 2. Sensitivity analysis and validation. *Journal of Geophysical Research-Atmospheres,* 105, 4385-4398

Wolf, B., Chwala, C., Fersch, B., Garvelmann, J., Junkermann, W., Zeeman, M. J., ... & Brugger, P. (2017). The scalex campaign: Scale-crossing land surface and boundary layer processes in the tereno-prealpine observatory. *Bulletin of the American Meteorological Society*, *98*(6), 1217-1234.

Wolf, B., Zheng, X.H., Brueggemann, N., Chen, W.W., Dannenmann, M., Han, X.G., Sutton, M.A., Wu, H.H., Yao, Z.S., Butterbach-Bahl, K. (2010). Grazing-induced reduction of natural nitrous oxide release from continental steppe. *Nature*, 464, 881-884.

Zacharias, S., Bogena, H., Samaniego, L., Mauder, M., Fuß, R., Pütz, T., et al. (2011). A network of terrestrial environmental observatories in Germany. *Vadose Zone Journal*, 10(3), 955-973.

Zhang, W., Liu, C., Zheng, X., Zhou, Z., Cui, F., Zhu, B., ... & Kiese, R. (2015). Comparison of the DNDC, LandscapeDNDC and IAP-N-GAS models for simulating nitrous oxide and nitric oxide emissions from the winter wheat–summer maize rotation system. *Agricultural Systems*, *140*, 1-10.

Chapter five - Conclusions and Future Work

1. Synthesis of significant contributions

From the analysis from Chapter 2: **“Dynamics of carbon sequestration in tropical dry forests along two successional gradients under climate change extremes”** we found that biomass and carbon storage increase in these TDF from younger forests to older forests, and has been increasing at each forest stand, which may be an indicator of forest recovery of these ecosystems. We obtained values of final AGB of 49.5 to 186.2 Mg ha^{-1} for TDF site in Brazil, and for the final BGB, we found values between 9.0 and 34.0 Mg ha^{-1}. For the site in Costa Rica, we obtained values of final AGB of 46.5 to 215.3 Mg ha^{-1} and for BGB from 13.6 to 38.6 Mg ha^{-1}. Moreover, we found some increases in the mortality rates after strong El Nino events, especially in the younger forests. At the same time, the DBH growth and recruitment rates were affected by these climatic events. Because of this, the net productivity of the forest stands varies interannually depending on the precipitation and climatic conditions of the area. Productivity in dry years was 40% lower than the average for all years. Wet years can also significantly increase productivity by almost 50% compared to the average of all years.

Our main results showed that carbon dynamics in TDF could be greatly influenced by climate variation and global climate change. Depending on their location, some dry forests are more influenced by climate variability than others, and differences between secondary stages are observed, where the youngest forests tend to be more vulnerable. We will expect to see in the years to come far greater carbon losses caused by increases in severe droughts and hurricane events (IPCC 2007; Sterl et al. 2008). These events can modify the carbon sequestration capacity of TDF and the recovery rates of secondary TDF in terms of carbon storage, forest structure and diversity. These changes in response to predicted increases of extreme drought events will jeopardize the ability of secondary TDF to recover faster after human intervention especially under extreme climatic events such as El Niño, causing significant diversity and biomass losses that will cost the ecosystem time and resources to recover from.

In the study in Chapter 3: “**Seasonality and budgets of soil greenhouse gas emissions from a tropical dry forest successional gradient in Costa Rica”** we found that at the start of the first rain events, large emissions pulses of CO_2 and N_2O are released from soils at all sites caused by the "Birch effect." These large pulses of CO_2 from the soil shift the net carbon balance of the intermediate forest site into a carbon source in the transition period from dry to the wet season. Even though more than 80% of annual N_2O emissions were released during this rewetting period, the reduction of the C sink calculated by global warming potentials was only ~1%.

Annual soil emissions of CO_2 were highest for the young secondary forest (8555.7 kg C ha^{-1} y^{-1}), followed by the old secondary forest (7419.6 kg C ha^{-1} y^{-1}) and the pasture (7223.7 kg C ha^{-1} y^{-1}). Annual emissions of N_2O were higher for the forest sites (0.39 and 0.43 kg N ha^{-1} y^{-1}) and lower in the pasture (0.09 kg N ha^{-1} y^{-1}). CH_4 uptake was higher in the old secondary forest (-2.61 kg ha^{-1} y^{-1}), followed by the pasture (-0.69 kg C ha^{-1} y^{-1}) and the young secondary forest (-0.58 kg C ha^{-1} y^{-1}). From multiple regression analyses, soil moisture was the best predictor for all three GHG emissions. N_2O fluxes were also influenced by microbial biomass. Annual CO_2 and N_2O soil fluxes of tropical dry forests in this study and obtained from a literature review (6.3 t C ha^{-1} y^{-1} and 0.5 kg N ha^{-1} y^{-1}) are much lower than the annual fluxes at wetter tropical forests (14.0 t C ha^{-1} y^{-1} and 2.5 kg N ha^{-1} y^{-1}). Moreover, tropical dry forest and pastures (-2.0 kg C ha^{-1} y^{-1} and -0.7 kg C ha^{-1} y^{-1}) are on average stronger sinks for CH_4 than wetter tropical forests (-1.9 kg C ha^{-1} y^{-1} and -0.6 kg C ha^{-1} y^{-1}).

Our results suggest TDF soils are important sources (CO_2, N_2O) and sinks (CH_4) of GHGs, but emissions are significantly lower than in tropical wet forest ecosystems. We found a strong control of precipitation events and thus soil water content on soil GHG fluxes and less importance of other soil environmental variables such as temperature, microbial biomass, and inorganic N concentration. Particularly, pulse emissions of CO_2 and N_2O at the transition from dry to wet season significantly influence the respective annual emission budget in the forest sites.

In Chapter 4: **"Spatio-temporal variability and uncertainties of greenhouse gas emissions in a pre-alpine Bavarian grassland based on model results"** we used a combination of manual and automatic soil chambers to measure the CO_2 and N_2O gas exchanges from the soil at different locations in a Bavarian grassland. Measurements were compared to simulated emissions of CO_2 and N_2O using the biogeochemical model LandscapeDNDC. Measurements of CO_2 fluxes using manual chambers, automatic chambers and modeled results showed a strong seasonality and similar patterns at all measured locations.

The LandscapeDNDC model was able to simulate the temporal trends of the measured daily CO_2 fluxes. At local scales, the results from the model improve when we used the average of all the simulations for the site than using the resulting simulation from averaged parameters to initialize the model. For N_2O emissions, we found significant differences between measured emissions and modeled emissions. For the environmental controls of CO_2 and N_2O, such as soil moisture and temperature, the model was able to simulate the seasonal patterns. Discrepancies between modeled and measured results could arise from inconsistencies or systematic errors in the input data of the model or biological processes that the model fails to fully characterize at local scales.

2. Future work and challenges

The studies that constitute this thesis showed the importance and the necessity of more detailed datasets where forest and grasslands ecosystems are monitored continuously at local scales. In terms of TDF carbon dynamics (chapter 2), we found few studies with forest inventories that have measured plots continuously in TDF and can characterize interannual variability in productivity, like in the case of our study (more than a decade) because of limited time and resources for the projects. We also found few studies with direct measurements of belowground biomass. Secondary TDF forests cover larger areas than old-growth forests in tropical regions, but they continue to be understudied, and our knowledge of carbon dynamics in these forests is rather scarce.

The variability of carbon stocks (above and below ground) and net greenhouse gas emissions over time can be evaluated (as showed in chapter 2 and 3), using a combination of direct measurements of forest inventory plots, remote-sensing techniques, and models based on accepted principles of statistical analysis (IPCC 2001). For carbon quantification, tree harvesting or forest inventories are the most reliable of all the methodologies, but they can be expensive, slow, and challenging to conduct at regional or global scales (Gibbs et al. 2007). More current remote sensing techniques (e.g., satellite images, airborne LIDAR, UAVs), allow scientists to acquire data for larger areas (e.g., Le Toan et al. 2011; Asner et al. 2012; Santoro, 2019). Also, remote sensing techniques applied on the ground at more local scales (e.g., carbon flux towers, optical phenology towers, wireless sensor networks) can acquire data with a high temporal resolution.

The study sites described in this thesis have been equipped and studied intensively using different remote sensing techniques. At the Santa Rosa National Park and Mata Seca State Park, optical phenology towers combined with wireless sensor networks in the forest understory and carbon flux towers (only at Santa Rosa National Park) have been used to determine seasonal greenness signals, phenological stages and primary productivity (e.g., Rankine et al. 2017; Castro et al. 2018). Also, airborne LIDAR has been used in Santa Rosa National Park for the identification and classification of forest successional stages by their forest structure (e.g., Castillo et al. 2012; Gu et al. 2018).

At the Fendt grassland in Bavaria Germany, intensive campaigns to collect data using flux towers, micrometeorology stations, hydrometeorological installations, soil wireless sensor networks, and airborne data have been carried for short periods (2 months in the summer) in the past. These intense campaigns intended to improve the spatial and temporal measurement resolutions, complement the permanent measurements with additional observed variables and validate the usage of innovative instruments, methods, and techniques that at the moment cannot be deployed over long time periods (Wolf et al. 2017).

Moreover, remote sensing data will always depend on ground measurements (e.g., forest inventories, permanent plots, and field samples) for calibration and validation. Remote sensing technologies can be costly, and some of them are criticized for not producing accurate results (Gibbs et al. 2007; Sanchez-Azofeifa et al. 2009; Zolkos et al. 2013). In conjunction with ground measurements, remote sensing information can help at regional and local scales to estimate impacts of deforestation and land-use change, climate change and detection of natural disasters.

On the other hand, soil greenhouse gas fluxes, which have significant effects on the global carbon and nitrogen cycle, have fewer methodologies and are subjected to errors in the estimation caused by assumptions about the carbon and nitrogen storage or the effects of forest conversion (Powers et al. 2004; Meir and Pennington 2011). At chapter 3, we found a limited number of studies measuring the net effect of all major greenhouse gas emissions from tropical soils with generally a low number of measurements (mostly < 10, max 30) across the year. Measuring GHG fluxes presents some logistical challenges and infrastructure constraints that influence the choice of e.g., automatic vs. manual chamber measurements. In our case, infrastructure and power supply did not allow for automatic measurements of soil GHG exchange at all the sites under investigation. However, our study is among the few with more than 25 measurements of GHG exchange across different hygric seasons. For our manual chamber measurements, we followed the informed sampling approach as suggested by Barton et al., (2015) to further reduce uncertainty in estimating seasonal and annual fluxes, i.e., more frequent sampling during times of expected high fluxes (in our case transition from dry to wet) and lower sampling frequency during the dry and wet season. Also, manual chamber measurements of CO_2, N_2O, and CH_4 exchange were put in relation to automatic and continuous measurements of soil CO_2 fluxes and NEE, which to our knowledge is the first time for a TDF ecosystem.

More information and studies are needed to asses the minimum required spatial and temporal data at local scales for the correct estimation of annual emissions at regional scales. It is known that soil fluxes respond to biogeochemical nutrient dynamics, soil physical properties, soil moisture, and soil temperature (Raich and Tufekciogul, 2000; Fornara et al. 2013), but their interactions and spatio-temporal dynamics at field scale remain unclear (Borchard et al. 2015). Although process-based models have been used to simulate soil emissions and carbon dynamics (chapter 4), these models are not completely reliable and can induce in the over or underestimation of GHG emissions since they rely heavily on field measurements at local scales for calibration and validation (Leip et al. 2011). More improvement is still required to simulate the spatial variability of GHG emissions and the validity of upscaling model estimates to larger regions.

3. Literature Cited

Asner, G. P., Mascaro, J., Muller-Landau, H. C., Vieilledent, G., Vaudry, R., Rasamoelina, M., ... & Van Breugel, M. (2012). A universal airborne LiDAR approach for tropical forest carbon mapping. *Oecologia*, *168*(4), 1147-1160.

Barton, L., Wolf, B., Rowlings, D., Scheer, C., Kiese, R., Grace, P., ... & Butterbach-Bahl, K. (2015). Sampling frequency affects estimates of annual nitrous oxide fluxes. *Scientific reports*, *5*(1), 1-9.

Borchard, N., Schirrmann, M., von Hebel, C., Schmidt, M., Baatz, R., Firbank, L., et al. 2015. Spatio-temporal drivers of soil and ecosystem carbon fluxes at field scale in an upland grassland in Germany. Agriculture, ecosystems & environment. 211: 84-93.

Castillo, M., Rivard, B., Sanchez-Azofeifa, A., Calvo-Alvarado, J., & Dubayah, R. (2012). LIDAR remote sensing for secondary Tropical Dry Forest identification. *Remote sensing of environment*, *121*, 132-143.

Castro, S. M., Sanchez-Azofeifa, G. A., & Sato, H. (2018). Effect of drought on productivity in a Costa Rican tropical dry forest. *Environmental Research Letters*, *13*(4), 045001.

Fornara, D.A., Banin, L., Crawley, M.J. 2013. Multi-nutrient vs. nitrogen-only effects on carbon sequestration in grassland soils. Global Change Biology. 19: 3848-3857.

Gibbs, H. K., Brown, S., Niles, J. O., & Foley, J. A. (2007). Monitoring and estimating tropical forest carbon stocks: making REDD a reality. *Environmental Research Letters*, *2*(4), 045023.

Gu, Z., Cao, S., & Sanchez-Azofeifa, G. A. (2018). Using LiDAR waveform metrics to describe and identify successional stages of tropical dry forests. *International journal of applied earth observation and geoinformation*, *73*, 482-492.

IPCC (2001). Climate Change 2001: Synthesis Report, ed. R.T. Watson and the Core Writing Team. Cambridge: Cambridge University Press.

IPCC (2007). Intergovernmental Panel on Climate Change Climate Change 2007: Synthesis Report. IPCC Publication, http://www.ipcc.ch/pdf/assessment-report/ar4/syr/ar4_syr.pdf (accessed 10 Dec. 2019).

Le Toan, T., Quegan, S., Davidson, M. W. J., Balzter, H., Paillou, P., Papathanassiou, K., ... & Ulander, L. (2011). The BIOMASS mission: Mapping global forest biomass to better understand the terrestrial carbon cycle. *Remote sensing of environment*, *115*(11), 2850-2860.

Leip, A., Busto, M., Corazza, M., Bergamaschi, P., Koeble, R., Dechow, R., ... & De Vries, W. (2011). Estimation of N2O fluxes at the regional scale: data, models, challenges. *Current Opinion in Environmental Sustainability*, *3*(5), 328-338.

Meir, P., & Pennington, R. T. (2011). Climatic change and seasonally dry tropical forests. In *Seasonally Dry Tropical Forests* (pp. 279-299). Island Press, Washington, DC.

Powers, J. S. (2004). Changes in soil carbon and nitrogen after contrasting land-use transitions in northeastern Costa Rica. *Ecosystems*, *7*(2), 134-146.

Raich, J., Tufekciogul, A. 2000. Vegetation and soil respiration: correlations and controls. Biogeochemistry. 48: 71-90.

Rankine, C., Sanchez-Azofeifa, G. A., Guzmán, J. A., Espirito-Santo, M. M., & Sharp, I. (2017). Comparing MODIS and near-surface vegetation indexes for monitoring tropical dry forest phenology along a successional gradient using optical phenology towers. *Environmental Research Letters*, *12*(10), 105007.

Sánchez-Azofeifa, G. A., Castro-Esau, K. L., Kurz, W. A., & Joyce, A. (2009). Monitoring carbon stocks in the tropics and the remote sensing operational limitations: from local to regional projects. *Ecological Applications*, *19*(2), 480-494.

Santoro, M., Cartus, O. (2019). ESA Biomass Climate Change Initiative (Biomass_cci): Global datasets of forest above-ground biomass for the year 2017, v1. Centre for Environmental Data Analysis, *02 December 2019*.

doi:10.5285/bedc59f37c9545c981a839eb552e4084. http://dx.doi.org/10.5285/bedc59f37c9545c981a839eb552e4084

Sterl, A., Severijns, C., Dijkstra, H., et al. (2008). When can we expect extremely high surface temperatures? *Geophysical Research Letters*, *35*(14).

Zolkos, S. G., Goetz, S. J., & Dubayah, R. (2013). A meta-analysis of terrestrial aboveground biomass estimation using lidar remote sensing. *Remote Sensing of Environment*, *128*, 289-298.

Thesis bibliography

Adegbeye, M. J., Reddy, P. R. K., Obaisi, A. I., Elghandour, M. M. M. Y., Oyebamiji, K. J., Salem, A. Z. M., ... & Camacho-Díaz, L. M. (2019). Sustainable agriculture options for production, nutritional mitigation of greenhouse gasses and pollution, and nutrient recycling in emerging and transitional nations- An overview. *Journal of Cleaner Production*, 118319.

Allen, C. D. et al. (2010). A global overview of drought and heat-induced tree mortality reveals emerging climate change risks for forests. *Forest ecology and management*, *259*(4), 660-684.

Allen, C. D., Breshears, D. D., McDowell, N. G. (2015). On underestimation of global vulnerability to tree mortality and forest die-off from hotter drought in the Anthropocene. *Ecosphere*, *6*(8), 1-55.

Allen, K., Dupuy, J. M., Gei, M. G. et al. (2017). Will seasonally dry tropical forests be sensitive or resistant to future changes in rainfall regimes?. *Environmental Research Letters*, *12*(2), 023001.

Allison, S., Wallenstein, M., and Bradford, M. (2010). Soil-carbon response to warming dependent on microbial physiology. *Nature Geosciences. 3,* 336-40.

Álvarez, M. et al. (2008). Ecology procedures. In: Nassar, J. M., Rodríguez, J. P., Sanchez-Azofeifa, G. A., Garvin, T., Quesada, M. eds. Manual of Methods: Human, Ecological and Biophysical Dimensions of Tropical Dry Forests. Caracas: Ediciones IVIC, Instituto Venezolano de Investigaciones Científicas (IVIC). p. 15-46.

Amthor, J.S. and Baldocchi, D.D. (2001). Terrestrial Higher Plant Respiration and Net Primary Production. In *Terrestrial Global Productivity*, Academic Press, 33-59

Anderegg, W. R., Kane, J. M., Anderegg, L. D. (2013). Consequences of widespread tree mortality triggered by drought and temperature stress. *Nature climate change*, *3*(1), 30.

Aryal, D. R., De Jong, B. H., Ochoa-Gaona, S., Mendoza-Vega, J., & Esparza-Olguin, L. (2015). Successional and seasonal variation in litterfall and associated nutrient transfer in semi-evergreen tropical forests of SE Mexico. *Nutrient cycling in agroecosystems*, *103*(1), 45-60.

Aryal, D. R., Hendricus, B., Jong, J. De, Mendoza-Vega, J., Ochoa-Gaona, S., & Esparza-Olguín, L. (2017). Soil Organic Carbon Stocks and Soil Respiration in Tropical Secondary Forests in Southern Mexico. Global Soil Security, 153–165. https://doi.org/10.1007/978-3-319-43394-3.

Asner, G. P., Mascaro, J., Muller-Landau, H. C., Vieilledent, G., Vaudry, R., Rasamoelina, M., ... & Van Breugel, M. (2012). A universal airborne LiDAR approach for tropical forest carbon mapping. *Oecologia*, *168*(4), 1147-1160.

Aubinet, M., Grelle, A., Ibrom, A., Rannik, Ü., Moncrieff, J., Foken, T., Kowalski, A.S., Martin, P.H., Berbigier, P., Bernhofer, C. et al. (1999). Estimates of the annual net carbon and water exchange of forests: The EUROFLUX methodology. In *Advances in Ecological Research*; Academic Press: Cambridge, MA, USA, Volume 30, pp. 113–175.

Baldocchi, D.D., Hincks, B.B., Meyers, T.P. (1988). Measuring biosphere-atmosphere exchanges of biologically related gases with micrometeorological methods. *Ecology*, *69*, 1331–1340.

Barton L., Wolf B., Rowlings D., Scheer C., Kiese R., Grace P., Stefanova K., Butterbach-Bahl K. (2015). Sampling frequency affects estimates of annual nitrous oxide fluxes. Scientific Reports 5, DOI: 10.1038/srep15912.

Becknell, J. M., & Powers, J. S. (2014). Stand age and soils as drivers of plant functional traits and aboveground biomass in secondary tropical dry forest. *Canadian Journal of Forest Research*, *44*(6), 604-613.

Becknell, J. M., Kucek, L. K., & Powers, J. S. (2012). Aboveground biomass in mature and secondary seasonally dry tropical forests: A literature review and global synthesis. *Forest Ecology and Management*, *276*, 88-95.

Bellassen, V., & Luyssaert, S. (2014). Carbon sequestration: Managing forests in uncertain times. *Nature*, *506*(7487), 153-155.

Bogena, H. R., Bol, R., Borchard, N., Brüggemann, N., Diekkrüger, B., Drüe, C., ... & Missong, A. (2015). A terrestrial observatory approach to the integrated investigation of the effects of deforestation on water, energy, and matter fluxes. *Science China Earth Sciences*, *58*(1), 61-75.

Bond-Lamberty, B., Thomson, A. (2010). Temperature-associated increases in the global soil respiration record. *Nature. 464*(7288), 579-582.

Borchard, N., Schirrmann, M., von Hebel, C., Schmidt, M., Baatz, R., Firbank, L., et al. 2015. Spatio-temporal drivers of soil and ecosystem carbon fluxes at field scale in an upland grassland in Germany. Agriculture, ecosystems & environment. 211: 84-93.

Borken, W., & Matzner, E. (2009). Reappraisal of drying and wetting effects on C and N mineralization and fluxes in soils. *Global Change Biology*, *15*(4), 808-824.

Bouwman, A. F., Boumans, L. J. M., & Batjes, N. H. (2002). Modeling global annual N2O and NO emissions from fertilized fields. *Global Biogeochemical Cycles*, *16*(4), 28-1.

Bradford, M. A., Wieder, W. R., Bonan, G. B., Fierer, N., Raymond, P. A., & Crowther, T. W. (2016). Managing uncertainty in soil carbon feedbacks to climate change. *Nature Climate Change*, *6*(8), 751-758.

Breuer, L., Papen, H., & Butterbach-Bahl, K. (2000). N_2O emission from tropical forest soils of Australia. *Journal of Geophysical Research Atmospheres*, *105*(D21), 26353–26367. https://doi.org/10.1029/2000JD900424

Brienen RJW, et al. (2015) Long-term decline of the Amazon carbon sink. *Nature,* 519, 344–348.

Brown, S., & Lugo, A. E. (1982). The storage and production of organic matter in tropical forests and their role in the global carbon cycle. *Biotropica*, 161-187.

Butterbach-Bahl, K., Baggs, E. M., Dannenmann, M., Kiese, R., & Zechmeister-Boltenstern, S. (2013). Nitrous oxide emissions from soils: how well do we understand the processes and their controls?. *Philosophical Transactions of the Royal Society B: Biological Sciences*, *368*(1621), 20130122.

Butterbach-Bahl, K., Denk, T., Grote, R., Haas, E., Havermann, F., Petersen, C. W., Kiese, R., Klatt, S., Kraus, D., Molina Herrera, S., Petersen, K., Werner, C., & Wolf, B. (2019). LandscapeDNDC v1. 30.0. https://ldndc.imk-ifu.kit.edu/products/ldndc-usersguide.pdf

Butterbach-Bahl, K., Kock, M., Willibald, G., Hewett, B., Buhagiar, S., Papen, H., Kiese, R. (2004). Temporal variations of fluxes of NO, NO_2, N_2O, CO_2, and CH_4 in a tropical rain forest ecosystem. *Global Biogeochemical Cycles*, 18, doi:10.1029/2004GB002243

Cai, W. et al. (2014). Increasing frequency of extreme El Niño events due to greenhouse warming. *Nature Climate Change*. 4(2): 111-116.

Calvo-Rodriguez, S., Sanchez-Azofeifa, A. G., Duran, S. M., and Espirito-Santo, M. M. (2017). Assessing ecosystem services in Neotropical dry forests: a systematic review. *Environmental Conservation*, *44*(1), 34-43.

Campo, J., & Vázquez-Yanes, C. (2004). Effects of nutrient limitation on aboveground carbon dynamics during tropical dry forest regeneration in Yucatán, Mexico. *Ecosystems*, *7*(3), 311-319.

Cao, S., Sanchez-Azofeifa, G. A., Duran, S. M., & Calvo-Rodriguez, S. (2016). Estimation of aboveground net primary productivity in secondary tropical dry forests using the Carnegie–Ames–Stanford approach (CASA) model. *Environmental Research Letters*, *11*(7), 075004.

Castaldi, S., & Aragosa, D. (2002). Factors influencing nitrification and denitrification variability in a natural and fire-disturbed Mediterranean shrubland. *Biology and Fertility of Soils*, *36*(6), 418–425. https://doi.org/10.1007/s00374-002-0549-2

Castaldi, S., Ermice, A., & Strumia, S. (2006). Fluxes of N_2O and CH_4 from soils of savannas and seasonally dry ecosystems. *Journal of Biogeography*, *33*(3), 401–415. https://doi.org/10.1111/j.1365-2699.2005.01447.x

Castillo, M., Rivard, B., Sanchez-Azofeifa, A., Calvo-Alvarado, J., & Dubayah, R. (2012). LIDAR remote sensing for secondary Tropical Dry Forest identification. *Remote sensing of environment*, *121*, 132-143.

Castro, S. M., Sanchez-Azofeifa, G. A., & Sato, H. (2018). Effect of drought on productivity in a Costa Rican tropical dry forest. *Environmental Research Letters*, *13*(4), 045001.

Cavaleri, M. A., Coble, A. P., Ryan, M. G., Bauerle, W. L., Loescher, H. W., & Oberbauer, S. F. (2017). Tropical rainforest carbon sink declines during El Niño as a result of reduced photosynthesis and increased respiration rates. *New Phytologist*, *216*(1), 136-149.

Chadwick, R., Good, P., Martin, G., & Rowell, D. P. (2016). Large rainfall changes consistently projected over substantial areas of tropical land. *Nature Climate Change*, *6*(2), 177.

Chave, J., Réjou-Méchain, M., Búrquez, A., Chidumayo, E., Colgan, M. S., Delitti, W. B., ... & Henry, M. (2014). Improved allometric models to estimate the aboveground biomass of tropical trees. *Global change biology*, *20*(10), 3177-3190.

Chazdon, R. L., Letcher, S. G., Van Breugel, M., Martínez-Ramos, M., Bongers, F., & Finegan, B. (2007). Rates of change in tree communities of secondary Neotropical forests following major disturbances. *Philosophical Transactions of the Royal Society B: Biological Sciences*, *362*(1478), 273-289.

Chazdon, R. L., Redondo-Brenes, A., Vilchez-Alvarado, B. (2005). Effects of climate and stand age on annual tree dynamics in tropical second-growth rain forests. *Ecology*, *86*(7), 1808-1815.

Chen, S., Zou, J., Hu, Z., Chen, H., & Lu, Y. (2014). Global annual soil respiration in relation to climate, soil properties and vegetation characteristics: Summary of available data. *Agricultural and Forest Meteorology*, *198*, 335-346.

Cifuentes Jara, M. (2008). Aboveground biomass and ecosystem carbon pools in tropical secondary forests growing in six life zones of Costa Rica. Oregon State University. https://ir.library.oregonstate.edu/concern/graduate_thesis_or_dissertations/jm214s40j

Clark, D. A. (2004). Sources or sinks? The responses of tropical forests to current and future climate and atmospheric composition. *Philosophical Transactions of the Royal Society B: Biological Sciences*, *359*(1443), 477–491. https://doi.org/10.1098/rstb.2003.1426

Condit, R., Ashton, P. S., Manokaran, N., Lafrankie, J. V., Hubbell, S. P., and Foster, R. B. (1999). Dynamics of the forest communities at Pasoh and Barro Colorado: Comparing two 50-ha plots. *Philosophical Transactions of the Royal Society of London. Series B: Biological Sciences*, 354, 1739-1748.

Curiel Yuste, J., Baldocchi, D. D., Gershenson, A., Goldstein, A., Misson, L., & Wong, S. (2007). Microbial soil respiration and its dependency on carbon inputs, soil temperature and moisture. *Global Change Biology*, *13*(9), 2018–2035. https://doi.org/10.1111/j.1365-2486.2007.01415.x

Dalal, R. C., & Allen, D. E. (2008). Greenhouse gas fluxes from natural ecosystems. *Australian Journal of Botany*, *56*(5), 369. https://doi.org/10.1071/bt07128

Davidson, E. A., Matson, P. A., Vitousek, P. M, et al. (1993). Processes regulating soil emissions of NO and N_2O in a seasonally dry tropical forest. *Ecology*, 74(1): 130–139.

Davidson, E. A., Nepstad, D. C., Ishida, F. Y., & Brando, P. M. (2008). Effects of an experimental drought and recovery on soil emissions of carbon dioxide, methane, nitrous oxide, and nitric oxide in a moist tropical forest. *Global Change Biology*, *14*(11), 2582-2590.

De Arruda, P. H. Z., Vourlitis, G. L., Santanna, F. B., Pinto Jr, O. B., Lobo, F. D. A., & Nogueira, J. D. S. (2016). Large net CO_2 loss from a grass-dominated tropical savanna in south-central Brazil in response to seasonal and interannual drought. *Journal of Geophysical Research: Biogeosciences*, *121*(8), 2110-2124.

Didan, K. (2015). MOD13Q1 MODIS/Terra, MYD13Q1 MODIS/Aqua Vegetation Indices 16-Day L3 Global 250m SIN Grid V006. NASA EOSDIS Land Processes DAAC. https://doi.org/10.5067/MODIS/MYD13Q1.006

Dupuy, J. M., Hernández-Stefanoni, J. L., Hernández-Juárez, R. A., Tetetla-Rangel, E., López-Martínez, J. O., Leyequién-Abarca, E., ... & May-Pat, F. (2012). Patterns and correlates of tropical dry forest structure and composition in a highly replicated chronosequence in Yucatan, Mexico. *Biotropica*, *44*(2), 151-162.

Enquist, B. J., & Leffler, A. J. (2001). Long-term tree ring chronologies from sympatric tropical dry-forest trees: individualistic responses to climatic variation. *Journal of Tropical Ecology*, *17*(1), 41-60.

Eviner, V. T. (2014). 10.6 Biogeochemical Interactions Governing Terrestrial Net Primary Production.

Farrick, K. K., & Branfireun, B. A. (2013). Left high and dry: a call to action for increased hydrological research in tropical dry forests. *Hydrological Processes*, *27*(22), 3254-3262.

Fest, B. J., Hinko-Najera, N., Wardlaw, T., Griffith, D. W., Livesley, S. J., & Arndt, S. K. (2017). Soil methane oxidation in both dry and wet temperate eucalypt forests shows a near-identical relationship with soil air-filled porosity. *Biogeosciences,* 14, 467-479. https://doi:10.5194/bg-14-467-2017

Flessa, H., Ruser, R., Schilling, R., Loftfield, N., Munch, J.C., Kaiser, E.A., Beese, F. (2002). N_2O and CH4 fluxes in potato fields: Automated measurement, management effects and temporal variation. *Geoderma*, 105, 307-325.

Fornara, D.A., Banin, L., Crawley, M.J. 2013. Multi-nutrient vs. nitrogen-only effects on carbon sequestration in grassland soils. Global Change Biology. 19: 3848-3857.

Fu, J., Gasche, R., Wang, N., Lu, H., Butterbach-Bahl, K., & Kiese, R. (2019). Dissolved organic carbon leaching from montane grasslands under contrasting climate, soil and management conditions. *Biogeochemistry*, *145*(1-2), 47-61.

Garcia-Montiel, D. C., Steudler, P. A., Piccolo, M. C., Melillo, J. M., Neill, C., & Cerri, C. C. (2001). Controls on soil nitrogen oxygen emissions from forest and pastures in the Brazilian Amazon. *Global Biogeochemical Cycles*, *15*(4), 1021–1030. https://doi.org/10.1029/2000GB001349

Gentry, A. H. (1988). Changes in plant community diversity and floristic composition on environmental and geographical gradients. *Annals of the Missouri botanical garden*, 1-34.

Gibbs, H. K., Brown, S., Niles, J. O., & Foley, J. A. (2007). Monitoring and estimating tropical forest carbon stocks: making REDD a reality. *Environmental Research Letters*, *2*(4), 045023.

Gibbs, H. K., Ruesch, A. S., Achard, F., Clayton, M. K., Holmgren, P., Ramankutty, N., Foley, J. A. (2010). Tropical forests were the primary sources of new agricultural land in the 1980s and 1990s. *Proceedings of the National Academy of Sciences, 107,* 16732- 16737.

Groffman, P. M., Butterbach-Bahl, K., Fulweiler, R. W., Gold, A. J., Morse, J. L., Stander, E. K., ... & Vidon, P. (2009). Challenges to incorporating spatially and temporally explicit phenomena (hotspots and hot moments) in denitrification models. *Biogeochemistry*, *93*(1-2), 49-77.

Gu, Z., Cao, S., & Sanchez-Azofeifa, G. A. (2018). Using LiDAR waveform metrics to describe and identify successional stages of tropical dry forests. *International journal of applied earth observation and geoinformation*, *73*, 482-492.

Guo, X., Drury, C. F., Yang, X., Daniel Reynolds, W., & Fan, R. (2014). The Extent of Soil Drying and Rewetting Affects Nitrous Oxide Emissions, Denitrification, and Nitrogen Mineralization. *Soil Science Society of America Journal*, *78*(1), 194. https://doi.org/10.2136/sssaj2013.06.0219

Gütlein, A., Gerschlauer, F., Kikoti, I., & Kiese, R. (2018). Impacts of climate and land use on N_2O and CH_4 fluxes from tropical ecosystems in the Mt. Kilimanjaro region, Tanzania. *Global Change Biology*, *24*(3), 1239–1255. https://doi.org/10.1111/gcb.13944

Haas, E., Klatt, S., Fröhlich, A., Kraft, P., Werner, C., Kiese, R., et al. (2013). LandscapeDNDC: a process model for simulation of biosphere–atmosphere–hydrosphere exchange processes at site and regional scale. *Landscape ecology*, 28(4), 615-636.

He, Y., Gibbons, J., & Rayment, M. (2016). A two-stage sampling strategy improves chamber-based estimates of greenhouse gas fluxes. *Agricultural and Forest Meteorology*, 228, 52-59.

Hofer, S. (2003). QuikChem Method 12-107-06-2-A. Determination of ammonia (Salicylate) in 2M KCl soil extracts by Flow Injection Analysis. Lachat Instruments. Colorado, USA. 10p.

Holdridge, L. R. (1967). *Life zone ecology*. San Jose: Tropical Science Center. 1967.

Houghton, R. A. (2013) The emissions of carbon from deforestation and degradation in the tropics: Past trends and future potential. *Carbon Management, 4*:539–546.

Hursh, A., Ballantyne, A., Cooper, L., Maneta, M., Kimball, J., & Watts, J. (2017). The sensitivity of soil respiration to soil temperature, moisture, and carbon supply at the global scale. *Global change biology*, *23*(5), 2090-2103.

Imbach, P., Molina, L., Locatelli, B., Roupsard, O., Mahé, G., Neilson, R., et al. (2012). Modeling potential equilibrium states of vegetation and terrestrial water cycle of Mesoamerica under climate change scenarios. *Journal of Hydrometeorology*, *13*(2), 665-680.

IPCC (2001). Climate Change 2001: Synthesis Report, ed. R.T. Watson and the Core Writing Team. Cambridge: Cambridge University Press.

IPCC (2006). *Guidelines for National Greenhouse Gas Inventories.* Intergovernmental Panel on Climate Change, ed. H. Eggleston, L. Buendia, K. Miwa, T. Ngara, & K. Tanabe. Japón: IGES (National Greenhouse Gas Inventories Programme).

IPCC (2007). Intergovernmental Panel on Climate Change 2007: Synthesis Report. IPCC Publication, http://www.ipcc.ch/pdf/assessment-report/ar4/syr/ar4_syr.pdf (accessed 10 Dec. 2019).

IPCC (2014). Climate Change 2014: Synthesis Report. Contribution of Working Groups I, II and III to the Fifth Assessment Report of the Intergovernmental Panel on Climate Change, 2–26. Cambridge University Press, Cambridge, United Kingdom and New York, NY, USA. https://doi.org/10.1017/CBO9781107415324.

IPCC. (2007). Climate change 2007: the physical science basis. In: *Contribution of working group I to the fourth assessment report of the intergovernmental panel on climate change*, ed. S. Solomon, D. Qin, M. Manning, Z. Chen, M. Marquis, K.B. Averyt, M. Tignor and H.L. Miller, pp 996. Cambridge, UK: Cambridge University Press.

Janzen, D. H. (1988). Tropical dry forests. *Biodiversity*, 130-137.

Janzen, D. H., Hallwachs, W., & Kappelle, M. (2016). Biodiversity conservation history and future in Costa Rica: The case of Área de Conservación Guanacaste (ACG). *Costa Rican Ecosystems. The University of Chicago Press, Chicago and London*, 290-341.

Jaramillo, V. J., Martinez-Yrizar, A., & Sanford, R. L. (2011). Primary productivity and biogeochemistry of seasonally dry tropical forests. In *Seasonally dry tropical forests* (pp. 109-128). Island Press, Washington, DC.

Kalacska, M., Sanchez-Azofeifa, G. A., Calvo-Alvarado, J. C., Quesada, M., Rivard, B., & Janzen, D. H. (2004). Species composition, similarity and diversity in three successional stages of a seasonally dry tropical forest. *Forest ecology and management*, *200*(1-3), 227-247.

Kalacska, M., Sanchez-Azofeifa, G. A., Rivard, B., Calvo-Alvarado, J. C., & Quesada, M. (2008). Baseline assessment for environmental services payments from satellite imagery: A case study from Costa Rica and Mexico. *Journal of environmental management*, *88*(2), 348-359.

Keating, B. A., Carberry, P. S., Hammer, G. L., Probert, M. E., Robertson, M. J., Holzworth, D., ... & McLean, G. (2003). An overview of APSIM, a model designed for farming systems simulation. *European journal of agronomy*, *18*(3-4), 267-288.

Kesik, M., Ambus, P., Baritz, R., Bruggemann, NB., Butterbach- Bahl, K., Damm, M., Duyzer, J., Horvath, L., Kiese, R., Kitzler, B., Leip, A., Li, C., Pihlatie, M., Pilegaard, K., Seufert, G., Simpson, D., Skiba, U., Smiatek, G., Vesala, T., Zechmeister- Boltenstern, S. (2005). Inventories of N_2O and NO emissions from European forest soils. *Biogeosciences*, 2, 353-375.

Kiese, R., Fersch B., Baessler C., Brosy C., Butterbach-Bahl K., Chwala C., Dannenmann M., Fu J., Gasche R., Grote R., Jahn C., Klatt J., Kunstmann H., Mauder M., Rödiger T., Smiatek

G., Soltani M., Steinbrecher R., Völksch I., Werhahn J., Wolf B., Zeeman M., Schmid H.P. (2018). The TERENO-preAlpine Observatory: integrating meteorological, hydrological and biogeochemical measurements and modelling. *Vadose Zone Journal*. 10.2136/vzj2018.03.0060.

Kiese, R., Hewett, B., Butterbach-Bahl, K. (2008b). Seasonal dynamic of gross nitrification and N_2O emission at two tropical rainforest sites in Queensland, Australia. *Plant and Soil*, 309, 211-226.

Kiese, R., Wochele, S., Butterbach-Bahl, K. (2008a). Site specific and regional estimates of methane uptake by tropical rainforest soils of north-eastern Australia. *Plant and Soil*, 309, 105-117.

Knepel, K. (2012). QuikChem Method 12-107-04-1-B. Determination of nitrate in 2M KCl soil extracts by Flow Injection Analysis. Lachat Instruments. Loveland, USA. 11p.

Lasky, J. R., Uriarte, M., and Muscarella, R. (2016). Synchrony, compensatory dynamics, and the functional trait basis of phenological diversity in a tropical dry forest tree community: effects of rainfall seasonality. *Environmental Research Letters*, *11*(11), 115003.

Lassey, K. R., Scheehle, E. A., & Kruger, D. (2005). Towards reconciling national emission inventories for methane with the global budget. *Environmental Sciences*, *2*(2-3), 193-204.

Le Quéré, C., Moriarty, R., Andrew, R. M., Canadell, J. G., Sitch, S., Korsbakken, J. I., ... & Houghton, R. A. (2015). Global carbon budget 2015. *Earth System Science Data*, *7*(2), 349-396.

Le Toan, T., Quegan, S., Davidson, M. W. J., Balzter, H., Paillou, P., Papathanassiou, K., ... & Ulander, L. (2011). The BIOMASS mission: Mapping global forest biomass to better understand the terrestrial carbon cycle. *Remote sensing of environment*, *115*(11), 2850-2860.

Lebrija-Trejos, E., Pérez-García, E. A., Meave, J. A., Poorter, L., & Bongers, F. (2011). Environmental changes during secondary succession in a tropical dry forest in Mexico. *Journal of Tropical Ecology*, *27*(5), 477–489. https://doi.org/10.1017/s0266467411000253

Leip, A., Busto, M., Corazza, M., Bergamaschi, P., Koeble, R., Dechow, R., ... & De Vries, W. (2011). Estimation of N2O fluxes at the regional scale: data, models, challenges. *Current Opinion in Environmental Sustainability*, *3*(5), 328-338.

Leiva, J. A., Rocha, O. J., Mata, R., & Gutiérrez-Soto, M. V. (2009). Cronología de la regeneración del bosque tropical seco en Santa Rosa, Guanacaste, Costa Rica: II. La vegetación en relación con el suelo. *Revista de Biología Tropical*, *57*(3), 817-836.

Li, C. (2000). Modeling trace gas emissions from agricultural ecosystems. *Nutrient Cycling Agro ecosystems*, 58, 259-276.

Li, C., Frolking, S., & Frolking, T. A. (1992a). A model of nitrous oxide evolution from soil driven by rainfall events: 1. Model structure and sensitivity. *Journal of Geophysical Research: Atmospheres*, *97*(D9), 9759-9776.

Li, C., Frolking, S., & Frolking, T. A. (1992b). A model of nitrous oxide evolution from soil driven by rainfall events: 2. Model applications. *Journal of Geophysical Research: Atmospheres*, *97*(D9), 9777-9783.

Lieberman, D., and Lieberman. M. (1987). Forest tree growth and dynamics at La Selva, Costa Rica (1969-1982). *Journal of Tropical Ecology*, 3, 347-358.

Linares-Palomino, R., Oliveira-Filho, A. T., & Pennington, R. T. (2011). Neotropical seasonally dry forests: diversity, endemism, and biogeography of woody plants. In *Seasonally dry tropical forests* (pp. 3-21). Island Press, Washington, DC.

Lopez, B. C., Rodriguez, R., Gracia, C. A., & Sabate, S. (2006). Climatic signals in growth and its relation to ENSO events of two Prosopis species following a latitudinal gradient in South America. *Global Change Biology*, *12*(5), 897-906.

Lugo, P. M. A., Medina, E., Money, H. A., Murphy, P. G., & Bullock, S. H. (2005). Dry forests of Central America and the Caribbean. *Seasonally dry tropical forests*, 9-34.

Luyssaert S, et al. (2008) Old-growth forests as global carbon sinks. *Nature, 455*, 213–215.

Madeira, B., Espírito-Santo, M. M. Do., Sanz D'angelo, V., Nunes, Y. R. F., Sanchez-Azofeifa, G. A., Fernandes, W., and Quesada, M. (2009). Changes in tree and liana communities along a successional gradient in a tropical dry forest in south-eastern Brazil. *Plant Ecology*, 201, 291–304.

Martínez-Ramos, M., Balvanera, P., Arreola Villa, F., Mora, F., Maass, J. M., and Maza-Villalobos Méndez, S. (2018). Effects of long-term inter-annual rainfall variation on the dynamics of regenerative communities during the old-field succession of a neotropical dry forest. *Forest Ecology and Management*, *426*, 91–100. https://doi.org/10.1016/j.foreco.2018.04.048

Martinez-Yrizar, A., Maass, J. M., Pérez-Jiménez, L. A., & Sarukhán, J. (1996). Net primary productivity of a tropical deciduous forest ecosystem in western Mexico. *Journal of Tropical Ecology*, *12*(1), 169-175.

Mattos, P. P., Braz, E. M., Domene, V. D., Sampaio, E. V. D. S. B., Gasson, P., Pareyn, F. G. C., ... & Araújo, E. D. L. (2015). Climate-tree growth relationships of Mimosa tenuiflora in seasonally dry tropical forest, Brazil. *Cerne*, *21*(1), 141-149.

Maza-Villalobos, S., Poorter, L., and Martínez-Ramos, M. (2013). Effects of ENSO and temporal rainfall variation on the dynamics of successional communities in old-field succession of a tropical dry forest. *PloS one*, *8*(12), e82040.

Meir, P., & Pennington, R. T. (2011). Climatic change and seasonally dry tropical forests. In *Seasonally Dry Tropical Forests* (pp. 279-299). Island Press, Washington, DC.

Mendivelso, H. A., Camarero, J. J., Gutiérrez, E., & Castaño-Naranjo, A. (2016). Climatic influences on leaf phenology, xylogenesis and radial stem changes at hourly to monthly scales in two tropical dry forests. *Agricultural and forest meteorology*, *216*, 20-36.

Miles, L., Newton, A., DeFries, R., Ravilious, C., May, I., Blyth, S., Kapos, V., Gordon J. (2006). A global overview of the conservation status of Tropical Dry Forests. *Journal of Biogeography*. 33, 491-505.

Mitchard, E. T. (2018). The tropical forest carbon cycle and climate change. *Nature*, *559*(7715), 527-534.

Moldrup, P., Olesen, T., Komatsu, T., Yoshikawa, S., Schjønning, P., & Rolston, D. E. (2003). Modeling diffusion and reaction in soils: X. A unifying model for solute and gas diffusivity in unsaturated soil. *Soil Science*, *168*(5), 321–337. https://doi.org/10.1097/00010694-200305000-00002

Molina-Herrera, S., Haas, E., Klatt, S., Kraus, D., Augustin, J., Magliulo, V., ... & Skiba, U. (2016). A modeling study on mitigation of N2O emissions and NO3 leaching at different agricultural sites across Europe using LandscapeDNDC. *Science of the Total Environment*, *553*, 128-140.

Muhr, J., Goldberg, S. D., Borken, W., & Gebauer, G. (2008). Repeated drying-rewetting cycles and their effects on the emission of CO_2, N_2O, NO, and CH_4 in a forest soil. *Journal of Plant Nutrition and Soil Science*, *171*(5), 719–728. https://doi.org/10.1002/jpln.200700302

Murphy, P. G., & Lugo, A. E. (1986). Ecology of tropical dry forest. *Annual review of ecology and systematics*, *17*(1), 67-88.

Myklebust, M. C., Hipps, L. E., & Ryel, R. J. (2008). Comparison of eddy covariance, chamber, and gradient methods of measuring soil CO2 efflux in an annual semi-arid grass, Bromus tectorum. *Agricultural and forest meteorology*, *148*(11), 1894-1907.

Navarro-García, F., Casermeiro, M. Á., & Schimel, J. P. (2012). When structure means conservation: Effect of aggregate structure in controlling microbial responses to rewetting events. *Soil Biology and Biochemistry*, *44*(1), 1–8. https://doi.org/10.1016/j.soilbio.2011.09.019

Neill, C., Piccolo, M.C., Cerri, C.C., Steudler, P.A., Melillo, J.M., Brito, M. (1997). Net nitrogen mineralization and net nitrification rates in soils following deforestation for pasture across the southwestern Brazilian Amazon Basin landscape. *Oecologia*, 110, 243 - 252

NOAA National Weather Service, National Centers for Environmental Prediction, Climate Prediction Center (2018). Cold and Warm Episodes by Season. Available: https://origin.cpc.ncep.noaa.gov/products/analysis_monitoring/ensostuff/ONI_v5.php

O'Connell, C. S., Ruan, L., & Silver, W. L. (2018). Drought drives rapid shifts in tropical rainforest soil biogeochemistry and greenhouse gas emissions. *Nature Communications*, *9*(1). https://doi.org/10.1038/s41467-018-03352-3

Oertel, C., Matschullat, J., Zurba, K., Zimmermann, F., Erasmi, S. (2016). Greenhouse gas emissions from soils - A review. *Chemie der Erde*. 76, 327–352.

Olhoff, A., & Christensen, J. M. (Eds.) (2019). *Lessons from a decade of emissions gap assessments*. United Nations Environment Programme.

ORNL DAAC. (2018). MODIS and VIIRS Land Products Global Subsetting and Visualization Tool. ORNL DAAC, Oak Ridge, Tennessee, USA. Accessed October 24, 2019. Subset obtained for MOD13Q1/MYD13Q1 product at 10.8427N,85.6165W, time period: 2016-10-23 to 2019-09-22, and subset size: 0.25 x 0.25 km. https://doi.org/10.3334/ORNLDAAC/1379

Pan, Y., et al. (2011) A large and persistent carbon sink in the world's forests. *Science,* 333, 988–993.

Papen, H., & Butterbach-Bahl, K. (1999). A 3-year continuous record of nitrogen trace gas fluxes from untreated and limed soil of a N-saturated spruce and beech forest ecosystem in Germany: 1. N_2O emissions. *Journal of Geophysical Research: Atmospheres*, *104*(D15), 18487-18503.

Parton, W. J., Hartman, M., Ojima, D., & Schimel, D. (1998). DAYCENT and its land surface submodel: description and testing. *Global and planetary Change*, *19*(1-4), 35-48.

Penman, J., Gytarsky, M., Hiraishi, T., Krug, T., Kruger, D., Pipatti, R., ... & Wagner, F. (2003). Good practice guidance for land use, land-use change and forestry. *Good practice guidance for land use, land-use change and forestry.*

Pennington, R. T., Lavin, M., and Oliveira-Filho, A. (2009). Woody plant diversity, evolution, and ecology in the tropics: perspectives from seasonally dry tropical forests. *Annual Review of Ecology, Evolution, and Systematics*, *40*, 437-457.

Pennington, R. T., Lavin, M., Prado, D. E., Pendry, C. A., Pell, S. K., and Butterworth, C. A. (2004). Historical climate change and speciation: neotropical seasonally dry forest plants show patterns of both Tertiary and Quaternary diversification. *Philosophical Transactions of the Royal Society of London B: Biological Sciences*, *359*(1443), 515-538.

Perez-Ruiz, E. R., Garatuza-Payan, J., Watts, C. J., Rodriguez, J. C., Yepez, E. A., & Scott, R. L. (2010). Carbon dioxide and water vapour exchange in a tropical dry forest as influenced by the North American Monsoon System (NAMS). *Journal of Arid Environments*, *74*(5), 556–563. https://doi.org/10.1016/j.jaridenv.2009.09.029

Poorter, L., and Markesteijn, L. (2008) Seedling traits determine drought tolerance of tropical tree species. *Biotropica* 40(3): 321–331.

Poorter, L., Bongers, F., Aide, T. M., Zambrano, A. M. A., Balvanera, P., Becknell, J. M., ... & Craven, D. (2016). Biomass resilience of Neotropical secondary forests. *Nature*, *530*(7589), 211-214.

Portillo-Quintero, C. A., & Sanchez-Azofeifa, G. A. (2010). Extent and conservation of tropical dry forests in the Americas. *Biological conservation*, *143*(1), 144-155.

Portillo-Quintero, C. A., Sanchez-Azofeifa, G. A., Calvo-Alvarado, J. C., Quesada, M., and Espírito-Santo, M. M. Do. (2014). The role of tropical dry forests for biodiversity, carbon and water conservation in the neotropics: lessons learned and opportunities for its sustainable management. *Regional Environmental Change,* 15: 1039-1049.

Portillo-Quintero, C., Sanchez-Azofeifa, A., Calvo-Alvarado, J., Quesada, M., & do Espirito Santo, M. M. (2015). The role of tropical dry forests for biodiversity, carbon and water conservation in the neotropics: lessons learned and opportunities for its sustainable management. *Regional Environmental Change*, *15*(6), 1039-1049.

Powers, J. S. (2004). Changes in soil carbon and nitrogen after contrasting land-use transitions in northeastern Costa Rica. *Ecosystems*, *7*(2), 134-146.

Powers, J. S., Becknell, J. M., Irving, J., & Perez-Aviles, D. (2009). Diversity and structure of regenerating tropical dry forests in Costa Rica: Geographic patterns and environmental drivers. *Forest Ecology and Management*, *258*(6), 959-970.

Powers, J.S., Tiffin, P. (2010). Plant functional type classifications in tropical dry forests in Costa Rica: leaf habit versus taxonomic approaches. *Functional Ecology*, 24, 927–936.

Pugh, T. A., Lindeskog, M., Smith, B., Poulter, B., Arneth, A., Haverd, V., & Calle, L. (2019). Role of forest regrowth in global carbon sink dynamics. *Proceedings of the National Academy of Sciences*, *116*(10), 4382-4387. www.pnas.org/cgi/doi/10.1073/pnas.1810512116

Raich, J. W., Potter, C. S., & Bhagawati, D. (2002). Interannual variability in global soil respiration, 1980–94. *Global Change Biology*, *8*(8), 800-812.

Raich, J. W., Schlesinger, W. H. (1992). The global carbon dioxide flux in soil respiration and its relationship to vegetation and climate. Tellus B. 44(2), 81-99.

Raich, J., Tufekciogul, A. 2000. Vegetation and soil respiration: correlations and controls. Biogeochemistry. 48: 71-90.

Raich, J.W., Potter, C.S. (1995). Global patterns of carbon dioxide emissions from soils. *Global Biogeochemical Cycles, 9*, 23-36.

Raich, J.W., Schlesinger, W.H. (1992). The global carbon dioxide flux in soil respiration and its relationship to vegetation and climate. Tellus, B44, pp. 81–99

Rankine, C., Sanchez-Azofeifa, G. A., Guzmán, J. A., Espirito-Santo, M. M., & Sharp, I. (2017). Comparing MODIS and near-surface vegetation indexes for monitoring tropical dry forest phenology along a successional gradient using optical phenology towers. *Environmental Research Letters*, *12*(10), 105007.

Read, L., & Lawrence, D. (2003). Recovery of biomass following shifting cultivation in dry tropical forests of the Yucatan. *Ecological Applications*, *13*(1), 85-97.

Remy, E., Gasche, R., Kiese, R., Wuyts, K., Verheyen, K., & Boeckx, P. (2017). Edge effects on N2O, NO and CH4 fluxes in two temperate forests. *Science of the Total Environment*, *575*, 1150-1155.

Robertson, G. P., & Groffman, P. M. (2007). Nitrogen transformations. In *Soil microbiology, ecology and biochemistry* (pp. 341-364). Academic Press.

Rosenkranz, P., Brüggemann, N., Papen, H., Xu, Z., Seufert, G., & Butterbach-Bahl, K. (2006). N 2 O, NO and CH 4 exchange, and microbial N turnover over a Mediterranean pine forest soil.

Rowland, L., da Costa, A. C. L., Galbraith, D. R., Oliveira, R. S., Binks, O.J. , Oliveira, A. A. R., Pullen, A. M, Doughty, C. E., Metcalfe, D. B., Vasconcelos, S. S., and Ferreira, L. V. (2015). Death from drought in tropical forests is triggered by hydraulics not carbon starvation. *Nature,* 528: 119–121.

Rozendaal, D. M., Chazdon, R. L., Arreola-Villa, F., Balvanera, P., Bentos, T. V., Dupuy, J. M., ... & Martínez-Ramos, M. (2017). Demographic drivers of aboveground biomass dynamics during secondary succession in neotropical dry and wet forests. *Ecosystems*, *20*(2), 340-353.

Ruser, R., Flessa, H., Russow, R., Schmidt, G., Buegger, F., & Munch, J. C. (2006). Emission of N2O, N2 and CO2 from soil fertilized with nitrate: effect of compaction, soil moisture and rewetting. *Soil Biology and Biochemistry*, *38*(2), 263-274.

Sanchez-Azofeifa, G. A., Calvo-Alvarado, J., Espiritu-Santo, M. M., Fernandes, G. W., Powers, J. S., and Quesada, M. (2013). Tropical dry forest in the Americas: the tropi-dry endeavour. *Tropical dry forests in the Americas: Ecology, conservation and management*, 1-16.

Sánchez-Azofeifa, G. A., Castro-Esau, K. L., Kurz, W. A., & Joyce, A. (2009). Monitoring carbon stocks in the tropics and the remote sensing operational limitations: from local to regional projects. *Ecological Applications*, *19*(2), 480-494.

Sanchez-Azofeifa, G. A., Quesada, M., Rodríguez, J. P., Nassar, J. M., Stoner, K. E., Castillo, A., ... & Fajardo, L. (2005). Research priorities for Neotropical dry forests 1. *Biotropica: The Journal of Biology and Conservation*, *37*(4), 477-485.

Sanchez-Azofeifa, G.A., Calvo-Alvarado, J.C., Espírito-Santo, M.M.Do., Fernandes, G.W., Powers, J., Quesada, M. (2014). Tropical Dry Forests in the Americas: The Tropi-Dry Endeavor. In: Tropical Dry Forests in the Americas: Ecology, Conservation, and Management. CRC Press, Boca Raton. pp 1-16

Sanchez-Azofeifa, G.A., Castro, K. L., Rivard, B., Kalacska, M. R. (2005). Research priorities for neotropical dry forests. *Biotropica*. 37, 477-485.

Santoro, M., Cartus, O. (2019). ESA Biomass Climate Change Initiative (Biomass_cci): Global datasets of forest above-ground biomass for the year 2017, v1. Centre for Environmental Data Analysis, *02 December 2019*. doi:10.5285/bedc59f37c9545c981a839eb552e4084. http://dx.doi.org/10.5285/bedc59f37c9545c981a839eb552e4084

Schaufler, G., Kitzler, B., Schindlbacher, A., Skiba, U., Sutton, M. A., & Zechmeister-Boltenstern, S. (2010). Greenhouse gas emissions from European soils under different land use: effects of soil moisture and temperature. *European Journal of Soil Science*, *61*(5), 683-696.

Schimel, J., Balser, T. C., & Wallenstein, M. (2007). Microbial stress-response physiology and its implications for ecosystem function. *Ecology*, *88*(6), 1386-1394.

Schulze, E.D., Luyssaert, S., Ciais, P., Freibauer, A., Janssens, I.A., Soussana, J.F., et al. (2009). Importance of methane and nitrous oxide for Europe's terrestrial greenhouse-gas balance. *Nature Geoscience*, 2, 842-850.

Singh, J. S., Singh, S., Raghubanshi, A. S., Singh, S., Kashyap, A. K., & Reddy, V. S. (1997). Effect of soil nitrogen, carbon and moisture on methane uptake by dry tropical forest soils. *Plant and Soil*, *196*(1), 115–121. https://doi.org/10.1023/A:1004233208325

Singh, K. P., & Kushwaha, C. P. (2005). Emerging paradigms of tree phenology in dry tropics. *Current Science*, 964-975.

Sitch, S., Huntingford, C., Gedney, N., Levy, P. E., Lomas, M., Piao, S. L., et al. (2008). Evaluation of the terrestrial carbon cycle, future plant geography and climate-carbon cycle feedbacks using five Dynamic Global Vegetation Models (DGVMs). *Global Change Biology*, *14*(9), 2015-2039.

Souza, S. R., Veloso, M. D., Espírito-Santo, M. M., Silva, J. O., Sanchez-Azofeifa, A., e Brito, B. G. S., & Fernandes, G. W. (2019). Litterfall dynamics along a successional gradient in a Brazilian tropical dry forest. *Forest Ecosystems*, *6*(1), 35.

Stange, F., Butterbach-Bahl, K., Papen, H., Zechmeister-Boltenstern, S., Li, C., Aber, J. (2000). A process-oriented model of N2O and NO emissions from forest soils 2. Sensitivity analysis and validation. *Journal of Geophysical Research-Atmospheres,* 105, 4385-4398

Steinhoff, D. F., Monaghan, A. J., and Clark, M. P. (2015). Projected impact of twenty-first century ENSO changes on rainfall over Central America and northwest South America from CMIP5 AOGCMs. *Climate Dynamics* 44(5-6): 1329-1349.

Sterl, A., Severijns, C., Dijkstra, H., et al. (2008). When can we expect extremely high surface temperatures? *Geophysical Research Letters*, *35*(14).

Van Der Heijden, G. M., Powers, J. S., & Schnitzer, S. A. (2015). Lianas reduce carbon accumulation and storage in tropical forests. *Proceedings of the National Academy of Sciences*, *112*(43), 13267-13271.

van Groenigen, K. J., Osenberg, C. W., Hungate, B. A. (2011). Increased soil emissions of potent greenhouse gases under increased atmospheric CO_2. *Nature, 475*(7355), 214-216.

van Haren, J. L. M., Handley, L. L., Biel, K. Y., Kudeyarov, V. N., McLain, J. E. T., Martens, D. A., & Colodner, D. C. (2005). Drought-induced nitrous oxide flux dynamics in an enclosed tropical forest. *Global Change Biology*, *11*(8), 1247–1257. https://doi.org/10.1111/j.1365-2486.2005.00987.x

Van Mantgem, P. J., Stephenson, N. L., and Byrne, J.C. (2009). Widespread increase of tree mortality rates in the western United States. *Science*. 323:521–524.

Vance, E. D., Brookes, P. C., & Jenkinson, D. S. (1987). An extraction method for measuring soil microbial biomass C. *Soil biology and Biochemistry*, 19 (6), 703-707.

Vargas, R., & Allen, M. F. (2008). Environmental controls and the influence of vegetation type, fine roots and rhizomorphs on diel and seasonal variation in soil respiration. *New Phytologist*, *179*(2), 460-471.

Veldkamp, E., Keller, M. & Nunez, M. (1998) Effects of pasture management on N2O and NO emissions from soils in the humid tropics of Costa Rica. *Global Biogeochemical Cycles*, 12, 71–79.

Verduzco, V. S., Garatuza-Payán, J., Yépez, E. A., Watts, C. J., Rodríguez, J. C., Robles-Morua, A., & Vivoni, E. R. (2015). Variations of net ecosystem production due to seasonal precipitation differences in a tropical dry forest of northwest Mexico. *Journal of Geophysical Research: Biogeosciences*, *120*(10), 2081–2094. https://doi.org/10.1002/2015JG003119

Wang, G., Cai, W., Gan, B., Wu, L., Santoso, A., Lin, X., Chen, Z., and McPhaden, M. J. (2017). Continued increase of extreme El Niño frequency long after 1.5 C warming stabilization. *Nature Climate Change* 7(8): 568-572.

Waring, B. G., & Powers, J. S. (2016). Unraveling the mechanisms underlying pulse dynamics of soil respiration in tropical dry forests. *Environmental Research Letters*, *11*(10). https://doi.org/10.1088/1748-9326/11/10/105005

Waring, R. H., Running, S. W. (2010). *Forest ecosystems: analysis at multiple scales*. Elsevier. Pp 59.

Welch, B., Gauci, V., & Sayer, E. J. (2019). Tree stem bases are sources of CH_4 and N_2O in a tropical forest on upland soil during the dry to wet season transition. *Global Change Biology*, *25*(1), 361–372. https://doi.org/10.1111/gcb.14498

Williams, M. A., & Xia, K. (2009). Characterization of the water soluble soil organic pool following the rewetting of dry soil in a drought-prone tallgrass prairie. *Soil Biology and Biochemistry*, *41*(1), 21–28. https://doi.org/10.1016/j.soilbio.2008.08.013

Wolf, B., Chwala, C., Fersch, B., Garvelmann, J., Junkermann, W., Zeeman, M. J., ... & Brugger, P. (2017). The scalex campaign: Scale-crossing land surface and boundary layer processes in the tereno-prealpine observatory. *Bulletin of the American Meteorological Society*, *98*(6), 1217-1234.

Wolf, B., Zheng, X.H., Brueggemann, N., Chen, W.W., Dannenmann, M., Han, X.G., Sutton, M.A., Wu, H.H., Yao, Z.S., Butterbach-Bahl, K. (2010). Grazing-induced reduction of natural nitrous oxide release from continental steppe. *Nature*, 464, 881-884.

Wood, T. E., & Silver, W. L. (2012). Strong spatial variability in trace gas dynamics following experimental drought in a humid tropical forest. *Global Biogeochemical Cycles*, *26*(3), 1–12. https://doi.org/10.1029/2010GB004014

Wright, S. J., & Calderón, O. (2006). Seasonal, El Nino and longer term changes in flower and seed production in a moist tropical forest. *Ecology letters*, *9*(1), 35-44.

Xu, L., Baldocchi, D. D., Tang, J. (2004). How soil moisture, rain pulses, and growth alter the response of ecosystem respiration to temperature. *Global Biogeochemical Cycles, 18*(4), 1-10.

Yepez, E. A., Scott, R. L., Cable, W. L., & Williams, D. G. (2007). Intraseasonal variation in water and carbon dioxide flux components in a semiarid riparian woodland. *Ecosystems*, *10*(7), 1100–1115. https://doi.org/10.1007/s10021-007-9079-y

Zacharias, S., Bogena, H., Samaniego, L., Mauder, M., Fuß, R., Pütz, T., et al. (2011). A network of terrestrial environmental observatories in Germany. *Vadose Zone Journal*, 10(3), 955-973.

Zhang, K., Zhu, Q., Liu, J., Wang, M., Zhou, X., Li, M., et al. (2019). Spatial and temporal variations of N_2O emissions from global forest and grassland ecosystems. *Agricultural and Forest Meteorology*, *266*, 129-139.

Zhang, W., Liu, C., Zheng, X., Zhou, Z., Cui, F., Zhu, B., ... & Kiese, R. (2015). Comparison of the DNDC, LandscapeDNDC and IAP-N-GAS models for simulating nitrous oxide and nitric oxide emissions from the winter wheat–summer maize rotation system. *Agricultural Systems*, *140*, 1-10.

Zolkos, S. G., Goetz, S. J., & Dubayah, R. (2013). A meta-analysis of terrestrial aboveground biomass estimation using lidar remote sensing. *Remote Sensing of Environment*, *128*, 289-298.

Appendix

Appendix for chapter two - Tropical Dry Forests carbon sequestration dynamics along successional gradients under climate change extremes

Appendix 1. Aboveground carbon (AGC) and belowground carbon (BGC) pools by forest stand (20, 30 and 50 year-old and old-growth = OG) for Mata Seca State Park (MSSP; initial 2007 and final 2017) and Santa Rosa National Park (SRNP-EMSS; initial 2007 and final 2019). Different letters in the same column indicate significant differences between forest stands in a post-hoc Tukey test ($p<0.001$).

Site	Initial (Mg C ha^{-1})	Final (Mg C ha^{-1})	Loss (Mg C ha^{-1} y^{-1})	Gain (Mg C ha^{-1} y^{-1})
AGC MSSP				
20	6.1 ± 1.8^{a}	28.1 ± 3.6^{a}	0.8 ± 0.3^{a}	3.1 ± 1.0^{a}
50	36.0 ± 12.9^{b}	44.6± 17.1^{b}	2.2 ± 0.9^{b}	4.9 ± 1.8^{a}
OG	71.0 ± 15.8^{c}	83.1 ± 7.4^{c}	2.5 ± 0.8^{b}	5.0 ± 1.0^{a}
BGC MSSP				
20	1.3 ± 0.3^{a}	4.2 ± 2.0^{a}	0.2 ± 0.1^{a}	0.6 ± 0.4^{a}
50	8.2 ± 2.2^{b}	8.5± 2.8^{a}	0.3 ± 0.3^{b}	1.1 ± 1.1^{ab}
OG	14.8 ± 2.2^{c}	16.0 ± 1.9^{b}	0.4 ± 0.3^{b}	1.6 ± 1.2^{b}
AGC SRNP-EMSS				
30	19.1 ± 15.3^{a}	21.8 ± 15.8^{a}	1.5 ± 1.2^{a}	3.0 ± 2.6^{a}
50	66.1 ± 24.8^{b}	71.5 ± 22.0^{b}	4.0 ± 1.4^{b}	8.5 ± 2.4^{a}
OG	95.7 ± 14.4^{b}	101.2 ± 23.1^{b}	4.2 ± 0.9^{b}	7.6 ± 1.8^{a}
BGC SRNP-EMSS				
30	3.0 ± 1.5^{a}	4.7 ± 2.8^{a}	0.2 ± 0.2^{a}	0.1 ± 0.1^{a}
50	11.6 ± 1.7^{b}	12.2 ± 3.2^{b}	0.4 ± 0.3^{a}	0.6 ± 0.4^{ab}
OG	14.8 ± 5.0^{b}	15.2 ± 1.6^{b}	0.6 ± 0.6^{a}	0.9 ± 0.5^{b}

Appendix 2. Mean annual temperature (MAT), annual precipitation (MAP), days of rain, potential evapotranspiration (PET), water deficit, and ONI (Oceanic Nino Index) at both sites from 2006 to 2017.

Brazil MSSP	**MAP (mm)**	**Days of rain**	**MAT (°C)**	**Water deficit (mm)**	**PET (mm)**	**ONI**
2006	890.25	72.00	23.98	773.54	1382.24	0.09
2007	990.40	53.00	24.34	766.30	1386.60	-0.57
2008	708.80	49.00	24.16	808.60	1412.70	-0.76
2009	1015.40	58.00	24.81	794.30	1427.50	0.33
2010	759.00	52.00	24.20	837.60	1412.60	-0.47
2011	1284.80	72.00	23.56	691.40	1371.40	-0.84
2012	625.50	55.00	24.79	863.50	1391.40	-0.13
2013	1104.30	63.00	24.73	884.50	1443.80	-0.29
2014	645.20	49.00	24.90	977.60	1441.10	0.13
2015	499.20	72.00	25.89	588.79	1442.89	1.48
2016	733.50	98.00	25.40	573.75	1501.47	0.36
2017	686.00	64.00	25.28	877.00	1449.46	-0.18
Costa Rica SRNP-EMSS	**MAP (mm)**	**Days of rain**	**MAT (°C)**	**Water deficit (mm)**	**PET (mm)**	**ONI**
2006	1132.10	133.00	25.61	552.77	1475.23	0.09
2007	3052.90	152.00	26.10	683.70	1509.50	-0.57
2008	2984.60	120.00	25.40	745.00	1447.40	-0.76
2009	1250.70	149.00	25.10	511.00	1426.80	0.33
2010	2819.30	117.00	26.40	591.60	1531.20	-0.47
2011	2568.10	133.00	26.33	556.30	1460.30	-0.84
2012	1258.00	142.00	26.36	623.90	1468.50	-0.13
2013	1591.90	87.00	26.90	837.50	1577.50	-0.29
2014	1114.90	99.00	27.09	741.30	1486.80	0.13
2015	627.00	79.00	28.43	1118.13	1664.48	1.48
2016	1754.00	148.00	27.34	756.09	1707.08	0.36
2017	2049.10	148.00	27.00	756.09	1707.08	-0.18

Appendix 3. Linear models to evaluate the effects of aboveground carbon (AGC), time since abandonment (TSA), number of species and stems for the average of all years combined, wet and dry years on carbon losses, carbon gain and annual growth.

		Estimate	**Std. Error**	**t value**	**Pr(>|t|)**	**Model**
carbon loss	(Intercept)	0.00	0.17	0.00		R^2 0.25
	TSA	-0.27	0.31	-0.87		p <0.05
	Stems	-0.28	0.23	-1.23		
	Species	0.09	0.22	0.39		
	AGC	-0.22	0.34	-0.63		
	CEC	0.00	0.19	0.00		
carbon gain	(Intercept)	0.00	0.14	0.00		R^2 0.47
	TSA	-0.49	0.26	-1.88	<0.05	p <0.01
	Stems	-0.10	0.19	-0.51		
	Species	-0.19	0.18	-1.03		
	AGC	-0.10	0.29	-0.34		
	CEC	0.16	0.16	1.00		
annual growth	(Intercept)	0.00	0.13	0.00		R^2 0.58
	TSA	-0.46	0.23	-1.99	<0.05	p <0.001
	Stems	-0.10	0.17	-0.58		
	Species	-0.27	0.16	-1.63		
	AGC	-0.12	0.26	-0.46		
	CEC	0.28	0.14	1.91	<0.05	

Appendix for chapter three - Seasonality and budgets of soil greenhouse gas emissions from a tropical dry forest successional gradient in Costa Rica

Appendix 4. Stepwise multiple linear regression with best models used to identify the environmental drivers affecting the temporal variability in soil GHG. Included parameters were WFPS (water-filled pore space), MB (microbial biomass), NH_4^+ (ammonium) and NO_3^- (nitrate).

Stage		Parameter	Coefficient	Std. Error	t value	p-value	Adjusted R^2	p-value
Early stage	CO_2	(Intercept)	-3.75	13.81	-0.27		0.78	<0.001
		WFPS %	2.93	0.33	8.83	<0.001		
Intermediate stage	CO_2	(Intercept)	3.48	16.45	0.12		0.6	<0.001
		WFPS %	2.53	0.41	6.24	<0.001		
Pasture	CO_2	(Intercept)	-1.68	21.67	21.67		0.38	<0.001
		WFPS %	1.74	0.43	4.06	<0.001		
All sites	CO_2	Intercept	7.77	11.08	0.7		0.5	<0.001
		WFPS %	2.14	0.25	8.6	<0.001		
Early stage	N_2O	(Intercept)	-7.23	4.02	-1.8	<0.05	0.25	<0.05
		WFPS %	0.24	0.07	3.18	<0.001		
		NH_4	0.19	0.11	1.73	<0.05		
Intermediate stage	N_2O	(Intercept)	2.74	5.23	0.52		0.37	<0.001
		WFPS %	0.48	0.12	3.91	<0.001		
		Microbial biomass	-0.08	0.04	-2.3	<0.001		
Pasture	N_2O	(Intercept)	11.37	5.54	2.05	<0.05	0.59	
		WFPS %	-0.03	0.02	-1.58			
		Microbial biomass	0.01	0.01	1.75	<0.05		
All sites	N_2O	Intercept	-3.53	2.65	-1.33		0.2	<0.001
		WFPS %	0.15	0.04	3.21	<0.001		
		NH_4	0.08	0.04	1.75	<0.05		
Early stage	CH_4	(Intercept)	-7.17	5.08	-1.41		0.06	
		NO_3	-0.36	0.22	-1.68			
Intermediate stage	CH_4	(Intercept)	-56.42	7.04	-8.05	<0.001	0.57	<0.001
		NH_4	1.6	0.44	3.58	<0.001		
		NO_3	0.61	0.33	1.82	<0.05		
Pasture	CH_4	(Intercept)	-10.43	4.09	-2.55	<0.001	0.57	<0.001
		WFPS %	0.06	0.09	0.73	<0.001		
		NO_3	0.9	1.16	0.87	<0.05		
All sites	CH_4	Intercept	-18.79	3.83	-4.9	<0.001	0.1	
		NH_4	0.19	0.13	1.54			

Appendix 5. Literature review of mean annual precipitation, temperature and soil fluxes of CO_2, N_2O, and CH_4 from neotropical ecosystems. Fluxes have been recalculated from the original units and expressed in kg N_2O-N ha^{-1} y^{-1} and CH_4-C ha^{-1} y^{-1} and in t CO_2-C ha^{-1} y^{-1}.

References	Vegetation	Country	MAP (mm)	MAT (°C)	CO_2 (t C ha^{-1} y^{-1})	N_2O (kg N ha^{-1} y^{-1})	CH_4 (kg C ha^{-1} y^{-1})	Number of campaigns
Vitousek et al. (1989)	Tropical dry forest (intact old forest)	Mexico	748	24.9		0.4		2 (1 dry, 1 wet)
Garcia-Mendez et al. (1991)	Tropical dry forest (intact old forest)	Mexico	748	24.9		0.7		9 (3 dry, 6 wet)
Davidson et al. (1993)	Tropical dry forest (intact old forest)	Mexico	748	24.9		0.4		12 (4 dry, 8 wet)
Castaldi et al. (2004)	Open tree savanna	Venezuela	1057	27.3		0.5	0.7	2 (1 dry, 1 wet)
Castaldi et al. (2004)	Woodland savanna	Venezuela	1057	27.3		0.5	-0.3	2 (1 dry, 1 wet)
Scharffe et al. (1990), Sanhueza et al. (1990)	Open tree savanna	Venezuela	1300	27		0.5		21
Scharffe et al. (1990), Sanhueza et al. (1990)	Semi-deciduous tropical dry forest	Venezuela	1300	27		1	-3.14	21
Vargas (2012)	Tropical dry forest (secondary young forest)	Mexico	1650	24.2	3.9			-
Anderson and Poth (1998)	Cerrado Forest (shrub-land)	Brazil	1350	25	5.4		-6.1	1 (1 dry, 0 wet)
This study	Tropical dry forest (secondary old forest)	Costa Rica	1624	26.7	7.4	0.4	-2.6	22 (6 dry, 16 wet)
This study	Tropical dry forest (secondary young forest)	Costa Rica	1624	26.7	8.6	0.4	-0.6	23 (7 dry, 16 wet)
Average TDF			**1200.5**	**26.0**	**6.3±2.1**	**0.5±0.2**	**-2.0±2.5**	
This study	Tropical dry forest (abandoned pasture)	Costa Rica	1624	26.7	7.2	0.1	-0.7	22 (6 dry, 16 wet)
Garcia-Mendez et al. (1991)	Tropical dry forest (abandoned pasture)	Mexico	748	24.9		0.5		9 (3 dry, 6 wet)
Average TDF pasture			**1186**	**25.8**	**7.2±0.0**	**0.3±0.3**	**-0.7±0.0**	
Keller et al. (1986)	Tropical moist forest	Brazil	1770	26	12.6	1.2	-3.2	4
Davidson et al. (2000)	Tropical wet forest (secondary old forest)	Brazil	1800	26	18			16 (11 dry, 5 wet)
Davidson et al. (2000)	Tropical wet forest (intact old forest)	Brazil	1800	26.6	20			16 (11 dry, 5 wet)
Verchot et al. (1999, 2000)	Tropical wet primary forest	Brazil	1850	26.6	20	2.4	-2.1	12
Verchot et al. (1999, 2000)	Tropical wet secondary forest	Brazil	1850	26.6	17.9	0.9	-1	12
Garcia-Montiel et al. (2004)	Tropical moist secondary forest	Brazil	2090	25.4	14.1	2.5		2 (1 dry, 1 wet)
Fernandes et al. (2002)	Tropical wet forest	Brazil	2200	25.5	5		-1.1	2 (1 dry, 1 wet)
Garcia-Montiel et al. (2004)	Tropical moist secondary forest	Brazil	2270	25	14.4	2.2		2 (1 dry, 1 wet)
Keller et al. (1990)	Tropical moist forest	Panama	2600	27			-2.8	2
Keller et al. (1990)	Tropical moist forest	Panama	2600	27			-1.3	3

Keller et al. (1994)	Tropical wet primary forest	Costa Rica	3962	25.8		5.9	-0.5	15
Keller et al. (1994)	Tropical wet secondary forest	Costa Rica	3962	25.8		3.7	-0.4	15
Matson and Vitousek (1987)	Premontane tropical forest	Costa Rica	2700	22		2.3		8
Keller et al. (1986)	Subtropical moist forest	Puerto Rico	3530	25.7	9	1.8	-4.9	2
Schwendenmann et al. (2003)	Tropical wet forest	Costa Rica	4200	26	10.7			50
Matson and Vitousek (1987)	Tropical wet forest	Costa Rica	4200	26		2.5		15
Sayer et al. (2007)	Tropical moist forest	Panama	2600	27	15.3			9
Cleveland et al. (2010)	Tropical rain forest	Costa Rica	5000	26.5	11.4			12
Average tropical forest			**2832.4**	**25.9**	**14.0±4.6**	**2.5±1.4**	**-1.9±1.5**	
Verchot et al. (1999, 2000)	Tropical wet forest (abandoned pasture)	Brazil	1850	26.6	10.4	0.1	-3.1	12
Fernandes et al. (2002)	Tropical wet forest (abandoned pasture)	Brazil	2200	25.5	7.5		1.2	2 (1 dry, 1 wet)
Keller et al. (1990)	Tropical moist forest (burned pasture)	Panama	2600	27			-0.7	2
Keller et al. (1990)	Tropical moist forest (abandoned pasture)	Panama	2600	27			-0.5	2
Keller et al. (1994)	Tropical wet forest (abandoned pasture)	Costa Rica	3962	25.8		0.8	0.3	15
Davidson et al. (2000)	Tropical rain forest (abandoned pasture)	Brazil	1800	26.6	10			16 (11 dry, 5 wet)
Average tropical pasture			**2502.0**	**26.4**	**9.3±1.6**	**0.4±0.5**	**-0.6±1.6**	

Appendix for chapter four - Spatio-temporal variability and uncertainties of greenhouse gas emissions in a pre-alpine Bavarian grassland

Appendix 6. Physico-chemical properties found at each node at 5, 20 and 50cm of depth.

Node	Depth cm	Bulk density (g/cm³)	Clay	Silt	Sand	C org (%)	N (%)	pH
1	5	0.95	51.40	46.00	2.60	6.87	0.71	5.04
1	20	1.22	56.30	42.90	0.80	2.06	0.20	5.39
1	50	1.00	42.80	55.60	1.60	2.09	0.19	5.77
2	5	1.15	57.40	39.90	2.70	9.01	0.92	5.61
2	20	1.06	66.80	32.80	0.40	3.76	0.35	6.21
2	50	0.21	61.60	38.30	0.10	9.45	0.78	5.42
3	5	1.02	63.30	35.10	1.60	8.43	0.80	4.89
3	20	0.91	71.10	27.80	1.10	3.74	0.36	5.69
3	50	0.22	74.10	25.80	0.10	22.85	1.37	5.44
4	5	0.89	63.30	35.10	1.60	11.12	1.07	5.12
4	20	0.77	71.10	27.80	1.10	6.57	0.56	6.13
4	50	0.24	74.10	25.80	0.10	17.26	0.96	5.02
5	5	1.35	28.90	40.00	31.10	4.02	0.44	7.72
5	20	1.52	27.30	43.00	29.70	1.91	0.23	5.36
5	50	1.66	22.20	41.00	36.80	1.19	0.13	5.64
6	5	1.36	51.40	46.00	2.60	5.67	0.62	5.42
6	20	1.46	56.30	42.90	0.80	1.39	0.15	5.59
6	50	1.45	42.80	55.60	1.60	0.91	0.11	5.19
7	5	0.86	57.40	39.90	2.70	8.37	0.93	7.53
7	20	1.20	66.80	32.80	0.40	1.97	0.20	7.04
7	50	0.86	61.60	38.30	0.10	3.95	0.28	5.63
8	5	1.04	55.00	41.50	3.50	8.64	0.89	5.88
8	20	1.22	67.20	32.40	0.40	3.05	0.25	4.94
8	50	0.89	52.20	46.80	1.00	4.95	0.39	4.49
9	5	0.81	62.60	36.30	1.10	9.42	0.93	5.65
9	20	0.89	65.00	34.80	0.20	4.10	0.35	5.09
9	50	0.31	73.40	26.50	0.10	21.00	0.97	4.95
10	5	1.44	34.00	49.50	16.50	5.53	0.60	7.54
10	20	1.48	33.90	47.80	18.30	2.10	0.24	4.83
10	50	1.54	25.90	46.10	28.00	0.88	0.10	5.70
11	5	1.10	31.10	47.80	21.10	5.01	0.55	5.20
11	20	1.43	31.20	45.70	23.10	1.59	0.18	4.84
11	50	1.46	28.30	48.50	23.20	0.58	0.07	5.99
12	5	0.93	51.90	44.40	3.70	8.45	0.93	7.64
12	20	1.34	58.20	40.90	0.90	1.37	0.15	5.42
12	50	1.48	37.80	57.20	5.00	0.54	0.07	5.05

13	5	1.22	55.00	41.50	3.50	6.18	0.73	5.13
13	20	1.26	67.20	32.40	0.40	2.36	0.23	5.83
13	50	1.01	52.20	46.80	1.00	2.38	0.22	4.90
14	5	0.85	62.60	36.30	1.10	9.90	1.01	5.42
14	20	0.83	65.00	34.80	0.20	3.54	0.32	7.17
14	50	0.27	73.40	26.50	0.10	15.12	0.99	5.19
15	5	1.52	32.40	49.50	18.10	5.25	0.57	5.61
15	20	1.54	33.30	50.30	16.40	2.10	0.24	5.86
15	50	1.49	22.70	38.70	38.60	0.55	0.08	4.48
16	5	1.11	32.40	49.50	18.10	5.62	0.61	5.24
16	20	1.41	33.30	50.30	16.40	1.56	0.18	5.25
16	50	1.44	22.70	38.70	38.60	0.92	0.08	5.46
17	5	1.38	55.00	41.50	3.50	5.97	0.67	5.02
17	20	1.67	67.20	32.40	0.40	1.71	0.20	5.54
17	50	1.75	52.20	46.80	1.00	0.72	0.09	5.69
18	5	1.24	62.60	36.30	1.10	7.45	0.78	5.63
18	20	1.44	65.00	34.80	0.20	2.35	0.26	5.07
18	50	1.53	73.40	26.50	0.10	0.78	0.10	5.31
19	5	1.40	55.00	41.50	3.50	9.69	1.05	5.44
19	20	1.38	67.20	32.40	0.40	2.97	0.26	5.29
19	50	0.47	52.20	46.80	1.00	14.62	0.92	4.84
20	5	1.11	62.60	36.30	1.10	7.65	0.84	7.58
20	20	1.40	65.00	34.80	0.20	4.53	0.27	5.68
20	50	1.26	73.40	26.50	0.10	1.34	0.14	5.01